Diplomarbeit

Magnetized Nuclear Matter

Ausgeführt am
Institut für Theoretische Physik
der Technischen Universität Wien

unter der Anleitung von
Priv.Doz. Dr. Andreas Schmitt

durch
Alexander Haber, BSc
Forsthausgasse 10/A2/22
1200 Wien

Wien, am 21.11.2014 ____________

I don't know anything, but I do know that
everything is interesting if you go into it deeply enough.

Richard P. Feynman

Contents

Abstract

Due to magnetic catalysis, a strong magnetic field enhances the chiral condensate and thus might also increase the vacuum mass of nucleons. In this thesis I show that magnetic catalysis can be incorporated into effective models for dense nuclear matter. In order to discuss the resulting effect on the transition between vacuum and nuclear matter, i.e. the baryon onset of nuclear matter, I apply two relativistic field-theoretical models, the Walecka model and an extended linear sigma model. In both models it can be shown that at sufficiently large magnetic fields, the creation of nuclear matter becomes energetically more costly due to the heaviness of the magnetized nucleons, although the binding energy is also found to be increased by the magnetic field. These results are connected to the correct renormalization in presence of magnetic fields, which is derived in this thesis. They are potentially important for dense nuclear matter in compact stars, especially since previous studies in the astrophysical context always ignored the effect of magnetic catalysis.

Kurzfassung

Auf Grund von magnetischer Katalyse verstärkt ein magnetisches Feld das chirale Kondensat, wodurch erwartet werden kann, dass auch die Vakuummasse der Nukleonen erhöht wird. In dieser Arbeit wird gezeigt, dass es möglich ist, magnetische Katalyse in effektiven Modellen für dichte Kernmaterie zu berücksichtigen. Um den Einfluss auf den Übergang von Vakuum zu Kernmaterie, der "Baryon onset" genannt wird, zu berechnen, kommen zwei relativistische feldtheoretische Modelle zum Einsatz, das Walecka Modell und ein erweitertes, lineares sigma Modell. In beiden Fällen kann gezeigt werden, dass die Erzeugung von Kernmaterie bei genügend großen Hintergrundfeldern durch die größere Masse der magnetisierten Nukleonen energetisch schwieriger wird, obwohl auch die Bindungsenergie durch das Magnetfeld erhöht wird. Diese Resultate, die mit einer korrekten Renormalisierung in Anwesenheit von konstanten Magnetfeldern in Zusammenhang stehen, sind potentiell wichtig für dichte Kernmaterie in kompakten Sternen, im Besonderen da vorhergehende astrophysikalische Studien den Effekt der magnetischen Katalyse stets vernachlässigt haben.

Units and conventions

In this thesis I use natural Heaviside-Lorentz units. This means that we set $\hbar = c = k_B = 1$, and choose electron volts as the unit of energy. As a consequence, lengths are given by inverse energies, $[l] = \frac{1}{eV}$. Sometimes, for comparison with existing literature, femtometers are used as a unit of length. One femtometer, sometimes called one Fermi, are $1\,\mathrm{fm} = 10^{-15}\,\mathrm{m}$and correspond to $1\,\mathrm{fm} = 1\frac{\hbar c}{\mathrm{MeV}} \approx 197.327\,\mathrm{MeV}^{-1}$. In order to be able to compare the strength of the occurring magnetic fields to the masses, we use $[qB] = \mathrm{GeV}^2$ and $[m] = \mathrm{GeV}$. In natural units the electric charge is dimensionless. This is not true if one wants to compare the field strengths to astrophysical literature, where Gaussian units are common. For the proton, the charge is given by the elementary charge, which can be calculated from the fine structure constant, $\alpha = \frac{e^2}{4\pi} \approx \frac{1}{137}$, leading to $e \approx 0.30$ in our system of units. Using this, one obtains the conversion for the magnetic field strength, $qB = 0.1\,\mathrm{GeV}^2$ is then equivalent to $B = 1.7 \times 10^{19}\,\mathrm{G}$.

For the metric we use the mostly-minus convention of particle physics, $g^{\mu\nu} = \mathrm{diag}(1, -1, -1, -1)$. Throughout this thesis, most of the thermodynamical quantities are expressed as densities, since we are working in the thermodynamic limit. For readability, the appendix "density" is omitted whenever it is clear in the given context.

1 Introduction

Compact stars are, solely beaten by black holes, the second densest objects in our universe. For a rough estimate how incredible dense they are, one can calculate the density by plugging in typical values of compact star radii, which are of the order of $R \sim 10$ km, and masses, which can be found in the range of one to two solar masses $M_\odot$. With these numbers we end up with a density a few times higher of the density of heavy nuclei, $\rho \sim 7 \times 10^{14}\,\mathrm{gcm}^{-3}$. Although compact stars are "only" at the second place, they can be even more interesting in some context. Whereas black holes can be described completely by only three parameters, namely their mass, charge and spin, compact stars can serve as a laboratory for quantum chromo dynamics (QCD). This can be seen by a look to the QCD phase diagram, which collects the equilibrium phases of QCD in the plane of the quark or baryon chemical potential μ and temperature T (see Fig. 1.1). Compared to the occurring chemical potential in compact stars, which are at the GeV scale, their temperatures are rather low. Therefore, we merely find them close to the $T = 0$ axis. What is not clear a priori, is in which phase they can be found. They might live in the region of hadronic matter where quarks are confined into nucleons, but may also penetrate the deconfined region, implying that we could find quark stars in our universe. Since a compact star has a density profile ranging from smaller densities at the surface to very high values at the core, all possible combinations of the latter are possible, including several mixed phases. In order to unveil the truth, we have to calculate measurable properties like mass-radius relations, cooling properties and rotation curves of compact stars, which are strongly affected by the state of matter inside. However, this region of low temperatures and intermediate densities is rather hard to tackle. At high values of both of them, the coupling between quarks becomes sufficiently weak to render quarks asymptotically free, so perturbation theory can be applied. At very low densities we can perform actual experiments in the laboratory. After all, Hadrons are very hard to describe in terms of their fundamental degrees of freedom, i.e. as a particle composite of quarks. This forces us to use effective models like they are used in this thesis. Particularly interesting for us is the transition line between the vacuum and the state of hadronic nuclear matter, which is called the baryon onset of nuclear matter.

Additionally, the phase diagram can be extended by several other axes, one of them being a background magnetic field. Since the magnetic flux is conserved in the creation of a compact star, the magnetic field grows strongly as the star shrinks after it ran out of fuel. In this context, compact stars with very strong magnetic fields are called magnetars. At the surface, the magnetic fields can reach up to $B \lesssim 10^{15}$ G [1], and are expected to be even higher in the core, possibly up to 10^{18-20} G [2, 3]. For comparison, the magnetic field of the earth is around $B \sim 0.6$ G and the strongest magnetic fields created in a laboratory are around $B \sim 10^5$ G. Magnetic fields might also play a prominent role in neutron star mergers, since they are emitting gravitational waves which can be observed directly. The emitted waves are very sensitive to the microscopic properties of the matter inside the star, i.e. the equation of state, which is again influenced by the magnetic field of the star [4]. In such a binary system, the magnetic field might become extremely large because of the magneto-rotational instability [5], such that magnetic corrections to the equation of state get very important. If one compares these field strengths to the square of the energy scale of QCD, $\Lambda_{QCD}^2 \sim 10^{18}$ G, one can expect that these fields indeed affect dense nuclear matter.

Although the baryon onset is known to be a first order phase transition and to take place at a baryon chemical potential of $\mu_0 = 922.7$ MeV at $B = 0$, it is rather unclear how this transition is changed in presence of a magnetic field. For quarks it is known that their mass is increased by an effect called "magnetic catalysis" [6–15], which actually happens due to an, by the magnetic field, increased chiral condensate [16–19]. Magnetic catalysis and the underlying chiral symmetry

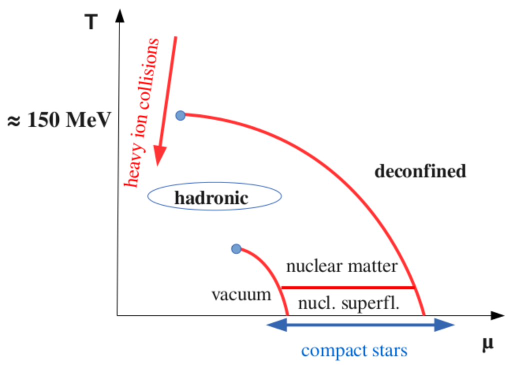

(a) Compact stars can be found nearly at $T = 0$ and intermediate chemical potentials. The onset of nuclear matter occurs around a quark chemical potential of $\mu_q = 300$ MeV . It is presented by the shorter, curved red line, separating the vacuum from the nuclear matter phase in the hadronic part of the diagram .

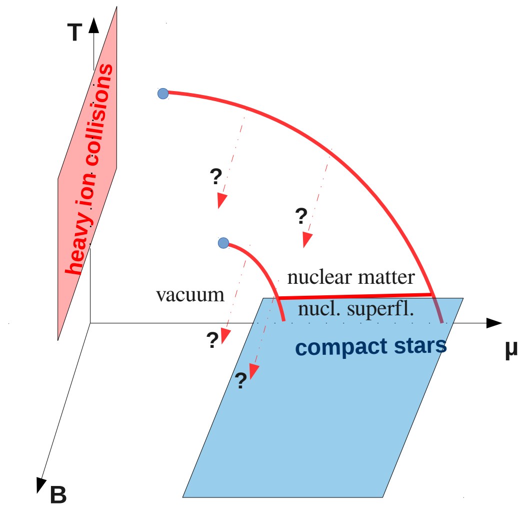

(b) In presence of a magnetic field it is unclear how the transition lines have to be continued into the magnetic direction. The transition from vacuum to nuclear matter will be studied in this work.

Figure 1.1: Sketch of the QCD phase diagram in the plane of quark chemical potential, temperature and background magnetic field. In this thesis the transition between the vacuum and nuclear matter in the hadronic phase and its extension into the direction of the magnetic axis at zero temperature is studied.

will be explained in some detail in the next chapter. Since nucleons are composited particles of quarks, magnetic catalysis can be expected to increase the vacuum mass of the nucleons too. This is not the only contribution to the baryon onset, since the binding energy of nuclear matter is also affected by external magnetic fields. Therefore, even if the vacuum mass is enhanced with the magnetic field, the behavior of the onset of nuclear matter is not trivial. I will show in this thesis, that the onset chemical potential as a function of the magnetic field indeed is not necessarily monotonic. In order to do so I apply to different relativistic field theoretical models, the Walecka model [20, 21], and an extended linear sigma model [22–29], which are introduced in Chap. 4 and Chap. 5.

Of course it is not the first time that dense nuclear matter in magnetic fields is studied, even more complicated models than the used ones in this thesis has been elaborated [30–37]. In all these works the divergent vacuum term has been simply omitted, like it was done in the Walecka model without magnetic field before. In this case it has been shown by Glendenning, that a correct renormalization can be done but only serves as minor correction [38–40]. This is still true for the unmagnetized vacuum part in the presence of a magnetic field, which I show in appendix B. Since magnetic catalysis is a vacuum effect, this “no-sea approximation” amounts to throwing out important physical effects, so at least the $B-$dependent part should be kept and properly renormalized, which is done in Chap. 3. This also has been done in the original works on magnetic catalysis as well in many following studies, like in the Nambu-Jona-Lasinio (NJL) model [41–46], a quark meson model [46–49] and the MIT bag model [50]. However, as far as we know, the resulting publication of this thesis [51], is the first to include the effect of magnetic catalysis in a relativistic mean-field description of nuclear matter. The effect of magnetic catalysis in the vacuum is calculated and presented in Chap. 6, whereas in Chap. 7 the full baryon onset of nuclear matter in a magnetic field is shown. These calculations do not make any qualitative predictions since the used models and parameters are unrealistic for nuclear matter in compact stars, where the occurring densities are expected to be much higher than considered here. Additionally we neglect the anomalous magnetic moment of the nucleons, we do not demand charge neutrality and beta equilibrium and only consider isospin symmetric matter. The isospin symmetry is only broken due to the different charges of neutrons and protons. The possible formation of a nucleonic superfluid is also neglected. Our study should merely be seen as a starting point for more realistic calculations or as a step back in order to improve existing studies of nuclear matter in strong magnetic fields.

2 Chiral symmetry of Quantum Chromodynamics

"Chiral" originates in the Greek word for hand, so chiral symmetry refers to systems where left and right handed objects exist and are treated equally. In quantum field theory, chiral symmetry means that the left and right handed components of a Dirac spinor transform independently under chiral transformations and the Lagrangian stays invariant. The strong interaction, which is described by quantum chromodynamics (QCD), is known to exhibit an approximate chiral symmetry. To understand this we take a look at the QCD Lagrangian:

$$\mathcal{L}_{QCD} = \bar{\psi}\left(i\gamma^{\mu}D_{\mu} + \mu\gamma_0 - M\right)\psi + \mathcal{L}_{gluons}\,. \tag{2.1}$$

Here, ψ denotes the Dirac spinor of the quark field in color, flavor and Dirac space, and $M = \mathrm{diag}\left(m_u, m_d, m_s\right)$ is the mass matrix in flavor space. Since the quark masses are not degenerated, the QCD Lagrangian is not isospin symmetric. $D_{\mu} = \partial_{\mu} - igT_a A_{\mu}^a$ denotes the covariant derivative containing the strong coupling constant g, the gauge fields A_{μ}^a and the generators of the $SU(3)_C$ color gauge group, $T_a = \frac{\lambda_a}{2}$, with the eight $(a = 1, ..., 8)$ Gell-Mann matrices λ_a. The gluonic part of the Lagrangian does not transform under chiral transformations of the quark spinors and is therefore of no interest here. The chemical potential enters like the temporal component of a gauge field with the zeroth Dirac gamma matrix γ_0 [52]. Since we neglect weak interactions, all flavors are conserved separately and enter the Lagrangian with their own chemical potential, so μ has to be considered as a diagonal matrix in flavor space as well. In order to decompose a general spinor into its left and right handed part we introduce the chirality projectors

$$P_R = \frac{1+\gamma_5}{2}, \qquad P_L = \frac{1-\gamma_5}{2}\,. \tag{2.2}$$

To show that these matrices obey the properties of projectors, which are idempotence, hermiticity, orthogonality and completeness,

$$P_{R/L}^2 = P_{R/L}, \qquad P_{R/L}^{\dagger} = P_{R/L}, \qquad P_L P_R = 0, \qquad P_R + P_L = 1\,, \tag{2.3}$$

it is enough to remember the definition of the fifth gamma matrix, $\gamma_5 = i\gamma_0\gamma_1\gamma_2\gamma_3$ that leads to $\gamma_5^2 = 1$ and $\gamma_5^{\dagger} = \gamma_5$.

The spinor can now be decomposed using these projectors:

$$\psi_{R/L} = P_{R/L}\psi\,,$$

such that the sum of the two parts yields the full spinor again, $\psi = P_R\psi + P_L\psi = \psi_R + \psi_L$. Since γ_5 anti commutates with all other gamma matrices, the decomposition of the Lagrangian looks like

$$\mathcal{L}_{QCD} = \bar{\psi}_R\left(i\gamma^{\mu}D_{\mu} + \mu\gamma_0\right)\psi_R + \bar{\psi}_L\left(i\gamma^{\mu}D_{\mu} + \mu\gamma_0\right)\psi_L - \bar{\psi}_R M\psi_L - \bar{\psi}_L M\psi_R + \mathcal{L}_{gluons}\,. \tag{2.4}$$

In the massless case, $M = 0$, the Lagrangian is chirally invariant, i.e. separate rotations of the left and right spinors leave it invariant. Therefore this limit is also called the chiral limit. As seen before we only consider matter with three flavors since the remaining three flavors (charm, top and bottom) are very heavy and normally not populated. Therefore the symmetry group structure is given by

$$U(3)_R \times U(3)_L\,, \tag{2.5}$$

and can be decomposed as

$$SU(3)_R \times SU(3)_L \times U(1)_L \times U(1)_R. \tag{2.6}$$

The Noether currents that correspond to these symmetries, $J^{\mu}_{a,R/L} = \bar{\psi}_{R/L}\gamma^{\mu}t_a\psi_{R/L}$ where $t_0 = \mathbf{1}$ and $t_a = T_a\,(a = 1, ...8)$, can be rewritten as an axial and a vector current. The vector current corresponds to the baryon conservation and is therefore also denoted as $U(1)_B$, the axial symmetry is broken due to quantum effects, which is called the axial anomaly. The actual flavor group symmetry $SU(3)_R \times SU(3)_L$ is called chiral symmetry group. In the case $M \neq 0$ but degenerated quark masses ($m_u = m_d = m_s$), the chiral symmetry is explicitly broken, but the simultaneous rotation of left and right handed spinors remains a symmetry, i.e. the remaining symmetry group is $SU(3)_{L+R}$.

Chiral symmetry can also be broken spontaneously by a **chiral condensate** of the form $\langle \bar{\psi}_L \psi_R \rangle$, which is only invariant under simultaneous right and left handed rotations. This means that the symmetry group $G = SU(3)_R \times SU(3)_L$ with $\dim G = 2\left(N^2 - 1\right) = 8 + 8 = 16$ is broken down to the subgroup $H = SU(3)_{L+R}$. with $\dim H = 8$. Since the coset space G/H is $\dim G - \dim H = 8$ dimensional we end up with 8 Goldstone bosons. Due to the explicit symmetry breaking these bosons are not exactly massless but acquire small masses and therefore are sometimes called pseudo-Goldstone bosons. These bosons form the well known pion octet containing the pions, kaons and η- mesons.

In this section I largely followed [53], where you can find more details on this subject.

2.1 Magnetic catalysis

In 1961 the physicists Nambu and Jona-Lasinio proposed the first time that "the nucleon mass arises largely as a self-energy of some primary fermion field through the same mechanism as the appearance of energy gap in the theory of superconductivity." [54, 55] This means, that the mass of the nucleons is mostly created dynamically by spontaneous symmetry breaking (SSB) of the (approximate) chiral symmetry. This concept suggests that external conditions or physical parameters, which alters the chiral condensate, also alter the mass of the nucleon! One of these external parameter is obviously a magnetic field. It has been shown that a sufficiently strong magnetic field tends to increase (or "catalyze") the chiral condensate or, more general, spin 0 fermion-antifermion condensates. This effect was therefore named "magnetic catalysis" [8–10, 14, 56]. The underlying physical mechanism is similar to the cooper pairing in superconductors described by BCS - theory (Bardeen-Cooper-Schrieffer). The magnetic field restricts the motion of a charged particle perpendicular to the field. Already at the classical level, the particle starts due spiral around the field lines with the cyclotron frequency ω_c. On a quantum mechanical level, this motion is quantized, where as the motion in direction of the field is, classically and on the quantum level, still free. If the particle is in the lowest possible energy state with zero energy contribution from the cyclic motion around the magnetic field, the problem becomes effectively 1+1 dimensional and the energy of the particle is simply given by $\epsilon_k = \sqrt{m^2 + k_{||}^2}$. This dimensional reduction leads, in complete analogy to BCS theory, to an nonvanishing condensate for an arbitrary small attractive interaction. Since the coupling in the QCD vacuum is rather strong, the chiral condensate also exists without magnetic field but is increased by the field. This is true for small temperatures. At high temperatures the situation is slightly more complicated, where an "inverse magnetic catalysis" can appear [18].

Due to the increasing chiral condensate, the magnetic field tends to increase the vacuum masses of quarks [6–15]. It is not obvious that an increasing quark mass also leads to an increased nucleon mass since the interaction between the quarks is also altered by the magnetic field. A recent work [57] concludes that the magnetic field tends to reduce the mass of neutrons, composited of quarks. In this work the effect of the chiral condensate has been neglected, so it is expected that these two effects will counteract and both affect the effective mass of the nucleon. It might be possible to include these effects in phenomenological models by taking the anomalous magnetic moment of the nucleons into account which indeed seems to decrease the nucleon mass [33]. In this thesis, nucleons are considered to be pointlike and the interaction between the quarks is neglected.

3 Landau free energy and renormalization

In this section I follow, if not specified otherwise, the publication of Florian Preis, Andreas Schmitt and the author of this thesis, Ref [51]. Further information is extracted from the pedagogical works of A. Schmitt and J. Kapusta, Refs [53, 58].

In this thesis I will investigate two different models in order to show how magnetic catalysis can be incorporated into phenomenological nuclear models. In a mean field approach, the effects of the various mesonic condensates can be absorbed into an effective dynamic nucleon mass M_N and an effective chemical potential, μ_*, leading to an essentially free fermionic quantum field theory. Due to the complete absorption of the effects of the nucleon interaction into the effective parameters, they become implicitly dependent on temperature and chemical potential. Note that the canonical variable to the baryon number N is still μ, where μ_* now refers to the energy at the Fermi level, $E_f = \mu_* = \sqrt{M^2 + k_F^2}$, with the Fermi momentum k_F. This is important for the correct thermodynamic relations. In this section we will derive the renormalized pressure in the presence of a magnetic field. It is shown that the renormalization is not straight forward any more if one includes a magnetic field and that the correct renormalization contains physical effects, especially magnetic catalysis, and therefore must not be neglected.

Since we allow for particle creation and annihilation we are working in a grand canonical ensemble and have to calculate the corresponding thermodynamic potential, the grand canonical potential or sometimes also called Landau free energy. Starting from the internal energy E successive Legendre transformations lead to the grand canonical potential,

$$\begin{aligned} \Omega &= E - TS - \mu N = -PV\,, \\ \frac{\Omega}{V} &= -P\,. \end{aligned} \tag{3.1}$$

From now on we will denote the Landau free energy *density* simply with Ω. Because of the connection of the free energy density to the pressure by multiplication with minus one, thermodynamical equilibrium is reached at the state with the highest pressure, i.e. with the lowest free energy.

In both models I consider, the free energy can be written in a very general way,

$$\Omega = \frac{B^2}{2} + U + \Omega_N\,. \tag{3.2}$$

The first term is the contribution of the magnetic field, which points, without loss of generality, into the z-direction, $B = (0, 0, B)^T$. This term can be derived from the electromagnetic part of the Lagrangian,

$$\mathcal{L}_{em} = -\frac{1}{4}F^{\mu\nu}F_{\mu\nu} = \frac{1}{2}\left(\boldsymbol{B}^2 + \boldsymbol{E}^2\right)\,, \tag{3.3}$$

where $F^{\mu\nu} = \partial^\mu A^\nu - \partial^\nu A^\mu$ is the totally antisymmetric field strength tensor including the electromagnetic potential A^μ. In the Landau gauge the potential has no temporal component, which corresponds to a vanishing electric field $\boldsymbol{E}$, and the curl of the spatial components of $A^\mu = (0, 0, Bx, 0)$ yields the desired magnetic field term, $\frac{B^2}{2}$. The second term is the model dependent tree-level potential which is completely independent of the nucleons, and the last term is the nucleonic part of the free energy. The concrete form of the tree-level potential does not matter for the renormalization and will be specified in the corresponding chapters separately.

The nucleonic pressure of a free field theory without magnetic field is well known and can be found in literature, for instance in Refs. [53, 58]. Since the magnetic field only couples to the charged protons and not to the neutral neutrons (the anomalous magnetic moment is neglected!), the isospin degeneracy is broken, so all the results presented here are valid for a single type of a spin-$\frac{1}{2}$ fermion. For neutrons and therefore uncharged matter, i.e. $qB = 0$, the evaluation of the path integral yields the free energy

$$\Omega_N\left(qB=0\right) = -2\sum_{e=\pm1}\int\limits_{-\infty}^{\infty}\frac{d^3\boldsymbol{k}}{(2\pi^3)}\left\{\epsilon_k + T\ln\left(1+e^{-\frac{\epsilon_k - e\mu_*}{T}}\right)\right\}, \tag{3.4}$$

where $e = -1$ corresponds to the anti-particle contribution that will vanish in the limit $T \to 0$ since the effective chemical potential is positive, $\mu_* > 0$, and the argument of the appearing Heaviside theta function $\Theta\left(-\mu_* - M\right)$ is always negative. The dispersion relation for a free particle is given by the relativistic energy-momentum relation,

$$\epsilon_k = \sqrt{k^2 + M^2}\,.$$

The integral over the excitation energies is divergent and has to be renormalized, what will be done for charged matter later in this chapter respectively in App. (B) for uncharged particles. The second part of the integral, which we will denote by $\Omega_{N,mat}$, can be solved analytically in the zero temperature limit using $\lim_{T\to0} T\ln\left(1+e^{\frac{x}{T}}\right) = x\Theta\left(x\right)$, where the theta function cuts off the momentum integral at the Fermi momentum k_F. In compact stars this limit is a good approximation, since the temperatures are typically in the keV range, whereas the masses and chemical potentials of the nucleons and quarks are at the MeV or even at the GeV scale.

$$\begin{aligned}
\Omega_{N,mat}(qB=0) &= -2\int\limits_{-\infty}^{\infty}\frac{d^3\boldsymbol{k}}{(2\pi^3)}\left\{T\ln\left(1+e^{-\frac{\epsilon_k-\mu_*}{T}}\right)\right\} \\
&\xrightarrow{T=0} \frac{\Theta\left(\mu_* - M\right)}{\pi^2}\int\limits_0^{k_F} dk\, k^2\left(\epsilon_k - \mu_*\right) \\
&= -\frac{\Theta\left(\mu_* - M\right)}{8\pi^2}\left[\left(\frac{2}{3}k_F^3 - M^2 k_F\right)\mu_* + M^4\ln\frac{k_F+\mu_*}{M}\right].
\end{aligned} \tag{3.5}$$

The theta function in the second line guaranties real energy states and therefore only allows a matter contribution to the free energy if the effective chemical potential μ_* is higher than the effective mass M.

3.1 Solution of the Dirac equation in presence of a magnetic field

In the presence of a magnetic field the derivation of the pressure following the path integral method is more complicated. However, it is enough to replace the dispersion relation by the dispersion relation of a charged particle in a magnetic field as well to partially replace the momentum integral. These replacement rules can be derived by solving the corresponding dirac equation. In order to do so I present a derivation which can be found in Ref. [59].

The Dirac equation is obtained as the Euler Lagrange equation of motion (EL-EOM) by variation with respect to $\bar{\psi}$ from the baryonic Lagrangian

$$\mathcal{L}_N = \bar{\psi}\left(i\gamma_\mu D^\mu - M + \mu\gamma^0\right)\psi\,, \tag{3.6}$$

where the magnetic field enters via the covariant derivative $D^\mu = \partial^\mu + iqA^\mu$. Without loss of generality we choose the magnetic field to point in the $z-$direction, i.e. $\boldsymbol{B} = B\hat{e}_z$. As explained before, this corresponds to a vector potential of the form $A^\mu = (0, 0, Bx, 0)$. The variation immediately yields

$$(i\gamma_\mu \partial^\mu + q\gamma_\mu A^\mu - M)\,\psi = 0\,. \tag{3.7}$$

The chemical potential is actually not a part of the Hamiltonian and is suppressed, we can add it at the end of the calculation to the energy eigenvalues obtained from the equation above. Since the temporal component of the vector potential is zero the equation reduces to

$$\left(i\gamma_\mu \partial^\mu + q\gamma_i A^i - M\right)\psi = 0\,. \tag{3.8}$$

Separating the time derivative from the spatial components and shifting it to the other side leads to the Schrödinger form of the Dirac equation with the corresponding Dirac Hamiltonian:

$$\begin{aligned} i\frac{\partial}{\partial t}\psi(X) &= \hat{H}\psi(X) && (3.9)\\ \hat{H} &= \gamma_0\left[\gamma_i\left(p^i + qA^i\right) + M\right]\,, && (3.10) \end{aligned}$$

were p^i denotes the momentum operator $-i\partial^i$. Since the Hamiltonian has no explicit time dependence we can calculate stationary solutions of the form $\psi(X) = e^{-ip_0 t}\psi(x,y,z)$, which leads to the stationary version of the Dirac equation for the time independent spinors,

$$\hat{H}\psi(x,y,z) = p_0\psi(x,y,z)\,. \tag{3.11}$$

To solve the problem in an elegant way we define an auxiliary operator $\hat{T}^0$ that commutes with the Hamiltonian and therefore omits the same eigenfunctions. This operator is known as the longitudinal polarization operator,

$$\hat{T}^0 = \frac{1}{M}\left[\gamma_0\gamma_i\gamma_5\left(p^i + qA^i\right)\right]\,. \tag{3.12}$$

The gamma structure of this operator is called Σ and can be expressed in the standard Dirac representation with help of the Pauli matrices σ^i :

$$\Sigma = \gamma_0\gamma_i\gamma_5 = \begin{pmatrix} \sigma^i & 0 \\ 0 & \sigma^i \end{pmatrix}\,. \tag{3.13}$$

It is straightforward to show that these operators commute, $\left[\hat{T}, \hat{H}\right] = 0$. Since this operator is block diagonal we express it in the form

$$\hat{T}^0 = \begin{pmatrix} \hat{\tau}^0 & 0 \\ 0 & \hat{\tau}^0 \end{pmatrix}\,, \tag{3.14}$$

where $\hat{\tau}^0$ is given by

$$\begin{aligned} \hat{\tau}^0 &= \frac{1}{M}\left[\sigma_i\left(p^i + qA^i\right)\right]\,, && (3.15)\\ &= \frac{1}{M}\left[\sigma_x\left(-i\frac{\partial}{\partial x}\right) + \sigma_y\left(-i\frac{\partial}{\partial y} + qBx\right) + \sigma_z\left(-i\frac{\partial}{\partial z}\right)\right]\,. \end{aligned}$$

Now we only have to solve the reduced eigenvalue problem for the auxiliary operator,

$$\hat{T}^0\psi = T^0\psi\,. \tag{3.16}$$

Due to its block diagonal structure this equation splits into two identical differential equations for the bispinors F. The entire solution is composed of two identical bispinors which can only differ by a multiplicative constant κ. Since the operator does neither depend on the coordinates y or z, we can separate the momentum in $y-$and $z-$direction and write down the now solely $x-$dependent Dirac spinor in the form

$$\psi(x,y,z) = e^{i(p_y y + p_z z)} \begin{pmatrix} F(x) \\ \kappa F(x) \end{pmatrix}, \qquad F(x) = \begin{pmatrix} f_1(x) \\ f_2(x) \end{pmatrix}. \tag{3.17}$$

At this point it is suitable to introduce a new variable $\xi = \sqrt{qB}\left(x + \frac{p_y}{qB}\right)$, with its derivative $\frac{d}{d\xi} = \frac{1}{\sqrt{qB}}\frac{d}{dx}$. Using again the standard representation of the Pauli matrices leads to the following system of differential equations for the bispinor $F(\xi)$ depending on the new variable ξ:

$$\frac{1}{M}\begin{pmatrix} p_z & -i\sqrt{qB}\frac{d}{d\xi} - ip_y - iqBx \\ -i\sqrt{qB}\frac{d}{d\xi} + ip_y + iqBx & -p_z \end{pmatrix}\begin{pmatrix} f_1 \\ f_2 \end{pmatrix} = T^0 \begin{pmatrix} f_1 \\ f_2 \end{pmatrix}. \tag{3.18}$$

In this equation we recognize operators similar to the ladder operators of the quantum mechanical harmonic oscillator:

$$a^+ = \frac{1}{\sqrt{2}}\left(\xi - \frac{d}{d\xi}\right), \qquad a^- = \frac{1}{\sqrt{2}}\left(\xi + \frac{d}{d\xi}\right). \tag{3.19}$$

As a function of these ladder operators the equation can be written as

$$\frac{1}{M}\begin{pmatrix} p_z & -i\sqrt{2qB}a^- \\ i\sqrt{2qB}a^+ & -p_z \end{pmatrix}\begin{pmatrix} f_1(\xi) \\ f_2(\xi) \end{pmatrix} = T^0 \begin{pmatrix} f_1(\xi) \\ f_2(\xi) \end{pmatrix}. \tag{3.20}$$

Performing the matrix multiplication yields two coupled equations for the functions f_1 and f_2. The first equation reads

$$f_1(\xi) = \frac{-i\sqrt{2qB}}{MT^0 - p_z} a^- f_2(\xi)\,. \tag{3.21}$$

If we insert this into the second equation we obtain a decoupled differential equation for the function $f_2(\xi)$:

$$\left(a^+ a^- - \frac{M^2\left(T^0\right)^2 - p_z^2}{2qB}\right) f_2(\xi) = 0\,. \tag{3.22}$$

Using the product rule (the derivative of the first ladder operator also acts on the position operator of the second one) we compute an equation that is identical to the quantum mechanical description of a harmonic oscillator:

$$\left(\frac{d^2}{d\xi^2} - \xi^2 + 1 + \frac{M^2\left(T^0\right)^2 - p_z^2}{qB}\right) f_2(\xi) \quad = \quad 0\,, \tag{3.23}$$

$$\left(-\frac{1}{2M}\frac{d^2}{d\xi^2} + \frac{1}{2M}\xi^2\right) f_2(\xi) \quad = \quad \underbrace{\frac{1}{2M}\left(1 + \frac{M\left(T^0\right)^2 - \frac{p_z^2}{M}}{qB}\right)}_{\hat{=}E} f_2(\xi)\,. \tag{3.24}$$

In comparison, the Schrödinger equation for the one dimensional harmonic oscillator is given by

$$\left(-\frac{1}{2M}\frac{d^2}{dx^2} - \frac{1}{2}M\omega^2 x^2\right)\psi = E\psi \tag{3.25}$$

and obeys the quantized solutions

$$E = \omega\left(\nu + \frac{1}{2}\right). \tag{3.26}$$

If we compare this to Eq. (3.24), we can read of the equivalence of the frequency $\omega^2 \hat{=} -\frac{1}{M^2}$ as the prefactor of the quadratic term and obtain, after some basic algebraic rearrangements, the eigenvalues of T^0:

$$T^{^0} = \pm\frac{1}{M}\sqrt{p_z^2 + 2\nu qB}\,. \tag{3.27}$$

The eigenfunctions are now given by the Harmonic oscillator functions which can be expressed by the Hermite polynomials. For the exact solutions, which are not of interest here, see [59] or [41].

Rewriting the original Hamiltonian in terms of the auxiliary operator allows us to compute the eigenvalues of the original problem.

$$\hat{H} = M\begin{pmatrix} I_2 & \hat{\tau}^0 \\ \hat{\tau}^0 & -I_2 \end{pmatrix}, \tag{3.28}$$

where I_2 is the 2×2 identity matrix. Since we already know the eigenvalues of $\hat{\tau}^0$ we obtain an algebraic system of equations for the desired eigenvalues p_0.

$$M\left[\begin{pmatrix} I_2 & 0 \\ 0 & -I_2 \end{pmatrix} + T^0\begin{pmatrix} 0 & I_2 \\ I_2 & 0 \end{pmatrix}\right]\begin{pmatrix} F(\xi) \\ \kappa F(\xi) \end{pmatrix} = p_0\begin{pmatrix} F(\xi) \\ \kappa F(\xi) \end{pmatrix}. \tag{3.29}$$

The solutions for p_0 finally turn out to be

$$p_0 = \epsilon_{k,\nu} = \pm\sqrt{p_z^2 + M^2 + 2\nu qB}\,. \tag{3.30}$$

We see that, compared to the B-independent dispersion relation $\epsilon_k = \sqrt{k^2 + M^2}$, only the momentum parallel to the magnetic field enters the relation. The perpendicular momentum is replaced by the discrete, quantized Landau levels. The Landau effect is a quantum mechanical effect which restricts the motion of a charged particle perpendicular to a magnetic field to quantized levels. Already at the classical level, a charged particle spirals around the magnetic field lines, in a quantum mechanical description these motion is now quantized, see Fig. 3.2. This effect can be seen in De-Haas-van-Alphen oscillations and is very well known in condensed matter physics for instance. The degeneracy of each level, i.e. the number of electrons that can populate a certain level, as well the level spacing depends on the magnetic field. If the field rises, more and more particles of the highest level drop into the energetic preferable lower level, which can contain more particles due to the larger field. At one point, all the particles have leaved the former highest level and the Fermi sphere becomes efficiently smaller. These successive clearance of the levels can be seen in various physical observables, for instance the baryon density at fixed chemical potential, see Fig. 3.1, or the magnetic susceptibility in condensed matter. If the magnetic field is high enough, all particles can be found in the ground state, $\nu = 0$, which is called the lowest Landau level (LLL), and the oscillations stop.

The momentum integral of the components parallel to the field has to be replaced by a discrete sum. Following Ref. ([41]), we confine our particle into a box with Volume $V = L_x L_y L_z$, assume periodic boundary conditions and write down the general expression for the free energy density,

$$\begin{aligned} \Omega &= -\frac{T}{V}\mathrm{Tr}\ln\frac{-i\omega_n + \mu - \epsilon}{T}, \\ &= -\frac{T}{L_x L_y L_z}\mathrm{Tr}\ln\frac{-i\omega_n + \mu - \epsilon}{T}, \end{aligned} \tag{3.31}$$

with the fermionic Matsubara frequencies ω_n and some suitable spectral decomposition ϵ of the Dirac Hamiltonian. For a particle in a box the spacing between two states in momentum space is

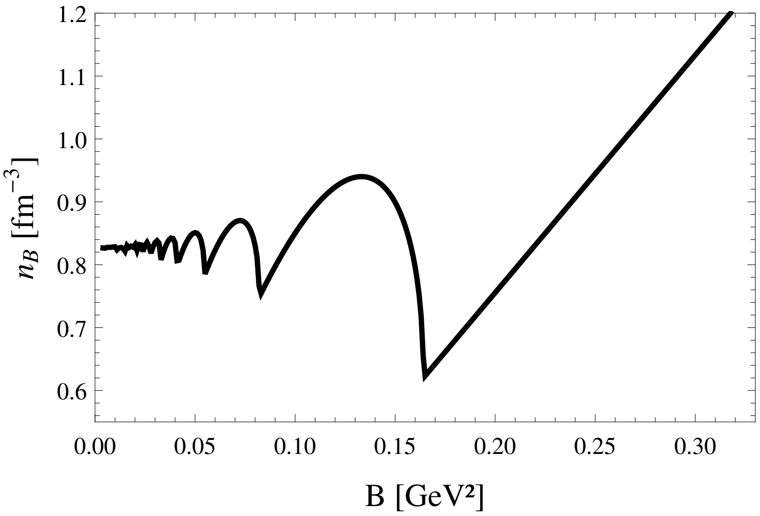

Figure 3.1: Baryon density of a free fermionic field at fixed chemical potential as a function of the magnetic field. The density shows the successive occupation of the Landau levels, called De-Haas-van-Alphen oscillations . Around 0.16 GeV^2, the magnetic field is high enough such that only the lowest Landau level (LLL) is occupied and the oscillations stop.

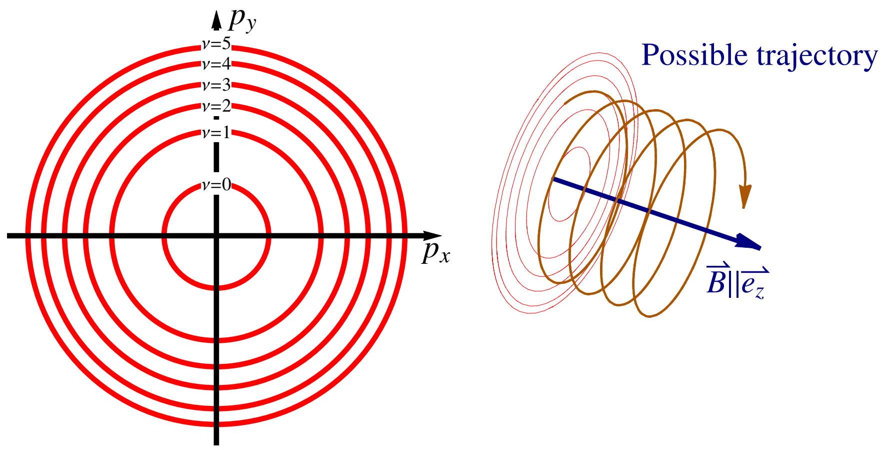

Figure 3.2: Due to the Landau level structure the energy levels perpendicular to the magnetic field, denoted by ν where $\nu = 0$ is the lowest Landau level (LLL), are discrete and quantized, which leads to the allowed particle trajectories in the right figure.

given by $\Delta k_i = \frac{2\pi}{L_i}$. Without magnetic field we replace $1/V$ with $\frac{\Delta k_x \Delta k_y \Delta k_z}{(2\pi)^3}$, which leads in the thermodynamic limit $V \to \infty$to the standard momentum integral $\int \frac{d^3\boldsymbol{k}}{(2\pi)^3}$. In the presence of a magnetic field the same can still be done for the unaffected momentum in z-direction. The momentum orthogonal to the field is replaced by the contribution of the Landau levels, so the trace has to be calculated as the sum over all Landau levels. In this case, each level is degenerated. In order to calculate the correct degeneracy factor we remember the variable transformation we performed in solving the Dirac equation, $\xi = \sqrt{qB}\left(x + \frac{k_y}{qB}\right)$. The extremal values of the momentum k_y can be found at $\xi = 0$, where x is restricted to $[0, L_x]$, so $k_{y,max} - k_{y,min} = L_x qB$. Since $\Delta k_y = \frac{2\pi}{L_y}$ is still valid and $\frac{k_{y,max} - k_{y,min}}{\Delta k_y} = L_x L_y qB/2\pi$, each energy level for a given k_z and ν is degenerated by a factor of $L_x L_y qB/2\pi$. Performing the transformation for k_z as before and taking the spin degeneracy α_ν, which we will calculate later, into account yields

$$\begin{aligned}\Omega &= -T \int \frac{dk_z}{2\pi} \sum_{\nu=0}^{\infty} \frac{L_x L_y}{L_x L_y} \frac{qB}{2\pi} \alpha_\nu \ln\left(\frac{-i\omega_n + \mu - \epsilon}{T}\right), \\ &= -T \int \frac{dk_z}{2\pi} \sum_{\nu=0}^{\infty} \frac{qB}{2\pi} \alpha_\nu \ln\left(\frac{-i\omega_n + \mu - \epsilon}{T}\right).\end{aligned} \tag{3.32}$$

If we compare this result to the non interacting one we can read off the replacement rule for the integral, which we will use from now on instead of performing all calculations bottom up:

$$2\int \frac{d^3\boldsymbol{k}}{(2\pi)^3} \to \frac{qB}{4\pi^2} \sum_{\nu=0}^{\infty} \alpha_\nu \int_{-\infty}^{\infty} dk_z\,, \tag{3.33}$$

where $\alpha_\nu = 2 - \delta_{\nu,0}$ is the spin degeneracy factor, which corresponds to the spin degeneracy factor 2 on the left hand side. One can see that all levels are occupied twice with exception of the LLL which is a spin singlet state. This can be read off from the spinor structure of the solution of the Dirac equation, see Ref. ([41]), Eq. (24). Two of the four components are proportional to the transition amplitude $\langle \xi | \nu - 1 \rangle$, the other two are proportional to $\langle \xi | \nu \rangle$. Since $\langle \xi | -1 \rangle = 0$ vanishes we see that for $\nu = 0$, i.e. the LLL, two of the four components are zero, so only one spin state is occupied.

Now we have all the ingredients to calculate the finite matter contribution of the charged particles. We simply use the replacement rules calculated above and insert it into the first line of Eq. (3.5). We apply the $T \to 0$ approximation as before and end up with another analytical solvable integral. Note that we changed the lower limit of integration to 0 where we use the symmetry of the integral, which yields an additional factor of 2 in the integrand.

$$\begin{aligned}\Omega_{N,mat} &= -\sum_{e=\pm 1} \frac{qBT}{2\pi^2} \sum_{\nu=0}^{\infty} \alpha_\nu \int_0^{\infty} dk_z \ln\left(1 + e^{-\frac{\epsilon_{k,\nu} - e\mu_*}{T}}\right), \\ &\overset{T=0}{\longrightarrow} \frac{qB}{4\pi^2} \Theta\left(\mu_* - M\right) \sum_{\nu=0}^{\nu_{max}} \alpha_\nu \int_0^{k_{F,\nu}} dk_z\, \left(\epsilon_{k,\nu} - \mu_*\right), \\ &= -\frac{qB}{4\pi^2} \Theta\left(\mu_* - M\right) \sum_{\nu=0}^{\nu_{max}} \alpha_\nu \left[\mu_* k_{F,\nu} - \left(M^2 + 2\nu qB\right) \ln \frac{k_{F,\nu} + \mu_*}{\sqrt{M^2 + 2\nu qB}}\right].\end{aligned} \tag{3.34}$$

In the second line the new B-dependent Fermi momentum in z-direction as well an upper limit of the Landau sum occur due to the theta function $\Theta\left(\mu_* - \epsilon_{k,\nu}\right)$. In order to see this, we take a closer look at the argument. The boundary of the integral is equal to the zero of the theta function,

$\mu_* - \sqrt{k_z^2 + M^2 + 2\nu qB} = 0$. Solving for k_z yields the new Fermi momentum dependent of the Landau level index ν,

$$k_{F,\nu} \equiv \sqrt{\mu_*^2 - (M^2 + 2\nu qB)} \tag{3.35}$$

For a given value of μ_*, the highest value for ν can be found for vanishing momentum, so ν_{max} is given by

$$\nu_{max} \equiv \frac{\mu_*^2 - M^2}{2qB} \,. \tag{3.36}$$

From this formula one can directly read of the condition for the validity of the LLL-approximation by requiring the r.h.s of ν_{max} to be smaller than one,

$$2qB < \mu_*^2 - M^2 \,. \tag{3.37}$$

3.2 Renormalization[1]

Since we have calculated the finite part of the matter contribution we turn back to the infinite contribution arising due to the integral over the excitation energies. For uncharged particles or vanishing magnetic fields this renormalization procedure has been carried out in literature and found to only serve minor corrections to the equation of state [38]. In App. (B) it is shown that its contribution to the onset in the Walecka model is negligible too.

For charged fermions in the presence of background magnetic fields, many works in literature have discussed the renormalization of the free energy although it has, to our knowledge, never been applied to to a relativistic mean field model for nuclear matter. Although it can be found in literature[60], I will present it in some detail since there exist different results in the community. I will show that these results are related by a different choice of the renormalization scale ℓ.

In order to regularize the divergent integral

$$\Omega_{N,sea} = -\frac{qB}{4\pi^2}\sum_{\nu=0}^{\infty}\alpha_\nu \int_{-\infty}^{\infty} dk_z \epsilon_{k,\nu} \tag{3.38}$$

we use the proper time method (see [61]) that has been widely used in the related literature, see Refs. [8–10, 41, 43], where it has been shown that dimensional regularization leads to the same result in Refs[44, 48, 50, 60]. Normally, this part is referred to as the vacuum contribution. Since it is proportional to the effective mass M it depends implicitly on the chemical potential and the temperature. Therefore, it is no vacuum contribution in the strict sense and we will rather refer to it as a contribution of the charged Dirac sea, $\Omega_{N,sea}$. To summarize we have decomposed the nucleonic contribution of the free energy $\Omega_N\left(M\left(B,\mu,T\right),\mu,T\right)$ into a matter- and a sea contribution,

$$\Omega_N = \Omega_{N,mat} + \Omega_{N,sea} \,. \tag{3.39}$$

The sea contribution depends, as mentioned before, only implicitly on the chemical potential and the temperature, $\Omega_{N,sea} = \Omega_{N,sea}\left(M\left(B,\mu,T\right),0,0\right)$. This decomposition is somehow arbitrary, however, had we only subtracted the "pure" magnetized vacuum, $\Omega_{N,sea}\left(M\left(B,0,0\right),0,0\right)$, the matter contribution would still not have been finite.

In order to regularize the sea contribution we start with rewriting the integrand by using the

[1] This section is an expanded discussion of chapter III of our paper [51].

Schwinger representation,

$$\frac{1}{x^a} = \frac{1}{\Gamma(a)} \int\limits_0^\infty d\tau\, \tau^{a-1} e^{-\tau x} \,, \tag{3.40}$$

which is an exact relation and yields

$$\Omega_{N,sea} = -\frac{qB}{\Gamma\left(-\frac{1}{2}\right) 2\pi^2} \int d\tau\, \tau^{-3/2} e^{-\tau M^2} \sum_{\nu=0}^{\infty} \alpha_\nu e^{-2\nu qB\tau} \int\limits_0^\infty dk_z e^{-\tau k^2} \,. \tag{3.41}$$

Here we identified the square of the dispersion relation with $x = k_z^2 + M^2 + 2\nu qB$ and therefore obtain $a = -\frac{1}{2}$. The value of the gamma function $\Gamma(n) = \int_0^\infty dt\, t^{n-1} e^{-t}$ evaluated at $-\frac{1}{2}$ is given by $\Gamma\left(-\frac{1}{2}\right) = -2\sqrt{\pi}$, which leaves us with

$$\Omega_{N,sea} = \frac{qB}{(2\pi)^2 \sqrt{\pi}} \int d\tau\, \tau^{-3/2} e^{-\tau M^2} \sum_{\nu=0}^{\infty} \alpha_\nu e^{-2\nu qB\tau} \int\limits_0^\infty dk_z e^{-\tau k^2} \,. \tag{3.42}$$

The separated momentum integral is a Gauss integral that can be computed analytically, $\int_0^\infty dk_z e^{-\tau k^2} = \frac{\sqrt{\pi}}{2\sqrt{\tau}}$. The sum over the exponential of the magnetic field, i.e. the sum over all Landau levels, converges to the hyperbolic cotangent, $\sum_{\nu=0}^{\infty} \alpha_\nu e^{-2\nu qB\tau} = \coth(qB\tau)$,

$$\Omega_{N,sea} = \frac{qB}{8\pi^2} \int\limits_0^\infty \frac{d\tau}{\tau^2} e^{-\tau M^2} \coth(qB\tau) \,. \tag{3.43}$$

This integral is still divergent, therefore we replace the lower boundary by the inverse square of the ultraviolet momentum cutoff $\Lambda, \frac{1}{\Lambda^2}$ (this is done in order to keep the arguments of the exponential functions in Eq. (3.42) dimensionless, such that the Schwinger variable τ has to carry units of inverse energy squared, $[\tau] = \frac{1}{E^2}$). Applying the limit $\lim_{qB\to 0} qB \coth qB\tau = \frac{1}{\tau}$ allows us to calculate the $B = 0$ contribution,

$$\begin{aligned} \Omega_{N,sea}(qB=0) &= \frac{1}{8\pi^2} \int\limits_{1/\Lambda^2}^\infty \frac{d\tau}{\tau^3} e^{-\tau M^2} \,, \\ &= \frac{1}{16\pi^2} \left[e^{-M^2/\Lambda^2} \left(\Lambda^4 - M^2\Lambda^2\right) - M^4 \Gamma\left(0, -\frac{M^2}{\Lambda^2}\right) \right] \,, \end{aligned} \tag{3.44}$$

with the incomplete Gamma function $\Gamma(a,x) = \int_x^\infty t^{a-1} e^{-t}$. This term can alternatively be calculated by integrating the B-independent vacuum term from Eq. (3.4) using a direct momentum cutoff for the regularization, see appendix B. As a first guess it sounds reasonable that the divergence originates only from this pure vacuum contribution. However, if this integral is subtracted from the original one, the result is still divergent.

$$\frac{qB}{8\pi^2} \int\limits_{\frac{1}{\Lambda^2}}^\infty \frac{d\tau}{\tau^2} e^{-\tau M^2} \coth(qB\tau) - \frac{1}{8\pi^2} \int\limits_{1/\Lambda^2}^\infty \frac{d\tau}{\tau^3} e^{-\tau M^2} = \frac{(qB)^2}{8\pi^2} \int\limits_{\frac{qB}{\Lambda^2}}^\infty \frac{ds}{s^2} \left(\coth s - \frac{1}{s}\right) e^{-2sx} \,, \tag{3.45}$$

where we introduced the abbreviation $x \equiv \frac{M^2}{2qB}$. Additionally, we performed a simple substitution of the form $qB\tau \equiv s$, which changes the lower boundary of the integral to $\frac{qB}{\Lambda^2}$. The divergence is located at the lower boundary of the integral, consequently it is called an ultra violet (UV) divergence. The infrared (IR) region is fine since the integral is exponentially damped. The general way to proceed is to add and subtract an additional integrand in such a way that the difference of them becomes finite and we only have to use a cutoff for the newly added integrand. In order to locate the exact origin of the divergence we take a look at the series expansion of the latter integrand.

$$\frac{(qB)^2}{8\pi^2}\frac{1}{s^2}\left(\coth s-\frac{1}{s}\right)e^{-2sx}=\frac{(qB)^2}{12\pi^2}\left(\frac{1}{2s}-x\right)+\mathcal{O}(s)\,, \tag{3.46}$$

which is, in lowest order, identical to the series expansion of a simpler integrand,

$$\frac{(qB)^2}{8\pi^2}\frac{1}{3s}e^{-2sx}=\frac{(qB)^2}{12\pi^2}\left(\frac{1}{2s}-x\right)+\mathcal{O}(s)\,.$$

In contrast to the complicated integral over the hyperbolic cotangent, this function can be integrated analytically using the cutoff for the lower boundary:

$$\frac{(qB)^2}{8\pi^2}\int\limits_{\frac{qB}{\Lambda^2}}^{\infty}ds\,\frac{1}{3s}e^{-2sx}=\frac{(qB)^2}{24\pi^2}\Gamma\left(0,\frac{M^2}{\Lambda^2}\right)\,.$$

We are now going to add this integrand to the $qB=0$ contribution which still can be regularized per cutoff as shown before, and subtract it from the difference of both contributions in order to make this integral finite. This allows us to extend the boundaries to the complete interval $[0,\infty)$.

$$\Omega_{N,sea}=\frac{(qB)^2}{8\pi^2}\int\limits_{\frac{qB}{\Lambda^2}}^{\infty}\frac{ds}{s^2}\left(\frac{1}{s}+\frac{s}{3}\right)e^{-2sx}+\frac{(qB)^2}{8\pi^2}\int\limits_{0}^{\infty}\frac{ds}{s^2}\left(\coth s-\frac{1}{s}-\frac{s}{3}\right)e^{-2sx}\,. \tag{3.47}$$

It is possible to rewrite the second part, which is finite, in such a way that we can extract the integral definition of the Hurwitz zeta-function, $\Gamma(n)\zeta(n,s)=\int_0^\infty\frac{t^{n-1}e^{-st}}{1-e^{-t}}$ for $\Re n>1$. For this purpose we use the exponential form of the hyperbolic cotangent, $\coth(s)=\frac{e^x+e^{-x}}{e^x-e^{-x}}=\frac{1+e^{-2x}}{1-e^{-2x}}$.

$$\begin{aligned}\frac{(qB)^2}{8\pi^2}\int\limits_{0}^{\infty}\frac{ds}{s^2}\left(\coth s-\frac{1}{s}-\frac{s}{3}\right)e^{-2sx}&=\frac{(qB)^2}{8\pi^2}\int\limits_{0}^{\infty}\frac{ds}{s^2}\left(\frac{1+e^{-2s}}{1-e^{-2s}}-\frac{1}{s}-\frac{s}{3}\right)e^{-2xs}=\\ \frac{(qB)^2}{4\pi}\int\limits_{0}^{\infty}du\left(\frac{u^ce^{-xu}}{1-e^{-u}}+\frac{u^ce^{-u(1+x)}}{1-e^{-u}}-2u^{c-1}e^{-xu}-\frac{1}{6}u^{c+1}e^{-xu}\right)\,.\end{aligned} \tag{3.48}$$

In the last line the substitution $2s=u$ is made and the constant $c=-2$ is introduced in order to read off the special functions mentioned above. The first two expressions represent the Hurwitz zeta-function, the second two terms are simple gamma functions. For the moment we neglect that $\Re c<1$ and leave it general, so we end up with

$$\frac{(qB)^2}{4\pi}\left[\Gamma(c+1)\zeta(c+1,x)+\Gamma(c+1)\zeta(c+1,1+x)-2x^{-c}\Gamma(c)-\frac{1}{3}x^{-2-c}\Gamma(2+c)\right]\,. \tag{3.49}$$

If we perform a series expansion around $c=-2$, we recognize that all divergent terms cancel as expected, and that all terms higher than zeroth order, $\mathcal{O}\left(c^0\right)$, are proportional to $c+2$ and therefore vanish in the limit $c\to-2$. After some simplifications one arrives at

$$
\begin{aligned}
\Omega_{N,sea} &= \Omega_{N,sea}\left(qB=0\right) + \frac{(qB)^2}{24\pi^2}\Gamma\left(0,\frac{M^2}{\Lambda^2}\right) + \\
&\frac{(qB)^2}{24\pi^2}\left[1-3x^2+\ln x+6x^2\ln x-6\zeta^{'}(-1,x)-6\zeta^{'}(-1,1+x)\right] .
\end{aligned} \tag{3.50}
$$

The second term originates from the additional integral which rendered the difference of the $B-$dependent and independent part finite. The Hurwitz zeta-function can be related to the normal zeta-function with the help of the Digamma function $\psi=\frac{\Gamma'(x)}{\Gamma(x)}$ via $\zeta'(-1,1+x)=x\ln x+\zeta'(-1,x)$ and $\zeta'(-1,x)=\zeta'(-1)+\frac{x^2}{2}-\frac{x}{2}\left(1+\ln 2\pi\right)+\psi^{(-2)}\left(x\right)$. For this purpose the $n-$th derivative of the Digamma function $\psi^{(n)}$ hast to be analytically continued to negative values of n. Using these identities and the definition of the Glaisher constant $\ln A=\frac{1}{12}-\zeta'(-1)$ with the numerical value $A\approx 1.282$, we compute

$$
\begin{aligned}
\Omega_{N,sea} &= \Omega_{N,sea}\left(qB=0\right) + \frac{(qB)^2}{24\pi^2}\Gamma\left(0,\frac{M^2}{\Lambda^2}\right) \\
&- \frac{(qB)^2}{2\pi^2}\left[\frac{x^2}{4}\left(3-2\ln x\right)+\frac{x}{2}\left(\ln\frac{x}{2\pi}-1\right)+\psi^{(-2)}\left(x\right)-\ln A-\frac{\ln x}{12}\right] .
\end{aligned} \tag{3.51}
$$

Beside the B-independent contribution, there is another divergent contribution in the limit $\Lambda\to\infty$ originating in the incomplete Gamma function $\Gamma\left(0,\frac{M^2}{\Lambda^2}\right)$ of the additional integrand. This contribution must now be absorbed into a renormalized magnetic field B_r and electric charge q_r. In order to do so we remember that the complete free energy also contains a free field contribution $\frac{B^2}{2}$. At first we expand $\Gamma\left(0,\frac{M^2}{\Lambda^2}\right)$ for large values of the cutoff,

$$
\begin{aligned}
\Gamma\left(0,\frac{M^2}{\Lambda^2}\right) &= -\left(\gamma_E+\ln\frac{M^2}{\Lambda^2}\right)+\mathcal{O}\left(\frac{M^2}{\Lambda^2}\right) , \\
&= -\left(\gamma_E+\ln\frac{M^2}{\ell^2}+\ln\frac{\ell^2}{\Lambda^2}\right)+\mathcal{O}\left(\frac{M^2}{\Lambda^2}\right) ,
\end{aligned} \tag{3.52}
$$

with the Euler-Mascheroni constant $\gamma_E\approx 0.577$. In the second line we introduced the renormalization scale ℓ via the identity $\ln\frac{\ell}{\ell}=\ln 1=0$. This allows us to separate the infinite cutoff by the introduction of a finite, for the moment arbitrary energy scale ℓ.

The next step is to introduce the renormalized coupling $q^2=Z_q^{-1}q_r^2$ and the renormalized magnetic field $B^2=Z_qB_r^2$ such that the product of them remains invariant, $q_rB_r=qB$. If one chose

$$
Z_q = 1+\frac{q_r^2}{12\pi^2}\left(\gamma_E+\ln\frac{\ell^2}{\Lambda^2}\right) , \tag{3.53}
$$

one can show that all divergent terms get absorbed into the new renormalized field and charge. As noted before, we expand the divergent term and also take the free field term into account and finally switch to the renormalized quantities.

$$
\begin{aligned}
\frac{B^2}{2}+\frac{(qB)^2}{24\pi^2}\Gamma\left(0,\frac{M^2}{\Lambda^2}\right) &= \frac{B^2}{2}-\frac{(qB)^2}{24\pi^2}\left(\gamma_E+\ln\frac{M^2}{\ell^2}+\ln\frac{\ell^2}{\Lambda^2}\right) , \\
&= \frac{B_r^2}{2}\left[Z_q-\frac{q_r^2}{12\pi^2}\left(\gamma_E+\ln\frac{M^2}{\ell^2}+\ln\frac{\ell^2}{\Lambda^2}\right)\right] , \\
&= \frac{B_r^2}{2}\left[1+\frac{q_r^2}{12\pi^2}\left(\gamma_E+\ln\frac{\ell^2}{\Lambda^2}\right)-\frac{q_r^2}{12\pi^2}\left(\gamma_E+\ln\frac{M^2}{\ell^2}+\ln\frac{\ell^2}{\Lambda^2}\right)\right] , \\
&= \frac{B_r^2}{2}-\frac{(q_rB_r)^2}{24\pi^2}\ln\frac{M^2}{\ell^2} .
\end{aligned} \tag{3.54}
$$

Note that the free field term $\frac{B_r^2}{2}$ is the only one where the magnetic field does not enter in combination with the charge. Consequently, the sea-contribution together with the free field part now reads

$$\begin{aligned}\Omega_{N,sea}+\frac{B_r^2}{2} &= \Omega\left(qB=0\right)+\frac{B_r^2}{2}-\frac{\left(q_rB_r\right)^2}{24\pi^2}\ln\frac{M^2}{\ell^2} \qquad (3.55)\\ &-\frac{\left(q_rB_r\right)^2}{2\pi^2}\left[\frac{x^2}{4}\left(3-2\ln x\right)+\frac{x}{2}\left(\ln\frac{x}{2\pi}-1\right)+\psi^{(-2)}(x)-\ln A-\frac{\ln x}{12}\right],\\ &= \Omega\left(qB=0\right)+\frac{B_r^2}{2}-\frac{\left(q_rB_r\right)^2}{24\pi^2}\ln\frac{2q_rB_r}{\ell^2A^{12}}\\ &-\frac{\left(q_rB_r\right)^2}{2\pi^2}\left[\frac{x^2}{4}\left(3-2\ln x\right)+\frac{x}{2}\left(\ln\frac{x}{2\pi}-1\right)+\psi^{(-2)}(x)\right], \qquad (3.56)\end{aligned}$$

where only renormalized quantities appear. For simplicity I will sometimes omit the index r for the renormalized quantities, keep in mind that no unrenormalized quantities appear in our calculations from now on. We have written the result in two different ways to make the discussion about the choice of the renormalization scale ℓ more transparent. There seem to be two natural choices for ℓ. If we choose the nucleon mass,$\ell = M$, we read off the nonvanishing terms in the first line, while, if we choose the magnetic field as a scale,$\ell = \sqrt{2q_rB_r}/A^6 \simeq 0.318\sqrt{q_rB_r}|$, the second line shows that this choice corresponds to keeping only terms that depend on M (plus the free field term). The choice for ℓ matters for evaluating observables such as the magnetization or the pressure itself. It has been pointed out in Ref. [60] (see also Ref. [62]), that only for $\ell = M$ the vacuum pressure for small magnetic fields $x \gg 1$ is proportional to B_r^2, receiving its sole contribution from the free field term because all other contributions are of order B_r^4 and higher,

$$x \gg 1: \qquad \frac{x^2}{4}\left(3-2\ln x\right)+\frac{x}{2}\left(\ln\frac{x}{2\pi}-1\right)+\psi^{(-2)}(x)-\frac{\ln A^{12}x}{12}=\frac{1}{720x^2}-\frac{1}{5040x^4}+\ldots \qquad (3.57)$$

In the regime of strong magnetic fields, where the dynamical mass becomes very small compared to $\sqrt{2q_rB_r}|$, i.e. $x \ll 1$, the momentum typically exchanged in scattering processes and hence the renormalization scale will be dominated by the scale set by the magnetic field, not by the mass. Presumably, the physically most appropriate choice for the renormalization scale is thus a combination of the mass and the magnetic field, $\ell \sim \sqrt{M^2+2qB}$, such that for small B the scale is dominated by the mass and vice versa. For our purpose, however, it is only important to notice that ℓ is a scale at which we evaluate the final physical result after minimizing the free energy: when we take the derivative of the free energy with respect to the dynamical mass M , we do so at **fixed** ℓ; and, when we determine the onset of nuclear matter we compare the free energy of the vacuum with the free energy of nuclear matter at the same value of ℓ. Therefore, we do not have to specify the renormalization scale, and the terms independent of M , i.e. the first two terms in the second line of Eq. (3.56) play no role.

To end this section we recap the final result of the free energy for one charged and one uncharged type of a spin $\frac{1}{2}$ fermion with which we are going to proceed in the next chapters.

$$
\begin{aligned}
\Omega &= \frac{B_r^2}{2} + U + \Omega_{N,mat} + \Omega_{N,sea} \\
&= \frac{B_r^2}{2} + U - \frac{qB}{4\pi^2}\Theta\left(\mu_* - M\right)\sum_{\nu=0}^{\nu_{max}} \alpha_\nu \left[\mu_* k_{F,\nu} - \left(M^2 + 2\nu qB\right)\ln\frac{k_{F,\nu} + \mu_*}{\sqrt{M^2 + 2\nu qB}}\right] \\
&\quad - \frac{\Theta\left(\mu_* - M\right)}{8\pi^2}\left[\left(\frac{2}{3}k_F^3 - M^2 k_F\right)\mu_* + M^4 \ln\frac{k_F + \mu_*}{M}\right] - \frac{\left(q_r B_r\right)^2}{24\pi^2}\ln\frac{2q_r B_r}{\ell^2 A^{12}} \\
&\quad - \frac{\left(q_r B_r\right)^2}{2\pi^2}\left[\frac{x^2}{4}\left(3 - 2\ln x\right) + \frac{x}{2}\left(\ln\frac{x}{2\pi} - 1\right) + \psi^{(-2)}(x)\right] .
\end{aligned}
\tag{3.58}
$$

4 The Walecka Model

The Walecka Model is a phenomenological, relativistic, field theoretical model that seeks to describe infinite nuclear matter and was investigated in his original form by Johnson and Teller [63], Duerr [64], and J.D. Walecka and Serot in Refs. [20, 65]. Later it was extended to its current form by including scalar selfinteractions by Boguta and Bodmer [66]. It has been studied intensively with and without magnetic field and can be found in many standard text books on dense matter or quantum hydrodynamics, see for instance Chap. 4 of the book on compact stars from Normann Glendenning [38], which I will largely follow in the introductory part of this chapter, or [53]. Additionally, there is a review of this model by Walecka itself in his book, see Ref. [67], or in a shorter article, see Ref. [68]. The fundamental degrees of freedom of the model are nuclei and the strong interaction between them is described via the exchange of the scalar σ- meson and the vector ω- meson. The Lagrangian consists of three parts,

$$\mathcal{L} = \mathcal{L}_N + \mathcal{L}_{\sigma,\omega} + \mathcal{L}_I \,, \tag{4.1}$$

where the nucleonic Lagrangian in his standard form looks like

$$\mathcal{L}_N = \bar{\psi}\left(i\gamma^\mu D_\mu - m_N + \mu\gamma^0\right)\psi \,, \tag{4.2}$$

where the Dirac spinor ψ is given by $\psi = \begin{pmatrix} \psi_n \\ \psi_p \end{pmatrix}$ with the neutron and proton spinor ψ_n and ψ_p. The parameter m_N presents the constant mass of the nucleon in vacuum, $m_N = 939$ MeV. The magnetic field enters again via the covariant derivative $D_\mu = \partial_\mu - iqA_\mu$ with the potential $A^\mu = (0, 0, -Bx, 0)$, i.e. $\boldsymbol{B} = B\hat{e}_z$. Since we take charged protons and uncharged neutrons simultaneously into account, the charge q in the covariant derivative is actually a diagonal matrix in flavor space, given by $q = \mathrm{diag}(e, 0)$. We only consider isospin symmetric matter, i.e. the masses of the nucleons are degenerate, they enter with the same chemical potential and the coupling for neutrons and protons to the mesons is identical. Consequently the mass matrix and the matrix for the chemical potentials are proportional to the identity matrix in flavor space.

The requirement of the Lagrangian to be a Lorentz scalar does not uniquely determine the form of the nucleon-meson interaction. From experiments it is well known that the strong interaction is repulsive at short distances and obeys a long attractive tail. This behavior can be modeled by a Yukawa interaction of the form $g_\sigma\bar{\psi}\sigma\psi$. The interaction Lagrangian $\mathcal{L}_I$ therefore reads

$$\mathcal{L}_I = g_\sigma \sigma\bar{\psi}\psi - g_\omega\bar{\psi}\omega_\mu\gamma^\mu\psi \,, \tag{4.3}$$

where the scalar field couples to the baryon scalar density $n_s = \bar{\psi}\psi$ and the vector meson to the baryon density, $n_B = \bar{\psi}\gamma^\mu\psi$. An analysis of two nonrelativistic Dirac particles interacting via a Yukawa interaction shows that the underlying classical potential is given by $V = -g^2\frac{e^{-\mu r}}{r}$, with the coupling constant g and the mass of the particle μ. Combining the two contributions of the mesons leads to a potential of the following form:

$$V(r) = \frac{g_\omega^2}{4\pi}\frac{e^{-m_\omega r}}{r} - \frac{g_\sigma^2}{4\pi}\frac{e^{-m_\sigma r}}{r} \,. \tag{4.4}$$

For a suitable choice of the parameters g_ω, g_σ, m_ω, and m_σ, the potential takes the experimentally discovered form shown in Fig. 4.1a. The connection to the Yukawa interaction can be made plausible by evaluating the corresponding Feynman diagram obtained from the interaction vortex.

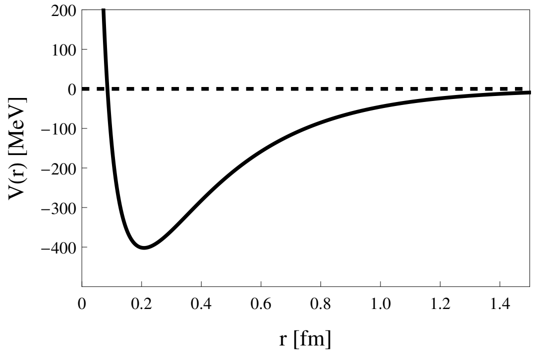

(a) Model of a nucleon-nucleon interaction obtained by two combined Yukawa potentials. For a suitable choice of the parameters, the model shows QCD like behavior; short range repulsion and long range attraction.

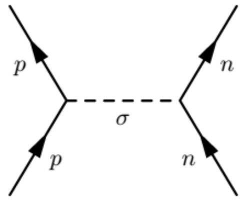

(b) Feynman diagram of the one meson exchange between two nucleons. The dashed line presents the exchanged boson, where the full lines present the in- and outgoing nucleons.

Figure 4.1

Working out the diagram for one boson is done as follows: the term $g_\sigma \bar{\psi}\sigma\psi$ can be drawn as two incoming nucleons, interacting via the exchange of the sigma meson, see right panel of Fig. 4.1a. The scattering amplitude of this diagram can be read of directly since each vertex contributes with a factor of the couplingig_σ, and the meson is incorporated by its propagator. For a massive boson neglecting scalar selfinteractions for the moment the propagator is given by $\frac{1}{k^2+m^2}$. It can be derived from the Fourier transformed equations of motion of the bosons. If we add up these contributions we obtain $V(k) = -g_\sigma^2 \frac{1}{k^2+m_\sigma^2}$. The Fourier transform of the classical Yukawa potential takes exactly the same form, $V(k) = -\frac{g_\sigma^2}{4\pi}\int d^3\boldsymbol{r}\, \frac{e^{-m_\sigma r}}{r} = -g_\sigma^2 \frac{1}{k^2+m_\sigma^2}$, which closes the connection.

The mesonic Lagrangian contains the mass and kinetic terms for both mesons as well scalar self interactions for the scalar meson that render the theory renormalizable.

$$\mathcal{L}_{\sigma,\omega} = \frac{1}{2}\left(\partial^\mu\sigma\partial_\mu\sigma - m_\sigma^2\sigma^2\right) - \frac{1}{4}\omega^{\mu\nu}\omega_{\mu\nu} + \frac{1}{2}m_\omega^2\omega^\mu\omega_\mu - \frac{b}{3}m_N\left(g_\sigma\sigma\right)^3 - \frac{c}{4}\left(g_\sigma\sigma\right)^4 , \tag{4.5}$$

where $\omega^{\mu\nu} \equiv \partial^\mu\omega^\nu - \partial^\nu\omega^\mu$ is the field strength tensor of the vector meson. The structure of the selfinteraction terms is chosen in such a way that the coupling constants b and c are dimensionless. The parameters of the models are the coupling constants g_σ and g_ω, the masses of the two mesons m_σ,m_ω and the nucleons m_N as well the coefficients of the scalar selfinteractions. The mass of the vector meson is rather well known and, following the particle data group (PDG, Ref. [69]), is given by approximately $m_\omega = 782$ MeV. The σ- meson is a rather broad resonance with a mass between $500 - 600$ MeV or even broader, we shall use a value of $m_\sigma = 550$ MeV. It is important to note that the vacuum nucleon mass is a fixed parameter of the model, it is not dynamically created by a chiral condensate. This means that the Walecka model can not describe chiral symmetry restoration, the chiral symmetry is always broken by definition. Therefore the scalar condensate can not be interpreted as the chiral condensate, because a vanishing expectation value for σ does not restore chiral symmetry like a vanishing chiral condensate is supposed to do. In the Walecka model σ is therefore a massive mode with mass m_σ in the chirally broken phase. The coupling constants will be fitted in order to reproduce experimental properties of nuclear matter at saturation later in this chapter.

As a first step we are going to calculate the equation of motions for all fields. The Euler Lagrange equations in quantum field theory are given by

$$\partial_\mu \frac{\partial \mathcal{L}}{\partial\left(\partial_\mu \phi\right)}-\frac{\partial \mathcal{L}}{\partial \phi}=0\,. \tag{4.6}$$

For the scalar meson the mesonic part of the Lagrangian is a simple free scalar field Lagrangian plus cubic and quartic interactions that yields the Klein-Gordon equation plus the derivatives of the self interaction terms, but becomes inhomogeneous due to the Yukawa interaction term. The right hand side is therefore not zero but given by the scalar density.

$$\left(\partial^\mu \partial_\mu+m_\sigma^2+b m_N g_\sigma^3 \sigma+c g_\sigma^4 \sigma^2\right) \sigma=g_\sigma \bar{\psi} \psi. \tag{4.7}$$

The equations for the vector meson can be taken from classical electromagnetism. The variation of the field strength tensor yields equations of the same form as the Maxwell equations, $-\partial_\mu \omega^{\mu\nu}=0$. The variation of the mass and the Yukawa term are straight forward, so we end up with

$$\begin{aligned} -\partial_\mu \omega^{\mu\nu}-m_\omega^2 \omega^\nu+g_\omega \bar{\psi} \gamma^\nu \psi &= 0\,, && (4.8)\\ \left(\partial^\mu \partial_\mu+m_\omega^2\right) \omega^\nu-\partial^\nu \partial_\mu \omega^\mu &= g_\omega \bar{\psi} \gamma^\nu \psi\,. && (4.9)\end{aligned}$$

The entire Lagrangian obeys a global $U(1)$ symmetry which corresponds to the baryon number conservation. The corresponding Noether current to this symmetry can be calculated by performing a local $U(1)$ transformation $\psi \rightarrow \psi^{\prime}=e^{i \alpha(x)} \psi$ and setting the variation of the new Lagrangian with respect to $\alpha(x)$ to zero. The result is given by the baryon current $j_\mu=\bar{\psi} \gamma_\mu \psi$ which is divergence-free, i.e. $\partial_\mu j^\mu=0$. Therefore, the r.h.s of Eq. (4.9) vanishes if one takes it divergence, so we obtain

$$\begin{aligned} \partial_\nu\left(\partial^\mu \partial_\mu+m_\omega^2\right) \omega^\nu-\partial_\nu \partial^\nu \partial_\mu \omega^\mu &= 0\,, \\ m_\omega^2 \partial_\nu \omega^\nu &= 0\,. && (4.10)\end{aligned}$$

This shows that the divergence of the ω field vanishes which means that we obtain an inhomogeneous Klein-Gordon equation for each component of the vector field, where the right hand side is given by the baryon current.

$$\left(\partial^\mu \partial_\mu+m_\omega^2\right) \omega^\nu=g_\omega \bar{\psi} \gamma^\nu \psi\,. \tag{4.11}$$

The last equation we have to calculate covers the nucleons, so we perform the variation with respect to $\bar{\psi}$ and calculate

$$\left[\gamma_\mu\left(i D^\mu-g_\omega \omega^\mu\right)-\left(m_N-g_\sigma \sigma\right)\right] \psi=0\,. \tag{4.12}$$

4.1 Mean Field Approximation

These three coupled differential equations of motion are rather difficult to solve. A common way to proceed is to apply a mean field approximation for the mesonic fields. As a first step we write the spacetime x dependent condensates as a sum of the mean field, i.e. a condensate or simply the expectation value of the field, which is uniform in space and time, and fluctuations around it.

$$\begin{aligned} \sigma(x) &\rightarrow \langle\sigma\rangle+\sigma(x)\,, && (4.13)\\ \omega_\mu(x) &\rightarrow \left\langle\omega_0 \delta_{0\mu}\right\rangle+\left\langle\omega_i \delta_{0i}\right\rangle+\omega_\mu(x)\,. && (4.14)\end{aligned}$$

For readability I will denote the condensates by $\bar{\sigma}$ respectively $\bar{\omega}_\mu$. The Kronecker delta $\delta_{\nu\mu}$ is used to carry over the Lorentz index structure. Since the fluctuations are proportional to the temperature we can neglect them in the mean field approximation due to the rather low temperatures in compact stars (compared to the nucleon masses or chemical potential). In the mean field Lagrangian all kinetic terms vanish,

$$\mathcal{L}_{\sigma,\omega} = -\frac{1}{2}m_\sigma^2\bar{\sigma}^2 + \frac{1}{2}m_\omega^2\bar{\omega}^\mu\bar{\omega}_\mu - \frac{b}{3}m_N\left(g_\sigma\bar{\sigma}\right)^3 - \frac{c}{4}\left(g_\sigma\bar{\sigma}\right)^4 , \tag{4.15}$$

$$\mathcal{L}_I = g_\sigma\bar{\sigma}\bar{\psi}\psi - g_\omega\bar{\psi}\bar{\omega}_0\gamma^0\psi - g_\omega\bar{\psi}\bar{\omega}_i\gamma^i\psi. \tag{4.16}$$

It is interesting to see that the scalar condensate now enters the Lagrangian like a mass term, since it is proportional to the square of the nucleonic field, $\bar{\psi}\psi$, and that the temporal component of the vector meson enters the Lagrangian like the zeroth component of a gauge field, i.e. like the chemical potential. Rearranging the terms in the total Lagrangian makes this conclusion even clearer:

$$\mathcal{L} = \bar{\psi}\left(i\gamma_\mu D^\mu - m_N + g_\sigma\bar{\sigma} + \gamma_0\left(\mu + g_\omega\bar{\omega}_0\right) + \gamma_i\bar{\omega}^i\right)\psi \tag{4.17}$$

$$-\frac{1}{2}m_\sigma^2\bar{\sigma}^2 - \frac{b}{3}m_N\left(g_\sigma\bar{\sigma}\right)^3 - \frac{c}{4}\left(g_\sigma\bar{\sigma}\right)^4 + \frac{1}{2}m_\omega^2\bar{\omega}^\mu\bar{\omega}_\mu . \tag{4.18}$$

We see that the $\bar{\sigma}$ condensate alters the mass whereas the $\bar{\omega}_0$ condensate reduces the chemical potential. This allows us to introduce the effective parameters mentioned before,

$$M_N = m_n - g_\sigma\bar{\sigma} , \tag{4.19}$$

$$\mu_* = \mu - g_\omega\bar{\omega}_0 . \tag{4.20}$$

In case of the vector meson one has to specify which components actually undergo condensation. In the absence of a magnetic field one can show that the spatial components do not form a condensate. On the one hand, this can be motivated physically: as long as there is no magnetic field the theory we are considering is isotropic, i.e. there is no preferred direction. A spatial condensate would render the theory unisotropic. On the mathematical side there are several ways to show that no anisotropic condensate is formed. The expectation value of the field can be calculated in two ways. The first one is to solve the equation of motions in the mean field approximation. The second approach is to search the state which minimizes the thermodynamic potential Ω, i.e. maximizes the pressure. In order to show that these approaches are equivalent, we remember that the pressure is given by the logarithm of the partition function,

$$\Omega = -T\ln Z . \tag{4.21}$$

The partition function is calculated via the path integral,

$$Z = \int \mathcal{D}\bar{\psi}\mathcal{D}\psi\mathcal{D}\sigma\mathcal{D}\omega \exp\int_X \mathcal{L} = \int \mathcal{D}\bar{\psi}\mathcal{D}\psi\mathcal{D}\sigma\mathcal{D}\omega \exp S , \tag{4.22}$$

where the action S is the spacetime integral over the Lagrangian density, $S = \int_X \mathcal{L}$. In thermal field theory, the imaginary time formalism is applied. This means that the temporal integral is actually performed over imaginary time $\tau = it$, which is associated with inverse temperature. This means the abbreviation $\int_X$ fully reads $\int d^4x = \int_0^\beta d\tau \int_{\mathbb{R}^3} d^3\boldsymbol{x}$ with the inverse temperature $\beta = \frac{1}{T}$. For an introduction to thermal quantum field theory read [58] or [52]. In the mean field approximation, the path integral over the mesonic fields is omitted. The extremal values of the potential are calculated by taking the derivative w.r.t. the condensate,

$$\frac{\partial \Omega}{\partial \bar{\sigma}} = -T \frac{1}{Z} \frac{\partial Z}{\partial \bar{\sigma}} = -T \frac{1}{Z} \int \mathcal{D}\bar{\psi}\mathcal{D}\psi \, \frac{\partial S}{\partial \bar{\sigma}} \exp S = -T \left\langle \frac{\partial S}{\partial \bar{\sigma}} \right\rangle \equiv 0 \,. \tag{4.23}$$

In the last line we used the definition of expectation values in thermodynamics. Since the variation of the action S w.r.t. the scalar condensate yields the EL-EOM in the mean field approximation, I have shown that these two methods are indeed equivalent. The mean field equations of motion, separated into temporal and spatial components, now read

$$\begin{aligned} \left(m_\sigma^2 + b m_N g_\sigma^3 \bar{\sigma} + c g_\sigma^4 \bar{\sigma}^2\right) \bar{\sigma} &= g_\sigma \left\langle \bar{\psi}\psi \right\rangle \,, \\ m_\omega^2 \bar{\omega}_0 &= g_\omega \left\langle \psi^\dagger \psi \right\rangle \,, \\ m_\omega^2 \bar{\omega}_i &= g_\omega \left\langle \bar{\psi}\gamma_i \psi \right\rangle \,, \end{aligned} \tag{4.24}$$

where we used $\bar{\psi} = \psi^\dagger \gamma_0$ and $\gamma_0^2 = 1$. In the first equation the scalar density $n_s = \left\langle \bar{\psi}\psi \right\rangle$ appears on the right hand side. In the second line, the expectation value of the number operator $N = \psi^\dagger \psi$ appears, which is known as the baryon density, $n_B = \left\langle \psi^\dagger \psi \right\rangle$. One way to show that there is indeed no spatial condensate is to calculate the ground state expectation value of the baryon three-current, what is done explicitly in chapter 4.6, p. 170 ff. of Ref. [38]. Another way is to show that the dispersion relation and therefore the pressure does not depend on the spatial components of the vector condensate. This can be seen rather directly. In the mean field approximation the partition function and therefore the pressure is calculated by the following path integral:

$$\begin{aligned} Z &= \int \mathcal{D}\bar{\psi}\mathcal{D}\psi \exp\left(\int_X \mathcal{L}\right) \,, \\ &= e^{\frac{V}{T}\left(-\frac{1}{2}m_\sigma^2\bar{\sigma}^2 + \frac{1}{2}m_\omega^2 \bar{\omega}^\mu \bar{\omega}_\mu\right)} \int \mathcal{D}\bar{\psi}\mathcal{D}\psi \exp\left(\int_X \bar{\psi}\left[i\gamma^\mu \partial_\mu - M_N + \mu^* \gamma_0 + g_\omega \bar{\omega}_i \gamma^i\right]\psi\right) \\ &= e^{\frac{V}{T}\left(-\frac{1}{2}m_\sigma^2\bar{\sigma}^2 + \frac{1}{2}m_\omega^2 \bar{\omega}^\mu \bar{\omega}_\mu\right)} \int \mathcal{D}\bar{\psi}\mathcal{D}\psi \exp\left(-\sum_K \bar{\psi}(K) \frac{G^{-1}(K)}{T} \psi(K)\right) \,. \end{aligned} \tag{4.25}$$

In the second line we pulled the constant condensates out of the path integral and performed the trivial spacetime integral. For the moment we have restricted our problem to a finite volume and will apply the thermodynamic limit $V \to \infty$ later on. Since we are going to work with the energy density the volume will drop out anyway. In the third line we inserted the discrete Fourier transformations of the nucleonic fields,

$$\psi(x) = \frac{1}{\sqrt{V}} \sum_K e^{-iKX} \psi(k), \qquad \bar{\psi}(x) = \frac{1}{\sqrt{V}} \sum_K e^{iKX} \bar{\psi}(k) \,. \tag{4.26}$$

where we use the conventions $K = (-i\omega_n, \boldsymbol{k})$, $X = (-i\tau, \boldsymbol{x})$ and $KX = k_0 x_0 - \boldsymbol{k} \cdot \boldsymbol{x}$ with the fermionic Matsubara frequencies $\omega_n = (2n+1)\pi T$. From the second respectively the third line we can read off the inverse propagator in momentum space,

$$G^{-1} = -\gamma^0 K^0 + \gamma_i K^i - \gamma_i \bar{\omega}^i - \mu^* \gamma^0 + M_N \,. \tag{4.27}$$

Here we see that one can redefine the three-momentum by adding the constant spatial components of the $\bar{\omega}$ condensate, $\tilde{k}^i \equiv k^i - g_\omega \bar{\omega}^i$. Path integrals of this forms are essentially integrals over

Grassman variables and obey the known solution

$$P = \frac{T}{V}\ln(Z) = -\tfrac{1}{2}m_\sigma^2\bar{\sigma}^2 - \tfrac{b}{3}m_N\left(g_\sigma\bar{\sigma}\right)^3 - \tfrac{c}{4}\left(g_\sigma\bar{\sigma}\right)^4 + \tfrac{1}{2}m_\omega^2\bar{\omega}_0^2 + \tfrac{1}{2}m_\omega^2\bar{\omega}^i\bar{\omega}_i + P_N\,. \tag{4.28}$$

The important step is to notice that the sum over all spatial momenta in the propagator turns into an integral over the whole $k-$space in the thermodynamic limit. Since we have absorbed the spatial components of the vector condensate into the shifted momenta $\tilde{k}^i$ and the integration measure $d^3\boldsymbol{k}$ is not affected by the constant shift, P_N does certainly not depend on $\bar{\omega}_i$ any more. If we now compute the derivative of the pressure with respect to $\bar{\omega}_i$, the only contribution arises from the former mass term in the Lagrangian,

$$0 \equiv \frac{\partial P}{\partial\bar{\omega}_i} = \frac{1}{2}m_\omega^2\bar{\omega}^i\,, \tag{4.29}$$

which implements directly

$$\bar{\omega}^i = 0\,. \tag{4.30}$$

In presence of a magnetic field the situation is less clear. The external magnetic field breaks the rotational invariance, so we introduce a preferred direction by hand and an anisotropic condensate is not excluded a priori. Mathematically it is possible to show that the dispersion relation and the pressure are still not affected by the $\bar{\omega}_i$ condensate. In order to do so we solve again the Dirac equation like in chapter 3.1 under consideration of the condensates. The equation then reads

$$\left(i\gamma_\mu\partial^\mu + q\gamma_i\left(A^i - \frac{g_\omega}{q}\bar{\omega}^i\right) - M_N\right)\psi = 0\,, \tag{4.31}$$

where we include the $\bar{\sigma}$ condensate in the effective mass M_N and the vector condensate in the shifted magnetic vector potential. The $\bar{\omega}_0$ condensate is included in the effective chemical potential which is again omitted in the Dirac equation. Already at this stage one can interpret the spatial condensate as a constant shift of the vector potential. The calculation can therefore be carried out in complete analogy to the case without condensates, where it is useful to define a new complex coordinate $\bar{x} = x - \frac{g_\omega}{\beta}\bar{\omega}_2 + \frac{g_\omega}{i\beta}\bar{\omega}_1$. The ladder operators are now given in terms of the slightly different variable $\xi = \sqrt{qB}\left(\bar{x} + \frac{p_y}{\beta}\right)$. From the former calculation we already know that only the spinors itself are altered by a coordinate change, not the dispersion relation. From this we can conclude again that the nucleonic pressure once again does not depend on $\bar{\omega}_i$, so the solely contribution arises again due to the former mass term, which leads again to $\bar{\omega}^i = 0$. On the physical side it is known that a constant magnetic field does not introduce a baryon current of the form $\langle\bar{\psi}\gamma_i\psi\rangle$, so our conclusions are consistent with the equation of motion for the anisotropic condensate since that means that the r.h.s in the last line of Eq. (4.24) vanishes too. The Lagrangian we are going to use in this thesis for the Walecka model from now on is therefore given by

$$\mathcal{L} = \bar{\psi}\left(i\gamma_\mu D^\mu - M_N + \gamma_0\mu_*\right)\psi - \frac{1}{2}m_\sigma^2\bar{\sigma}^2 - \frac{b}{3}m_N\left(g_\sigma\bar{\sigma}\right)^3 - \frac{c}{4}\left(g_\sigma\bar{\sigma}\right)^4 + \frac{1}{2}m_\omega^2\bar{\omega}_0^2\,. \tag{4.32}$$

From the Lagrangian we can read off the tree-level potential of the Walecka model,

$$U = \frac{1}{2}m_\sigma^2\bar{\sigma}^2 + \frac{b}{3}m_N\left(g_\sigma\bar{\sigma}\right)^3 + \frac{c}{4}\left(g_\sigma\bar{\sigma}\right)^4 - \frac{1}{2}m_\omega^2\bar{\omega}_o^2\,. \tag{4.33}$$

4.2 Self-consistency equations

The equations that determine the behavior of the condensates are obtained by maximizing the pressure, i.e. minimizing the thermodynamical potential Ω:

$$\frac{\partial\Omega}{\partial\bar{\sigma}} = 0\,, \qquad \frac{\partial\Omega}{\partial\bar{\omega}_0} = 0\,. \tag{4.34}$$

They are often called self-consistency equations, in analogy to calculations on superfluidity sometimes also gap equations. Starting from Eq. (3.58), we can collect all the contributions we need.

$$\frac{\partial\Omega}{\partial\bar{\sigma}} = \frac{\partial U}{\partial\bar{\sigma}} + \frac{\partial\Omega_{N,mat}}{\partial\bar{\sigma}} + \frac{\partial\Omega_{N,sea}}{\partial\bar{\sigma}}\,, \tag{4.35}$$

$$\frac{\partial\Omega}{\partial\bar{\omega}_0} = \frac{\partial U}{\partial\bar{\omega}_0} + \frac{\partial\Omega_{N,mat}}{\partial\bar{\omega}_0} + \frac{\partial\Omega_{N,sea}}{\partial\bar{\omega}_0}\,. \tag{4.36}$$

It does not matter if the $T \to 0$ approximation is applied before or after the momentum integration, so we already start with the zero temperature expressions for the free energy. The derivative of the tree-level potential is straight forward,

$$\frac{\partial U}{\partial\bar{\sigma}} = m_\sigma^2\bar{\sigma} + g_\sigma\left[bm_N\,(g_\sigma\bar{\sigma})^2 + c\,(g_\sigma\bar{\sigma})^3\right]\,. \tag{4.37}$$

For the other contributions we apply the chain rule twice in order to transfer a derivative w.r.t. $\bar{\sigma}$ at first to a derivative w.r.t. the effective mass M_N, $\frac{\partial}{\partial\bar{\sigma}} = \frac{\partial M}{\partial\bar{\sigma}}\frac{\partial}{\partial M} = -g_\sigma\frac{\partial}{\partial M}$ and finally, using the definition of $x \equiv \frac{M_N^2}{2qB}$, into a x-derivative, $\frac{\partial}{\partial\bar{\sigma}} = \frac{\partial M_N}{\partial\bar{\sigma}}\frac{\partial x}{\partial M_N}\frac{\partial}{\partial x} = -g_\sigma\frac{M_N}{qB}\frac{\partial}{\partial x}$.

$$\frac{\partial\Omega_{N,sea}}{\partial\bar{\sigma}} = g_\sigma\frac{M_N}{qB}\frac{\partial}{\partial x}\left\{\frac{(qB)^2}{24\pi^2}\ln\frac{2qB}{\ell^2A^{12}} + \right. \tag{4.38}$$

$$\left.\frac{(qB)^2}{2\pi^2}\left[\frac{x^2}{4}\left(3-2\ln x\right) + \frac{x}{2}\left(\ln\frac{x}{2\pi} - 1\right) + \psi^{(-2)}(x)\right]\right\}. \tag{4.39}$$

Since we perform this calculation at a fixed value of ℓ the first term vanishes and we obtain

$$\frac{\partial\Omega_{N,sea}}{\partial\bar{\sigma}} = g_\sigma\frac{qBM_N}{2\pi^2}\left[\frac{x}{2}\left(3-2\ln x\right) - \frac{x}{2} + \frac{1}{2}\left(\ln\frac{x}{2\pi} - 1\right) + \frac{1}{2} + \psi^{(-1)}(x)\right]\,,$$

$$= g_\sigma\frac{qBM_N}{2\pi^2}\left[x\left(1-\ln x\right) + \frac{1}{2}\ln\frac{x}{2\pi} + \psi^{(-1)}(x)\right]\,. \tag{4.40}$$

It is instructive to start all over again with the temperature dependent integral expressions of the free energy (Eq. (3.5)+Eq. (3.34)), where we already neglect the antiparticle states and sum up the contributions of protons and neutrons.

$$\Omega_{N,mat} = -\frac{qBT}{2\pi^2}\sum_{\nu=0}^{\infty}\alpha_\nu\int_0^\infty dk_z\ln\left(1+e^{-\frac{\epsilon_{k,\nu}-\mu_*}{T}}\right) - 2T\int_{-\infty}^{\infty}\frac{d^3\boldsymbol{k}}{(2\pi^3)}\ln\left(1+e^{-\frac{\epsilon_k-\mu_*}{T}}\right)\,. \tag{4.41}$$

In Eq. (4.24), we have seen that the variation of the Lagrangian includes the scalar respectively the baryon density $n_s = \langle\bar{\psi}\psi\rangle$ and $n_B = \langle\psi^\dagger\psi\rangle$. Since the left hand side of the equations is equivalent to the derivative of the tree-level potential U, the right hand side have to arise due to the contribution of the matter part of the free energy. Therefore we can draw the connection

$$n_s = \langle\bar{\psi}\psi\rangle = \frac{\partial\Omega_{N,mat}}{\partial M_N}\,, \qquad n_B = \langle\psi^\dagger\psi\rangle = \frac{\partial\Omega_{N,mat}}{\partial\mu_*}\,, \tag{4.42}$$

where we have divided by the negative of the coupling constants $-g_\sigma$ and $-g_\omega$. Especially the second definition is very intuitive since it also follows directly from the thermodynamic relation, $n = -\frac{\partial \Omega}{\partial \mu} = \frac{\partial P}{\partial \mu}$. Secondly, if one computes the derivative of the integral expression one obtains

$$n_B = \frac{\partial \Omega_{N,mat}}{\partial \mu_*} = \frac{qB}{2\pi}\sum_{\nu=0}^{\infty}\alpha_\nu \int_{-\infty}^{\infty}\frac{dk_z}{2\pi} f(\epsilon_{k,\nu}-\mu_*) + 2\int \frac{d^3\mathbf{k}}{(2\pi)^3} f(\epsilon_k - \mu_*)\,, \tag{4.43}$$

$$\xrightarrow{T=0} \Theta(\mu_* - M_N)\left(\frac{qB}{2\pi^2}\sum_{\nu=0}^{\nu_{\max}}\alpha_\nu k_{F,\nu} + \frac{k_F^3}{3\pi^2}\right). \tag{4.44}$$

We see that the baryon density is computed as the by the Fermi distribution function $f(x) = \frac{1}{e^{x/T}+1}$ weighted integral over all states which is exactly the definition of the particle density, as stated before. In the limit $T \to 0$, the Fermi distribution $f(x)$ becomes a step function $\Theta(x)$ which cuts off the integral and the sum over all Landau levels at the Fermi surface. The scalar density is calculated in analogy by

$$n_s = \frac{\partial \Omega_{N,\mathrm{mat}}}{\partial M_N} = \frac{qB}{2\pi}\sum_{\nu=0}^{\infty}\alpha_\nu \int_{-\infty}^{\infty}\frac{dk_z}{2\pi}\frac{M_N}{\epsilon_{k,\nu}} f(\epsilon_{k,\nu}-\mu_*) + 2\int \frac{d^3\mathbf{k}}{(2\pi)^3}\frac{M_N}{\epsilon_k} f(\epsilon_k - \mu_*)\,, \tag{4.45}$$

$$\xrightarrow{T=0} \Theta(\mu_* - M_N)\left[\frac{qBM_N}{2\pi^2}\sum_{\nu=0}^{\nu_{\max}}\alpha_\nu \ln\frac{\mu_* + k_{F,\nu}}{\sqrt{M_N^2 + 2\nu qB}} + \frac{M_N}{2\pi^2}\left(k_F\mu_* - M_N^2 \ln\frac{k_F + \mu_*}{M_N}\right)\right], \tag{4.46}$$

where the $T \to 0$ limit is obtained in the same way since the integrals can be solved analytically too.

Since the sea contribution does not depend on the vector condensate at all, the only other contribution is the trivial derivative of the tree-level potential, $\frac{\partial U}{\partial \bar{\omega}_0} = -m_\omega^2 \bar{\omega}_0$. To summarize, the complete set of equations read

$$n_s = \frac{m_\sigma^2 \bar{\sigma}}{g_\sigma} + b m_N (g_\sigma \bar{\sigma})^2 + c(g_\sigma\bar{\sigma})^3 + \frac{qBM_N}{2\pi^2}\left[x(1-\ln x) + \frac{1}{2}\ln\frac{x}{2\pi} + \ln\Gamma(x)\right], \tag{4.47}$$

$$n_B = \frac{m_\omega^2 \bar{\omega}_0}{g_\omega}. \tag{4.48}$$

Note that we used the definition of the Digamma function $\psi = \frac{\Gamma'(x)}{\Gamma(x)}$ in the first line to obtain $\psi^{(-1)} = \int dx\, \frac{\Gamma'(x)}{\Gamma(x)} = \ln\Gamma(x)$.

4.3 Parameter Fit

In order to use the model quantitatively, we have to assign numerical values to the four coupling constants g_σ, g_ω, b and c. The parameters are fitted in such a way that the model reproduces saturation properties of infinite nuclear matter at zero magnetic field. This fit procedure is described in all standard text books about dense matter, see for instance Refs. [38, 53, 58]

The pressure of the model as a function of the baryon density can be divided into two areas, one with positive and one with negative pressure. The point $P = 0$ separates the unstable part with negative pressure from the stable part of the theory. The density that corresponds to $P(n_B) = 0$ is called saturation density. At this density, matter can exist in equilibrium without any external pressure, coming for instance from gravity. The numerical value can be obtained for example from a droplet model [70], a liquid droplet model[71] or by electron scattering experiments[72, 73]. The broadly accepted value can be found in the standard literature [38, 53, 58] or in the nuclear data tables [74] and is given by $n_0 = 0.153$ fm^{-3}. The second value we require the model to reproduce is

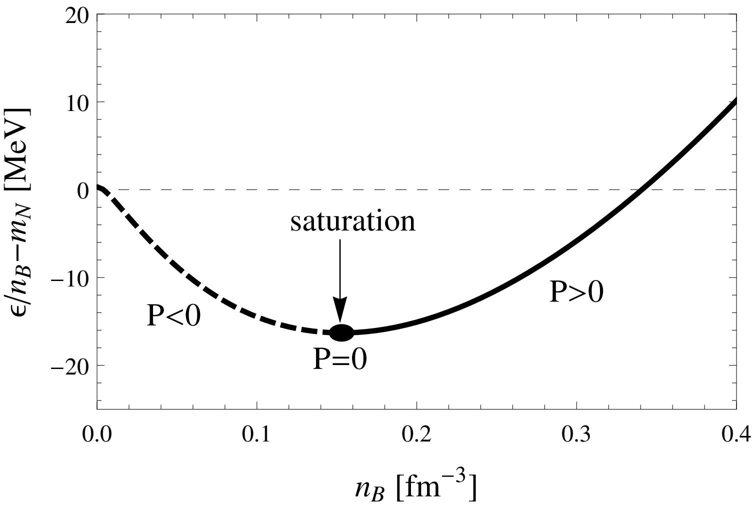

Figure 4.2: Binding energy per nucleon at $T = 0$ as a function of the baryon density. At a density of $n_B = 0.153\,\mathrm{fm}^{-3}$, the pressure is zero and the binding energy has a minimum fitted to $E_{bind} = -16.3$ MeV. At this point, called saturation density, nuclear matter is self bound, i.e. stable without any external pressure. The region to the left with negative pressure is actually unstable and therefore dashed.

the binding energy per nucleon of infinite nuclear matter. Of course this quantity is experimentally hard to access, however the total binding energy per nucleon of finite matter can be measured. This energy can be split into various contributions, namely a volume term, a surface term, a Coulomb term, an asymmetry and a pairing term. The underlying theory is the liquid drop model, the formula for the binding energy is known as the Bethe-Weiszäcker formula with the terms arranged in the same order as described above.

$$E_B = a_V A - a_S A^{2/3} - a_C \frac{Z^2}{A^{1/3}} - a_A \frac{(A-2Z)^2}{A} - \delta(A, Z)\,. \tag{4.49}$$

In this context we are able to specify what we actually mean with the expression dense nuclear matter: we are dealing with infinite, symmetric ($Z = A/2$), nuclear matter. In the limit $A \to \infty$, the surface term $-a_S \frac{1}{A^{1/3}}$ vanishes and we are left over with the volume contribution only. The Coulomb contribution does diverge, so we assume overall charge neutral matter. From a very general comparison of the electrostatic and the gravitational energy one can show that compact stars are indeed charge neutral [53]. However, we will neglect the influence of the electrons required for the charge neutrality in this thesis and leave this as a further project. From [38, 53, 58] we extract a value of $E_{bind} = \left(\frac{\varepsilon}{n_B} - m_N\right)|_{n_0} = -16.3$ MeV. Note that ε is the energy density of the system and not the single particle dispersion relation ϵ_k, defined via the thermodynamical relation $P = -\varepsilon + \mu n_B$. The critical potential at the onset of nuclear matter is the energy you need to add a nucleon to a bulk of nuclear matter and is, due to the interactions between the nucleons, lowered by the binding energy. Specifying the binding energy therefore also fixes the onset chemical potential at saturation,

$$\mu_0 = m_N + E_{bind} = 922.7\,\mathrm{MeV}\,. \tag{4.50}$$

We will use this relation later in this work in order to extract the behavior of the binding energy at the onset.

These two parameters also can be reproduced without scalar interactions. Beside renormalizability, the reproduction of the compression modulus K and the dynamical mass at saturation is another reason to introduce scalar self interactions. The compression modulus K is also known as the incompressibility. The incompressibility is a measure for the stiffness of nuclear matter. This means that "soft", i.e. easily compressible matter has a small change in the pressure upon changing the density. This can be seen using the thermodynamic relation $P = -\varepsilon + \mu n_B$ and the fact that ε/n_B hast a minimum at n_0, i.e. $\frac{\partial(\varepsilon/n_B)}{\partial n_B}|_{n_0} = 0$. This corresponds to soft equations of state, which means that soft systems are not able to withstand that high pressures like less softer systems, leading to a smaller maximum in the mass radius relations. It is defined by

$$K \equiv k_F^2 \frac{\partial^2 (\varepsilon/n_B)}{\partial k_F^2} \,. \tag{4.51}$$

Rewriting the Fermi momentum in terms of the density, $n_B = \frac{2}{3}k_F^3$ (the additional factor 2 arises due to the degeneration of protons and neutrons at $B = 0$), yields

$$K = 9 n_B \frac{\partial^2 \varepsilon}{\partial n_B^2} \,. \tag{4.52}$$

Calculating the first derivative with the help of $\varepsilon = \mu n_B - P$ gives $\frac{\partial \varepsilon}{\partial n_B}|_\mu = \mu - \frac{\partial \bar{\sigma}}{\partial n_B} \overbrace{\frac{\partial P}{\partial \bar{\sigma}}}^{=0} - \frac{\partial \bar{\omega}_0}{\partial n_B} \overbrace{\frac{\partial P}{\partial \bar{\omega}_0}}^{=0} - \overbrace{\frac{\partial P}{\partial n_B}}^{==}|_{\mu,\bar{\sigma},\bar{\omega}_0} = \mu = g_\omega \bar{\omega}_0 + \sqrt{k_F^2 + M_N^2}$, where we have used the self-consistency equations and the definition of $\mu_* = \mu - g_\omega \bar{\omega}_0 = \sqrt{k_F^2 + M_N^2}$. From the fact that the derivative $\partial_{n_B} \frac{\varepsilon}{n_B}$ vanishes at saturation one can show that $\frac{P}{n_B} = \frac{\partial P}{\partial n_B}|_{\mu,\bar{\sigma},\bar{\omega}_0}$. This expression is identical zero at saturation since the pressure at saturation is zero. As explained, the function $\frac{\varepsilon}{n_B}$ has a minimum at saturation. This can be used to obtain

$$0 \quad = \quad \frac{\partial}{\partial n_B}\frac{\varepsilon}{n_B} = \frac{1}{n_B}\left(\frac{\partial \varepsilon}{\partial n_B} - \frac{\varepsilon}{n_B}\right) , \qquad \to \qquad \frac{\varepsilon}{n_B} = \frac{\partial \varepsilon}{\partial n_B} = \mu \,. \tag{4.53}$$

$$\frac{\partial^2}{\partial n_B^2}\frac{\varepsilon}{n_B} \quad = \quad \frac{1}{n_B}\frac{\partial \mu}{\partial n_B} \,. \tag{4.54}$$

From these relations we can deduce $m_N + \frac{E_{bind}}{A} = \frac{\varepsilon}{n_B} = \bar{\omega}_0 g_\omega + \sqrt{k_F^2 + M_N^2} = \left(\frac{g_\omega}{m_\omega}\right)^2 n_B + \sqrt{k_F^2 + M_N^2}$, where we have used the field equation for the vector condensate in the form $n_B = \frac{m_\omega^2}{g_\omega}\bar{\omega}_0$. Altogether, we can write the compression modulus in the form of

$$K = 9 n_B \frac{\partial \mu}{\partial n_B} \,. \tag{4.55}$$

Inserting $\mu = \left(\frac{g_\omega}{m_\omega}\right)^2 n_B + \sqrt{k_F^2 + M_N^2}$ leads to

$$\frac{\partial \mu}{\partial n_B} = \left(\frac{g_\omega}{m_\omega}\right)^2 + \frac{1}{\mu_*}\left(k \frac{\partial k}{\partial n_B} - M g_\sigma \frac{\partial \bar{\sigma}}{\partial n_B}\right) \,. \tag{4.56}$$

At the end we invert the connection between the density and the Fermi momentum k_F, $k_F = \left(\frac{3}{2}n_B\right)^{1/3}$ and use the field equation for the $\bar{\sigma}$ condensate in the integral form. After some manip-

m_σ [MeV]	m_ω [MeV]	m_N [MeV]	g_ω	g_σ	b	c
550	782	939	8.1617	8.4264	8.7788×10^{-3}	6.8358×10^{-3}

K [MeV]	M_N	E_{bind} [MeV]	$n_0\,\mathrm{fm}^{-3}$
250	$0.8\,m_N$	-16.3	0.153

Table 4.1: Set of all parameters used in the Walecka model, including the fitted coupling constants, the mass parameters of the Lagrangian and the saturation properties of nuclear matter we use for fitting the coupling constants.

ulation we end up with

$$K = \frac{6k_F^3}{\pi^2}\left(\frac{g_\omega}{m_\omega}\right)^2 + \frac{3k_F^2}{\mu_*} - \frac{6k_F^3}{\pi^2}\left(\frac{M_N}{\mu_*}\right)^2 \left[\frac{\partial^2 U}{\partial M_N^2} + \frac{2}{\pi^2}\int_0^{k_F} dk \frac{k^4}{\epsilon_k^3}\right]^{-1} . \tag{4.57}$$

The value for the incompressibility is uncertain and there exist several numbers ranging from $200-300$ MeV [75, 76]. For the following I will assume a value of $K = 250$ MeV. The last saturation property we need to reproduce is the effective mass at the onset at saturation density, where I will assume a value of $M_N = 0.8m_N$. This value also comes with a big uncertainty, ranging from $(0.7-0.8)\,m_N$ [38, 39, 77, 78] or even smaller [79, 80]. However, we have chosen a value on the upper end of the range because lower values tend to be in conflict with vacuum properties in the eLSM, see appendix A in [51] or App. (D).

Finally, we are able to compute the numerical values for the coupling constants. From $n_B = \frac{2}{3}k_F^3$ we know the value of the Fermi momentum at saturation, $k_{F,0} = 259.148$ MeV. Since we demand that $\mu = 922.7$ at the onset and we require $M_N = 0.8m_N$, we can deduce directly the value of $g_\omega \bar{\omega}_0 = \mu - \sqrt{k_F^2 - M_N^2} = 921.905$ MeV. Inserting this into the equation of motion allows us to calculate $g_\omega = \sqrt{g_\omega \bar{\omega}_0 m_\omega^2 / n_0} = 8.1617$. Now we are left with the following set of equations:

$$\begin{aligned} P(n_0) &= 0\,, \\ K &= 250\,\mathrm{MeV}\,, \\ \frac{\partial P}{\partial \bar{\sigma}}|_{n_0} &= 0\,, \\ M_N &= 0.8m_N\,. \end{aligned} \tag{4.58}$$

These four equations allow us to determine the values of the four unknowns left, g_σ,b, c and $\bar{\sigma}$ at the onset at saturation which is of no particular interest for us. The result of the calculation an the summary of all parameters used until now can be found in Tab. 4.1.

5 Extended Linear Sigma Model (eLSM)

Before I will present the results of our calculations, I will introduce another model in order to show that magnetic catalysis is indeed a general, model independent, phenomenon in nuclear matter which can be incorporated using correct renormalization. Additionally, one gains some insight which ingredients of our theory influence the onset the most.

The extended linear sigma model, sometimes also called the parity doublet model, is a state of the art effective chiral model and has been used recently to calculate vacuum properties of QCD [26, 27], saturation densities of dense and cold nuclear matter [25] and anisotropic chiral phase transitions, so called chiral density waves [81].

As explained earlier, an explicit nucleon mass term $\sim \bar{\psi} m_N \psi$ breaks chiral symmetry explicitly and can not be incorporated into such a chiral invariant model. In the standard linear sigma model, the mass of the nucleon is therefore to the biggest part created by the chiral condensate [82, 83]. However, it is possible that also other condensates, like a gluon condenste, sometimes called "glueball" [84], or a tetraquark [26] condensate, contribute significantly to the nucleon mass. Furthermore, it is known that the standard linear sigma model can not reproduce stable nuclear matter properties. If the mass is generated solely by the chiral condensate, the linear sigma model can not represent saturated nuclear matter, neither can the chiral phase transition be described correctly [25]. These issues can be resolved by introducing a chiral invariant mass term m_0, which does not originate in the chiral condensate. In order to do so, a chiral partner of the nucleon is introduced via the mirror assignment, which was first discussed in Ref. [82]. As a natural choice for the chiral partner of the nucleon, the lightest stable state with the correct quantum numbers $J^P = \frac{1}{2}^-$ listed by the PDG [69] is used, $N(1535)$. In order to explain the mirror assignment one has to note that the chiral partner carries opposite parity. This leads to a different transformation under chiral rotations. If we introduce the two baryonic fields ψ_1 and ψ_2 as part of the bispinor $\Psi = (\psi_1, \psi_2)^T$, both of them being a bispinor in isospin space itself, the two components transform oppositely under chiral rotations. The right and left components of ψ_1 transform "correctly", i.e. with the transformation U_R respectively U_L, but the components of ψ_2 transform in the opposite way,

$$\psi_{1R} \to U_R \psi_{1R},\, \psi_{1L} \to U_L \psi_{1L},\, \psi_{2R} \to U_L \psi_{2R},\, \psi_{2L} \to U_L \psi_{2L}\,. \tag{5.1}$$

This behavior allows us to introduce a mass term m_0 in the Lagrangian that indeed does preserve chiral symmetry,

$$\mathcal{L}_{m_0} = -m_0 \left(\bar{\psi}_{1L}\psi_{2R} - \bar{\psi}_{1R}\psi_{2L} - \bar{\psi}_{2L}\psi_{1R} - \bar{\psi}_{2R}\psi_{1L} \right)\,. \tag{5.2}$$

Using the fact that $U_L U_R = U_R U_L = \mathbf{1}$ and that complex conjugation and transposition leads to a change in the ordering of the rotation matrix U and the spinor ψ, as well turns U_L to U_R and vice versa, e.g. $\overline{(U_L \psi_{1L})} = \bar{\psi}_{1L} U_R$, one can show that each term conserves chiral symmetry separately.

$$\bar{\psi}_{1L}\psi_{2R} \to \overline{(U_L\psi_{1L})} U_L \psi_{2R} = \bar{\psi}_{1L} U_R U_L \psi_{2R} = \bar{\psi}_{1L}\psi_{2R}\,, \tag{5.3}$$

and similar for the other three terms. This mass term can be rewritten with the help of the chiral projectors presented in Sec. 2. Studying the first two terms unveils the general principle: $\bar{\psi}_{1L}\psi_{2R} - \bar{\psi}_{1R}\psi_{2L} = \bar{\psi}_1 P_R P_R \psi_2 - \bar{\psi}_1 P_L P_L \psi_2 = \bar{\psi}_1 P_R \psi_2 - \bar{\psi}_1 P_L \psi_2 = \frac{1}{2}\bar{\psi}_1 \left[(1+\gamma_5) - (1-\gamma_5)\right]\psi_2 = \bar{\psi}_1 \gamma_5 \psi_2$. Performing the same calculation for the other terms yields

$$\mathcal{L}_{m_0} = -m_0 \left(\bar{\psi}_1 \gamma_5 \psi_2 - \bar{\psi}_2 \gamma_5 \psi_1 \right)\,. \tag{5.4}$$

The complete chiral symmetric Lagrangian can be found for instance in Ref. [26], Eq. (4) or in far more detail in Ref. [85]. In this Lagrangian many other mesons, like the ρ-meson, are included. However, since we work again in the mean field approximation we only keep the contributions of the mesons which acquire a non zero expectation value, i.e. σ, ω and the tetraquark field χ; for the pion, parity conservation demands $\boldsymbol{\pi} = 0$. The effective Lagrangian of the model in the form we use it can be found in [26, 27, 51] and can be decomposed in a nucleonic, a mesonic and an interaction term,

$$\mathcal{L} = \mathcal{L}_N + \mathcal{L}_{mes} + \mathcal{L}_I \, . \tag{5.5}$$

The nucleonic sector reads

$$\mathcal{L}_N = \bar{\Psi} \left(i\gamma_\mu D^\mu + \gamma^0 \mu \right) \Psi \, , \tag{5.6}$$

where the magnetic field enters again via the covariant derivative D^μ. Remember that Ψ denotes the bispinor in mirror space, in which the Dirac operator $i\gamma_\mu D^\mu + \gamma^0\mu$ is diagonal. The relevant mesonic part is given by

$$\mathcal{L}_{\text{mes}} = \frac{1}{2}\partial_\mu\sigma\partial^\mu\sigma + \frac{1}{2}m^2\sigma^2 + \epsilon\sigma - \frac{\lambda}{4}\sigma^4 - \frac{1}{4}\omega_{\mu\nu}\omega^{\mu\nu} + \frac{1}{2}m_\omega^2\omega_\mu\omega^\mu + \frac{1}{2}(\partial_\mu\chi\partial^\mu\chi - m_\chi^2\chi^2) + g\chi\sigma^2 \, . \tag{5.7}$$

The term linear in σ models the explicit chiral symmetry breaking by small, nonvanishing quark masses in QCD and renders the chiral symmetry an approximate symmetry in the eLSM. This can be seen by taking the derivative of the Lagrangian w.r.t. to σ, where the zero solution is nonexistent due to the then constant term ϵ. Whereas the ω meson is, like in the Walecka model, identified with the resonance $\omega(782)$, there are, according to Ref. [26], two possible choices for the σ-meson: the resonances $f_0(500)$ and $f_0(1370)$. Note that in the original paper cited before, Ref. [26], $f_0(600)$ is used. This deviation can easily be explained; shortly after the publication of the mentioned paper the particle was renamed by the PDG to $f_0(500)$ since its mass actually seems to be lower[69]. The first assignment seems to be unfavored for the description of QCD vacuum properties, so the σ field has another meaning than before [86]. Especially, the parameter m has the wrong sign to model chiral symmetry breaking. It is important to note that the σ and the χ field are mixed due to the interaction term $g\chi\sigma^2$ and can therefore not considered to present physical particles. This issue will be solved in the next section.

The last part of the Lagrangian of the eLSM covers the interactions between the nucleonic fields and the mesons and is given as a matrix in mirror space,

$$\mathcal{L}_I = \bar{\Psi} \begin{pmatrix} -\frac{\hat{g}_1\sigma}{2} - g_\omega\gamma_\mu\omega^\mu & a\chi\gamma^5 \\ -a\chi\gamma^5 & -\frac{\hat{g}_2\sigma}{2} - g_\omega\gamma_\mu\omega^\mu \end{pmatrix} \Psi \, . \tag{5.8}$$

The off-diagonal components give raise to the chiral invariant mass term, where the mass is generated dynamically by the tetraquark condensate. This means that we neglect the influence of the glueball condensate $\bar{G}$ in $m_0 = a\bar{\chi} + b\bar{G}$ in accordance with Ref. [26]. Like in the mesonic sector, the fields ψ_1 and ψ_2 are mixed due to the off-diagonal components in the interaction Lagrangian. Since there is no explicit mass term we can calculate the physical masses from the matrix that couples the fields $\bar{\Psi}$ and Ψ, where we have to apply the mean field approximation at first. Effectively, we are searching the eigenvalues of the energy operator $i\partial_t$ at vanishing three momentum $\mathbf{k}$, which corresponds to the spatial derivative in position space. Since the time derivative in the Dirac operator is multiplied by γ_0, we are actually looking for the eigenvalues of the matrix

$$\gamma_0 M = \begin{pmatrix} -\frac{\hat{g}_1\bar{\sigma}}{2}\gamma_0 & a\bar{\chi}\gamma^5\gamma_0 \\ -a\bar{\chi}\gamma^5\gamma_0 & -\frac{\hat{g}_2\bar{\sigma}}{2}\gamma_0 \end{pmatrix} , \tag{5.9}$$

which are the effective masses of the nucleon and its chiral partner.

$$m_{N,N^*} = \pm\frac{\hat{g}_1 - \hat{g}_2}{4}\bar{\sigma} + \sqrt{(a\bar{\chi})^2 + \left(\frac{\hat{g}_1 + \hat{g}_2}{4}\right)^2 \bar{\sigma}^2}\,. \tag{5.10}$$

Another standard way to obtain this result is to calculate the full inverse propagator in momentum space G^{-1}, obtained by a Fourier transformation of the Dirac fields. In the absence of a magnetic field, the determinant of the propagator in momentum space is

$$\begin{aligned}\det G^{-1} \;=\; &\Big\{(a\bar{\chi})^4 - 2(a\bar{\chi})^2\left[(k_0+\mu_*)^2 - \left(k^2 + m_1 m_2\right)\right] \\ &+ \left[(k_0+\mu_*)^2 - \left(k^2+m_1^2\right)\right]\left[(k_0+\mu_*)^2 - \left(k^2+m_2^2\right)\right]\Big\}^2 ,\end{aligned} \tag{5.11}$$

where we have abbreviated $m_1 \equiv \hat{g}_1\bar{\sigma}/2$, $m_2 \equiv \hat{g}_2\bar{\sigma}/2$. Since the vector meson enters the Lagrangian in the same way as in the Walecka model the definition of the effective chemical potential $\mu_* = \mu - g_\omega\bar{\omega}$ is unchanged. The zeros of the determinant are $\epsilon_{k,i} - \mu_*$ with the excitation energies $\epsilon_{k,i} = \sqrt{k^2 + M_i^2}$, where the index i distinguishes between the nucleon and its chiral partner, $i = N, N^*$, which leads to the same masses as presented before. The degeneracy of the two masses is broken due to the appearance of the chiral condensate $\bar{\sigma}$. This is in contrast to the standard linear sigma model, the naive assignment and the mirror assignment without chiral invariant mass term, i.e. $m_0 = 0$. In these three cases, the nucleon mass is entirely created by the chiral condensate [25]. For the sake of completeness, I write down the transformation matrix connecting the fields occurring in the Lagrangian, ψ_1 and ψ_2, to the physical fields N^* and N, taken from Ref. [25], Eq. (7).

$$\begin{pmatrix} N \\ N^* \end{pmatrix} = \frac{1}{\sqrt{2\cosh\delta}}\begin{pmatrix} e^{\delta/2} & \gamma_5 e^{-\delta/2} \\ \gamma_5 e^{-\delta/2} & -e^{\delta/2}\end{pmatrix}\begin{pmatrix} \psi_1 \\ \psi_2 \end{pmatrix}, \tag{5.12}$$

with the nucleonic mixing angle δ, defined by $\sinh\delta = -\frac{(\hat{g}_1+\hat{g}_2)\bar{\sigma}}{2m_0}$ or equally by $\cosh\delta = \frac{M_N + M_{N^*}}{2m_0}$.

5.1 Mean field approximation

The Lagrangian presented before omits fields that do not acquire a vacuum expectation value and therefore form no condensate. However, in a more complete treatment, one might include other mesonic fields like pions. This allows us to use the tree-level pion mass as another fit parameter. The complete mesonic Lagrangian before turning to the mean field approximation then reads

$$\mathcal{L}_{mes} = \mathcal{L}_{kin} + \mathcal{L}_\omega + \frac{1}{2}m^2\left(\sigma^2+\pi^2\right) - \frac{\lambda}{4}\left(\sigma^2+\pi^2\right)^2 + \epsilon\sigma - \frac{1}{2}m_\chi^2\chi^2 + g\chi\left(\sigma^2+\pi^2\right), \tag{5.13}$$

with the kinetic part $\mathcal{L}_{kin}$ of the mesonic Lagrangian

$$\mathcal{L}_{kin} = \frac{1}{2}\left(\partial_\mu\sigma\partial^\mu\sigma + \partial_\mu\boldsymbol{\pi}\cdot\partial^\mu\boldsymbol{\pi} + \partial_\mu\chi\partial^\mu\chi\right), \tag{5.14}$$

and the part describing the ω meson,

$$\mathcal{L}_\omega = -\frac{1}{4}\omega_{\mu\nu}\omega^{\mu\nu} + \frac{1}{2}m_\omega^2\omega_\mu\omega^\mu\,. \tag{5.15}$$

Since there are three different kinds of pions, the π^0, $\pi^+$and the π^-, we denote the vector of the pion fields, also called the pion triplet, by a bold letter $\boldsymbol{\pi}$. The pion enters the Lagrangian in a similar fashion as the chiral condensate, the only difference can be found in the explicit symmetry breaking modeling linear term $\epsilon\sigma$. In order to conserve parity we assume that the pion does not form a condensate, $\bar{\boldsymbol{\pi}} = 0$. One has to be more careful in presence of a magnetic field since it breaks isospin and rotation symmetry. However, in our approach the pion does not occur in the effective mass since it does not contribute to the Yukawa interaction and consequently does not alter the effective mass, leaving the vacuum result $\boldsymbol{\pi} = 0$ unaffected by the magnetic field. Before turning to the mean field approximation we renormalize the pion triplet with the pion wavefunction renormalization constant $Z = 1.67$, $\boldsymbol{\pi} \to Z\boldsymbol{\pi}$, in accordance with [85, 86]. The next step is to apply the mean field approximation, i.e. expanding the fields around the vev by replacing $\sigma \to \bar{\sigma} + \sigma$ and $\chi \to \bar{\chi} + \chi$. The vector condensate $\bar{\omega}_0$ is absorbed into the effective chemical potential in the nucleonic part of the full Lagrangian and therefore neglected for the following considerations. The Lagrangian is now given by

$$\mathcal{L} = \mathcal{L}_{kin} + \mathcal{L}_\omega - U(\bar{\sigma}, \bar{\chi}) + \mathcal{L}^{(1)} - \frac{1}{2}(\sigma, \chi) \begin{pmatrix} m_\sigma^2 & -2g\bar{\sigma} \\ -2g\bar{\sigma} & m_\chi^2 \end{pmatrix} \begin{pmatrix} \sigma \\ \chi \end{pmatrix} - \frac{1}{2} m_\pi^2 \pi^2 + \mathcal{L}_{I_m} . \quad (5.16)$$

The kinetic part stays unaffected and we have extracted the tree-level potential of the eLSM,

$$U(\bar{\sigma}, \bar{\chi}) = -\frac{1}{2} m^2 \bar{\sigma}^2 - \epsilon \bar{\sigma} + \frac{\lambda}{4} \bar{\sigma}^4 - \frac{1}{2} m_\omega^2 \bar{\omega}_0^2 + \frac{1}{2} m_\chi^2 \bar{\chi}^2 - g \bar{\chi} \bar{\sigma}^2 . \quad (5.17)$$

The square of the tree-level masses m_π^2 and m_σ^2 can be found by reading off all prefactors from terms of the form $-\frac{1}{2} m^2 \phi^2$, where ϕ denotes the corresponding field.

$$\begin{aligned} m_\sigma^2 &= 3\lambda\bar{\sigma}^2 - m^2 - 2g\bar{\chi} \,, & (5.18) \\ m_\pi^2 &= Z^2 \left(\lambda\bar{\sigma}^2 - m^2 - 2g\bar{\chi} \right) . & (5.19) \end{aligned}$$

In order to determine the condensates at tree-level one have to extremize the tree-level potential,

$$\begin{aligned} \frac{\partial U}{\partial \bar{\sigma}} &= 0 \quad \to \quad -m^2\bar{\sigma} + \lambda\bar{\sigma}^3 - \epsilon - 2g\bar{\chi}\bar{\sigma} = 0 \,, & (5.20) \\ \frac{\partial U}{\partial \bar{\chi}} &= 0 \quad \to \quad m_\chi^2 \bar{\chi} - g\bar{\sigma}^2 = 0 \,. & (5.21) \end{aligned}$$

In the first line we recognize the tree-level mass of the pion and can therefore write $\epsilon = \frac{m_\pi^2}{Z^2}\bar{\sigma}$. The second equation connects the chiral condensate and the tetraquark condensate by $\bar{\chi} = \frac{g\bar{\sigma}^2}{m_\chi^2}$. The interactions of the mesons are contained in $\mathcal{L}_{I_m}$ in the following way,

$$\mathcal{L}_{I_m} = -\lambda\bar{\sigma}\sigma \left(\sigma^2 + \pi^2 \right) - \frac{\lambda}{4} \left(\sigma^2 + \pi^2 \right)^2 + g\chi \left(\sigma^2 + \pi^2 \right) . \quad (5.22)$$

Since we are going to neglect the fluctuations later on, this part has no relevance for us. Additionally, there are terms linear in the fluctuations σ and χ,

$$\mathcal{L}^{(1)} = \left(m^2\bar{\sigma} - \lambda\bar{\sigma}^3 + \epsilon + 2g\bar{\chi}\bar{\sigma} \right) \sigma + \left(g\bar{\sigma}^2 - m_\chi^2 \bar{\chi} \right) \chi \,. \quad (5.23)$$

One sees that the brackets in front of the fluctuations are equivalent to the equations of motion for the condensates, where the fluctuations are set to zero, hence this part of the Lagrangian vanishes.

In the mean field approximation we can read off the potential for the fields σ and χ, which is responsible for the mixing of the fields.

$$V(\sigma, \chi) = \frac{1}{2} (\sigma\, \chi) \begin{pmatrix} m_\chi^2 & -2g\bar{\sigma} \\ -2g\bar{\sigma} & m_\sigma^2 \end{pmatrix} \begin{pmatrix} \sigma \\ \chi \end{pmatrix} . \quad (5.24)$$

If we denote the physical fields with h and s, the relation between the fields can be calculated with help of the ansatz

$$\begin{pmatrix} h \\ s \end{pmatrix} = \begin{pmatrix} \cos(\theta) & \sin(\theta) \\ -\sin(\theta) & \cos(\theta) \end{pmatrix} \begin{pmatrix} \chi \\ \sigma \end{pmatrix}, \tag{5.25}$$

where the transformation matrix is a general two-dimensional rotation matrix. If we want to calculate the mixing angle we have to invert the latter equation, i.e. replace $\theta \to -\theta$, and insert this ansatz into the Lagrangian. Demanding that in this new basis no mixing between the new fields occur allows us to calculate the mixing angle. Another way to proceed is to calculate the eigenvalues of the potential, which are the masses of the new fields m_h and m_s.

$$m_h^2 = \frac{1}{2}\left(m_\sigma^2 + m_\chi^2\right) - \sqrt{\left(m_\sigma^2 - m_\chi^2\right)^2 + (4g\bar{\sigma})^2}\,, \tag{5.26}$$

$$m_s^2 = \frac{1}{2}\left(m_\sigma^2 + m_\chi^2\right) + \sqrt{\left(m_\sigma^2 - m_\chi^2\right)^2 + (4g\bar{\sigma})^2}\,. \tag{5.27}$$

The lighter particle is now identified with the resonance $f_0\,(500)$, which we have denoted as scalar σ meson in the Walecka model, and the heavier particle with $f_0\,(1370)$.

The matrix that is used for the change of basis can be calculated by computing the normalized eigenvectors of the potential and writing them column by column into a matrix. Comparing this matrix to the inverse rotation matrix we can read off the mixing angle;

$$\theta = -\arctan\left(\frac{m_\sigma^2 - m_\chi^2}{4g\bar{\sigma}} - \frac{\sqrt{\left(m_\sigma^2 - m_\chi^2\right)^2 + (4g\bar{\sigma})^2}}{4g\bar{\sigma}}\right), \tag{5.28}$$

which is, for positive values of $m_\sigma^2 - m_\chi^2$, identical to the function found in Ref. [26].

5.2 Self-consistency Equations

In the previous sections the dispersion relation for the extended linear sigma model without magnetic field has been derived. Since the magnetic field couples equally to the fermionic fields ψ_1 and ψ_2, the implementation of the field via the covariant derivative is straightforward. The dispersion relation has to be replaced by the magnetic version $\epsilon_{k,\nu} = \sqrt{k_z^2 + 2\nu qB + M_i^2}$ for both states M_N and M_{N^*}, and all momentum integrals are replaced as in Eq. (3.33). The tree-level potential of the eLSM in the mean field approximation is given by Eq. (5.17). Due to the appearance of a third condensate we have to solve three self-consistency equations;

$$\frac{\partial\Omega}{\partial\bar{\sigma}} = 0\,, \qquad \frac{\partial\Omega}{\partial\bar{\chi}} = 0\,, \qquad \frac{\partial\Omega}{\partial\bar{\omega}_0} = 0\,, \tag{5.29}$$

where we have to use the general expression of the free energy from Eq. (3.58). Additionally, a sum over the two baryonic states has to be added. Transforming again the derivative w.r.t. the condensates into a mass derivative allows us to widely use the results of the Walecka model. For the matter and the sea contribution, beside the appearance of a second baryonic state N^* and a different expression for the effective masses, nothing has changed, hence we can write down the three equations immediately.

$$
\begin{aligned}
\epsilon + m^2\bar{\sigma} - \lambda\bar{\sigma}^3 + 2g\bar{\chi}\bar{\sigma} &= \sum_{i=N,N^*}\left\{ -\frac{M_i|qB|}{2\pi^2}\left[x_i(1-\ln x_i) + \frac{1}{2}\ln\frac{x_i}{2\pi} + \ln\Gamma(x_i)\right] + \frac{\partial\Omega_{N,\text{mat}}}{\partial M_i}\right\}\frac{\partial M_i}{\partial\bar{\sigma}}\,, \\
g\bar{\sigma}^2 - m_\chi^2\bar{\chi} &= \sum_{i=N,N^*}\left\{ -\frac{M_i|qB|}{2\pi^2}\left[x_i(1-\ln x_i) + \frac{1}{2}\ln\frac{x_i}{2\pi} + \ln\Gamma(x_i)\right] + \frac{\partial\Omega_{N,\text{mat}}}{\partial M_i}\right\}\frac{\partial M_i}{\partial\bar{\chi}}\,, \\
n_B &= \frac{m_\omega^2\left(\mu-\mu_*\right)}{g_\omega^2}\,,
\end{aligned}
\tag{5.30}
$$

with the obvious generalization of the abbreviation $x_i = \frac{M_i^2}{2qB}$. The third equation is precisely the same as in the Walecka model, rewritten with the help of the definition of the effective chemical potential $\mu_* = \mu - g_\omega\bar{\omega}_0$. The l.h.s. of the first two equations are the minimization of the potential, i.e. the vacuum equations (the r.h.s. is zero in the vacuum). The first equation contains the constant term ϵ which prevents the trivial solution $\bar{\sigma} = 0$ and is therefore capable of the explicit symmetry breaking of the chiral symmetry.

The derivative of the masses are the same for both states concerning the tetraquark, but differ for the chiral condensate since it is responsible for the mass splitting.

$$
\frac{\partial M_i}{\partial\bar{\sigma}} = \frac{\left(\frac{\hat{g}_1+\hat{g}_2}{4}\right)^2\bar{\sigma}}{\sqrt{\left(\frac{\hat{g}_1+\hat{g}_2}{4}\right)^2\bar{\sigma}^2 + (a\bar{\chi})^2}} \pm \frac{\hat{g}_1-\hat{g}_2}{4}\,,
\tag{5.31}
$$

$$
\frac{\partial M_i}{\partial\bar{\chi}} = \frac{a^2\bar{\chi}}{\sqrt{\left(\frac{\hat{g}_1+\hat{g}_2}{4}\right)^2\bar{\sigma}^2 + (a\bar{\chi})^2}}\,.
\tag{5.32}
$$

The matter contribution is the same as in the Walecka model, given by the scalar density expanded by the chiral partner. Since we are interested in the zero-temperature onset of nuclear matter, which occurs at energies well below M_{N^*}, the nucleonic states of the chiral partner will not be occupied in any of our results and can be neglected in the biggest part of the calculations. This can be understood by the fact that each partner enters with its own Heaviside function $\Theta\left(\mu_* - M_i\right)$ and we are working at energies below the mass of N^* with $M_{N^*} = 1535$ MeV. This is not true for the sea contribution where its role is, as I am going to show later, non negligible. To estimate the contribution of general baryonic states at given magnetic fields one expands the sea contribution for large x_i, i.e. $M_i^2 \gg 2qB$.

$$
x_i(1-\ln x_i) + \frac{1}{2}\ln\frac{x_i}{2\pi} + \ln\Gamma(x_i) = \frac{1}{12x_i} - \frac{1}{360x_i^3} + \mathcal{O}\left(\frac{1}{x_i^5}\right)\,.
\tag{5.33}
$$

Here one can see that only inverse powers of x_i occur, therefore at a given magnetic field, heavier states are more suppressed. Although the maximal magnetic fields we use in our calculations are in the range of one GeV, which is certainly less than the mass of $N(1535)$, its influence will be significant, which shows that neglecting baryonic states is not trivial and has to be done carefully. Eventually the model can be more predictive including further baryonic states, possibly even hyperons (baryons with nonvanishing strangeness). Nevertheless, our results should be seen as a first correction to nuclear field theories involving magnetic fields, so we leave all improvements of the model for later projects.

5.3 Parameter fit

For a meaningful comparison of the two models, we require the eLSM to reproduce the same saturation properties like the Waecka model, which forces us to adapt the parameters given in Ref. [26]. In principle, there is no big difference to the procedure carried out for the Walecka model, beside the fact that the eLSM has more independent parameters. The other two main differences concern the vacuum pressure and the compression modulus. Whereas in the Walecka model the vacuum pressure is zero, the finite vacuum expectation value of the tetraquark and the chiral condensate lead to a constant, nonvanishing vacuum pressure in the eLSM. Saturation therefore denotes the point of equal pressure of vacuum and matter. Secondly, the expression for the compression modulus in Eq. (4.57) has to be modified,

$$\frac{\partial^2 U}{\partial M_N^2} \to \frac{\partial^2 U}{\partial M_N^2} - \left(\frac{\partial^2 U}{\partial M_N \partial M_{N^*}}\right)^2 / \frac{\partial^2 U}{\partial M_{N^*}^2} \,, \tag{5.34}$$

because minimization with respect to both condensates have to be taken into account in computing the connection between M_N and n_B.

In the mesonic section, we have 6 parameters to fit, m, ϵ, λ, m_ω, m_χ and g. As in the Walecka model we use $m_\omega = 782\,\text{MeV}$. If we write the vacuum solution as $\bar{\sigma} = Zf_\pi$, we can reparametrize m and λ with help of the tree-level masses,

$$\lambda = \frac{1}{2\,(Zf_\pi)^2}\left(m_\sigma^2 - \frac{m_\pi^2}{Z^2}\right), \qquad m^2 = \frac{1}{2}\left(m_\sigma^2 - 3\frac{m_\pi^2}{Z^2}\right) - \frac{2g^2\,(Zf_\pi)^2}{m_\chi^2} \,, \tag{5.35}$$

with the pion wavefunction renormalization constant $Z = 1.67$ mentioned before and the pion decay constant $f_\pi = 92.4$ MeV.[2] This reparametrization is allowed since the value of the vacuum solution has no direct physical meaning. We may require that in the vacuum, the baryonic masses m_N and m_{N^*} are reproduced, which can be guaranteed by the fit of the parameters $\hat{g}_1$, $\hat{g}_2$ and a. Using $\epsilon = \frac{m_\pi^2}{Z^2}\bar{\sigma} = \frac{f_\pi m_\pi^2}{Z}$ immediately fixes $\epsilon = 1.0690 \times 10^6$ MeV^3. With these results the remaining constants m, λ, m_χ and g are functions of m_σ, m_χ and g. In the nucleonic section we have four additional parameters describing the coupling between the nucleonic and mesonic fields, $\hat{g}_1$, $\hat{g}_2$, g_ω and a. In total, we have to fit 7 parameters. The experimental input we use are the same saturation properties as in the Walecka model, namely the saturation density, the binding energy, the compression modulus and the effective mass at the onset, all at saturation. Additionally, we want to reproduce the vacuum masses of the two baryonic states, $m_N = 939$ MeV and $m_{N^*} = 1535$ MeV. As in the Walecka model the derivation of g_ω decouples since it is described by the same equation, leaving its value unchanged. Since the remaining equations are hard to solve numerically we follow a step by step procedure. One can see that we only have 6 properties we want to fit but 7 available parameters. We use the remaining freedom to fit the physical masses m_h and m_s as good as possible to the resonances $f_0(500)$ and $f_0(1370)$. For instance one can start by guessing a certain value for the parameter a and express the coupling constants $\hat{g}_1$ and $\hat{g}_2$ as a function of the constants m_N and m_{N^*} and the vacuum parameters a, g, and m_χ,

$$\begin{aligned} \hat{g}_1 &= \hat{g}_1(a, g, m_\chi)\,, \\ \hat{g}_2 &= \hat{g}_2(a, g, m_\chi)\,. \end{aligned} \tag{5.36}$$

For the five variables left, which are the three mentioned above and the value of the condensates at the onset, we use the remaining two self-consistency equations $\frac{\partial\Omega}{\partial\bar{\sigma}} = \frac{\partial\Omega}{\partial\bar{\chi}} = 0$ at $B = 0$, the

[2] These relations are the corrected versions of the expressions for λ and m^2 in Eq. (14) of Ref. [26].

ϵ [MeV^3]	m [MeV]	λ	g [MeV]	m_χ [MeV]	m_ω [MeV]
1.6090×10^6	518.75	13.950	1422.7	1310.4	782

$\hat{g}_1$	$\hat{g}_2$	g_ω	a
10.239	17.964	8.1617	29.836

Table 5.1: Set of parameters in the eLSM obtained by fitting the model to the presented nuclear saturation and vacuum properties.

condition that the pressure at the onset is identical to the vacuum pressure, the expression for the compression modulus and the fact that we require $M_N = 0.8\, m_N$ at the onset. Now one can compute how the change of the starting value for a changes the physical masses m_h and m_s. We decided to fit one of them exactly to $f_0(1370)$, which leads to the parameters presented in Tab. 5.1. With this parameter set we obtain $m_\sigma = 819.31$ MeV and $m_\chi = 1310.4$ MeV, leading to $m_h = 1370.0$ MeV per construction and $m_s = 715.1$ MeV, which is still in rough accordance with $f_0(500)$. These parameters are somehow arbitrary since the effective mass at the onset, the compression modulus and especially the choice of fitting $f_0(1370)$ exactly are arbitrary. Compared to the parameters used in Refs. [26, 29], we have improved the fit to nuclear matter at saturation by loosing some quality in the description of vacuum properties like the meson masses. It is interesting that these differences lead to a role reversal of m_h and m_s. With our parameter set, the$f_0(500)$ is predominantly given by σ (= a quark-antiquark state), while$f_0(1370)$ is predominantly given by χ (= a tetraquark state). In principle, this can be seen by calculating the mixing angle, however it is quite intuitive since m_s is much closer to m_σ than to m_χ and vice versa. We have checked that such a role reversal is unavoidable if one requires the reproduction of the mentioned saturation properties, no matter how the parameter a is chosen. The main reason is our more realistic choice of the effective mass at saturation $M_N = 0.8 m_N$ (while the original parameter sets lead to $M_N = 0.9 m_N$). Choosing an even lower effective mass would make it very difficult for the model in its present form to reproduce the resonances $f_0(500)$ and $f_0(1370)$ at all, which explains our choice of the effective mass at the onset at saturation close to the upper bound of the experimental spectrum.

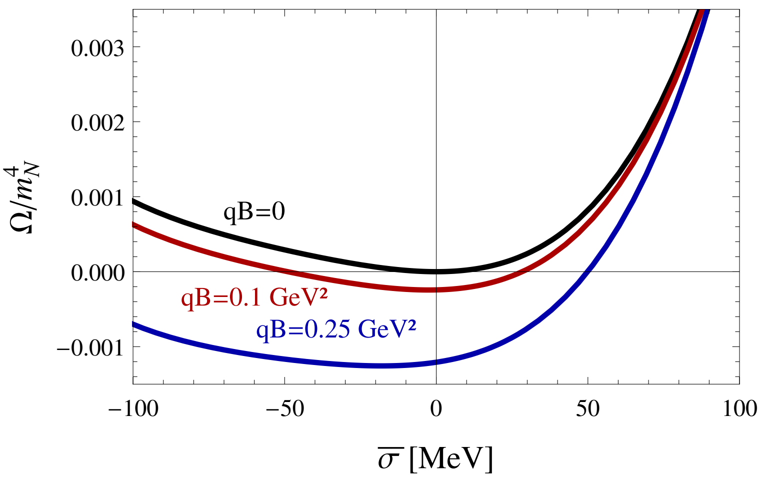

Figure 6.1: Vacuum free energy in the Walecka model as a function of the meson condensate for different values of the magnetic field. One can see that the minimum of the free energy becomes more and more negative with increasing magnetic field, leading to an increased effective mass of the nucleon.

6 Vacuum Solutions

I am now going to discuss the solution of the vacuum equations in both models and show that both of them are capable of describing magnetic catalysis. Vacuum refers to $\mu_* < M$, i.e. there is no nucleonic contribution to the pressure, but it does not imply $B = 0$.

6.1 Walecka Model

In both models, the scalar as well the baryon density are zero in the vacuum, $n_B = n_s = 0$, therefore the self-consistency equations are reduced trivially by one equation, since the vector condensate is always vanishing, $\bar{\omega}_0 = 0$. In the vacuum nothing should depend on the chemical potential, so it is physically consistent that the effective chemical potential has no influence too. In the Walecka model only one equation is left,

$$\frac{m_\sigma^2 \bar{\sigma}}{g_\sigma} + b m_N (g_\sigma \bar{\sigma})^2 + c(g_\sigma \bar{\sigma})^3 + \frac{qBM_N}{2\pi^2}\left[x(1-\ln x) + \frac{1}{2}\ln\frac{x}{2\pi} + \ln\Gamma(x)\right] = 0\,. \tag{6.1}$$

In absence of the magnetic field, the equation is obviously solved trivially by $\bar{\sigma} = 0$. (In the limit $B \to 0$ the sea contribution vanishes as expected, even if this can not be seen directly since x depends on the magnetic field to.) Since the neutron is uncharged, $q = 0$, its mass is also not affected by the magnetic field in the vacuum, only by finite baryon densities. The other solutions can be obtained by solving the remaining quadratic equation;

$$\bar{\sigma}_{1,2} = -\frac{b m_N}{2 g_\sigma c} \pm \sqrt{\left(\frac{b m_N}{2 g_\sigma c}\right)^2 - \frac{m_\sigma^2}{g_\sigma^4 c}}\,. \tag{6.2}$$

For the chosen set of parameters presented in Tab. 4.1, there is no further real solution, rendering $\bar{\sigma} = 0$ to the only existing one. This makes a lot of sense from a physical point of view: in the vacuum at $B = 0$ the effective mass $M_N = m_N - g_\sigma \bar{\sigma}$ is always equal to the mass parameter m_N of the Lagrangian, since there is nothing that influences the mass. This is always true, also for a slightly different set of parameters, but in this case, other real solutions appear, which we consequently have to neglect (see App. D).

For small magnetic fields, i.e. for big values of $x = \frac{M_N^2}{2qB}$, we can expand the sea contribution of the self-consistency equations,

$$\frac{qBM}{2\pi^2}\left[x(1-\ln x)+\frac{1}{2}\ln\frac{x}{2\pi}+\ln\Gamma(x)\right]=\frac{(qB)^2}{12\pi^2\left(m_N+g_\sigma\bar{\sigma}\right)}+\mathcal{O}\left(B^4\right)\,, \tag{6.3}$$

where we see that the lowest order is given by $\mathcal{O}\left(B^2\right)$. Therefore, we assume a quadratic ansatz for the effective mass at small field strengths of the form

$$M_N = m_N\left(1+\left(\frac{qB}{qB_0}\right)^2\right)\,, \tag{6.4}$$

which accounts for the fact that the effective mass at vanishing magnetic field is m_N. In order to calculate the numerical value of B_0 we recognize that at $B = B_0$ the effective mass is twice the nucleon mass, $M_N = 2m_N$. Rewriting Eq. (6.1) in terms of the effective mass, $g_\sigma\bar{\sigma} = m_N - M_N$, and then setting $B = B_0$ and $M_N = 2m_N$ allows us to solve for B_0. At small magnetic fields the behavior of the effective mass is consequently given by

$$\frac{M_N\left(\mu=T=0\right)}{m_N}\simeq 1+\frac{g_\sigma^2\,(qB)^2}{12\pi^2 m_N^2 m_\sigma^2}\simeq 1+\left(\frac{qB}{0.67\text{GeV}^2}\right)\,. \tag{6.5}$$

For high magnetic fields the model in its present form can not be trusted any more. Fitting the parameters to the same experimental values except for the effective mass at the onset, which is changed to $M_N = 0.78\,m_N$, reveals this fact rather clearly. In this new parameter set, which is discussed in App. D, the physical solution ceases to exist around $qB \simeq 0.3\,\text{GeV}^2$. It might be possible to cure this problem by allowing for B-dependent meson masses. In the current approach within the mean field approximation, in both models the mesons do not feel the magnetic field at all. Such an effect could be included for instance via meson loop corrections or a more microscopic approach. Throughout this thesis I will neglect such effects on the meson masses and couplings.

The remaining equation Eq. (6.1) has to be solved numerically, the result in comparison to the analytic result for small B is shown in Fig. 6.2.

The full numerical result is plotted with the black, solid line. One can clearly see that the effective mass increases with the magnetic field. This effect is called magnetic catalysis and presents one of the main results of this thesis. As far as we know, it is the first time that magnetic catalysis has been incorporated into effective models for nuclear matter. For $B \to 0$ the mass converges to the vacuum value of $m_N = 939$ MeV. For small magnetic fields, the analytic solution, which is represented by the blue, dash-dotted line, fits the numerical result quite well, for higher magnetic fields the raise in the mass is higher than the analytical approximation. The constant, red, dashed line would be the result if the B-dependent sea contribution is neglected. Without the additional, field dependent term, $\bar{\sigma} = 0$ is the only solution for all values of the magnetic field, where a vanishing condensate leads to a constant mass. The same is true for the uncharged partners, which is, in the case of the Walecka model, the neutron. The mass of the neutron in the vacuum is constant, it is only affected by finite baryon densities.

6.2 eLSM

In the extended linear sigma model, the free energy in the vacuum at $B = 0$ is simply the tree-level potential, defined in Eq. (5.17). The equations to solve in this case are the minimization of the tree-level potential w.r.t. to the three condensates. Since the role of the vector condensate $\bar{\omega}_0$ is

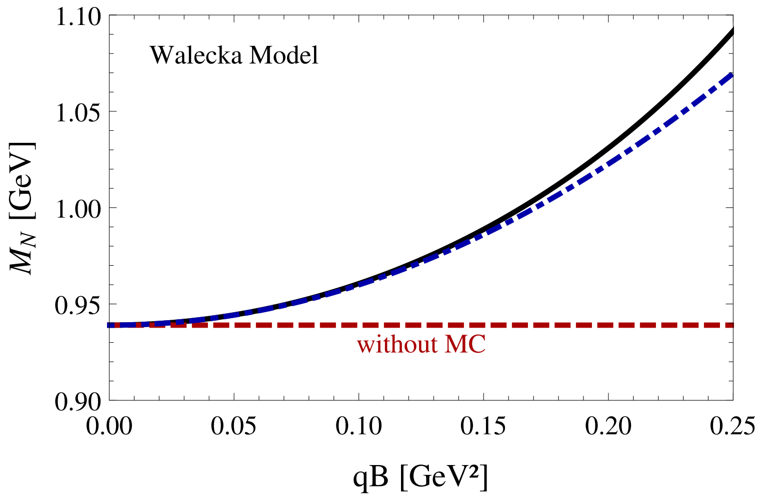

Figure 6.2: Effective nucleon mass at $\mu = T = 0$ as a function of the magnetic field in the Walecka model. The solid black line shows the full numerical result. One can see that the mass of the nucleon increases with the magnetic field, which is the effect of magnetic catalysis. The dashed-dotted, blue line represents the analytical result for small magnetic fields. The straight, red, dashed line would be the result without magnetic catalysis. In this case, where the B-dependent sea contribution is neglected, the nucleon mass does not depend on the field and stays constant at $M_N = m_N = 939$ MeV, which is also true for the uncharged neutron. For comparison to astrophysical units, a field strength of $qB = 0.1\,\mathrm{GeV}^2$, given in natural Heaviside-Lorentz units, corresponds to $B = 1.7 \times 10^{19}$ G in Gaussian units, where $q = e \backsimeq 0.30$.

exactly the same as in the Walecka model, one still obtains $\bar{\omega}_0 = 0$. The remaining two equations are given by

$$\frac{\partial U}{\partial \bar{\chi}} = \frac{\partial U}{\partial \bar{\sigma}} = 0\,, \tag{6.6}$$

$$\begin{aligned} \epsilon + m^2\bar{\sigma} - \lambda\bar{\sigma}^3 + 2g\bar{\chi}\bar{\sigma} &= 0\,, & (6.7)\\ g\bar{\sigma}^2 - m_\chi^2\bar{\chi} &= 0\,. & (6.8)\end{aligned}$$

The second equation relates the tetraquark condensate in the vacuum to the square of the chiral condensate. Inserting this relation into the first equation leads to an cubic equation for the chiral condensate, which can be solved analytically. The equation and its solution are given by

$$0 = \epsilon + m^2\bar{\sigma} - \lambda\bar{\sigma}^3 + \frac{2g^2\bar{\sigma}^3}{m_\chi^2}\,, \tag{6.9}$$

$$\bar{\sigma}(\mu = T = B = 0) = \frac{2m}{\sqrt{3}\sqrt{\lambda - \frac{2g^2}{m_\chi^2}}}\cos\left[\frac{1}{3}\arccos\left(\frac{3\sqrt{3}\epsilon}{2m^3}\sqrt{\lambda - \frac{2g^2}{m_\chi^2}}\right)\right] \simeq 154.3\,\mathrm{MeV} \tag{6.10}$$

For the numerical value we have inserted the values obtained by the parameter fit in Sec. 5.1. In the parametrization used there, the solution can be converted to $\bar{\sigma}(\mu = T = B = 0) = Zf_\pi \backsimeq 154.3$ MeV, which is shown explicitly in appendix C. For the tetraquark condensate one therefore obtains a numerical value of

$$\bar{\chi} = \frac{g\bar{\sigma}^2}{m_\chi^2} \backsimeq 27.9\,\mathrm{MeV}\,. \tag{6.11}$$

Inserting these values into the expression for the masses of the nucleon and its chiral partner one computes per construction $m_N = M_N(\mu = T = B = 0) = 939$ MeV and $m_{N^*} = M_{N^*}(\mu = T = B = 0) = 1535$ MeV. With the help of these results, the tree-level potential can be plotted as a

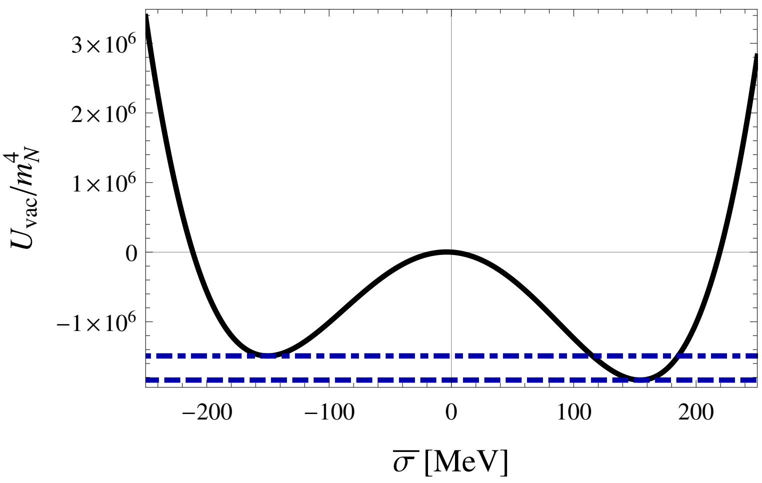

Figure 6.3: tree-level potential of the eLSM in the vacuum as a function of the chiral condensate $\bar{\sigma}$. Due to the linear term $\epsilon\bar{\sigma}$ in the potential, the function is not completely symmetric but slightly shifted, resulting in just one global minimum. This is the result of explicit symmetry breaking.

function of one variable, the chiral condensate, which is done in Fig. 5.17. Due to the explicit symmetry breaking of the chiral symmetry by the linear term in the potential, $\epsilon\bar{\sigma}$, the function is not completely symmetric. If a symmetry is explicitly broken but still approximately realized, the resulting Goldstone bosons, after the spontaneous breaking of the approximate global symmetry, acquire small masses. This happens because there is a small slope in the circle of the mexican hat, which results from rotation of the plotted potential around the central axis. In case of chiral symmetry breaking, the (pseudo-) Goldstone bosons are the three pions of the piontriplett. In order to take these particles into account one has to work beyond the mean field approximation, which is not done in this thesis.

In similarity to the Walecka model, both condensates, $\bar{\chi}$ and $\bar{\sigma}$, increase quadratically with the magnetic field. This is in agreement with chiral perturbation theory [12] (in the chiral limit, the behavior is linear in the magnetic field [11, 87]), and also with the quark-meson model [45] and the holographic Sakai-Sugimoto model [88]; see Ref. [19] for a comparison of lattice QCD results with the various model predictions. Inserting this ansatz into the first two equations of Eq. (5.30), one can calculate the coefficients in the eLSM analytically. Unfortunately there is no simple expression like in the Walecka model, so I only quote the numeric result for the nucleon mass,

$$M_N(\mu = T = 0) \backsimeq m_N \left(1 + \left(\frac{qB}{0.51\,\mathrm{GeV}^2}\right)^2\right) . \tag{6.12}$$

Since this result is actually obtained by assuming an ansatz for the condensates and not for the mass itself, it is also valid for the behavior of the mass of the chiral partner, only the vacuum mass m_N has to be replaced by m_{N^*} on the r.h.s. of the equation. The full numerical result is presented in Fig. 6.4.

The numerical result is again plotted in solid black. Similar to the Walecka model, the mass increases with the magnetic field, proving that magnetic catalysis can also be incorporated into the extended linear sigma model and in the huge variety of similar models. As stated at the very beginning of this thesis, magnetic catalysis seems to be a model independent effect that can be included into models for dense nuclear matter. The chosen range of the magnetic field is very large so that one can see the expected linear increase of the mass at high magnetic fields. At small magnetic fields the result coincidences again with the analytical approximation. For uncharged

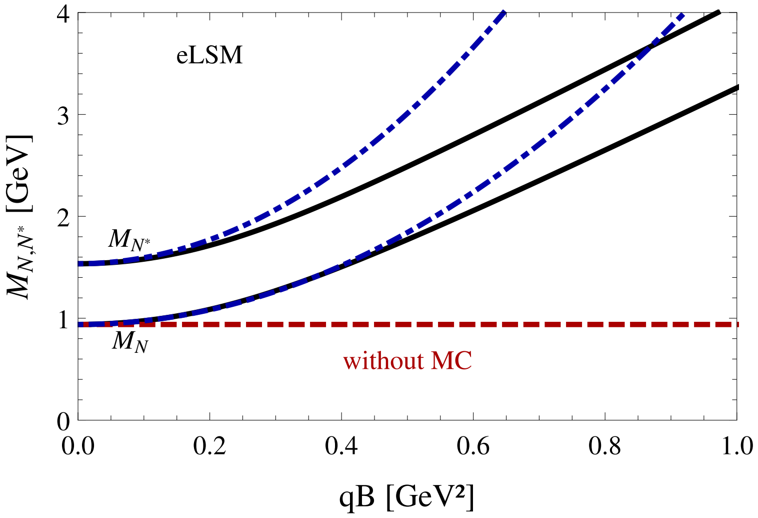

Figure 6.4: Effective mass of the nucleon and its chiral partner in the vacuum, $\mu = T = 0$, as a function of the magnetic field, in the extended linear sigma model. The solid black lines show the full numerical result for the nucleon and its chiral partner, starting from the $B = 0$ values $m_N = 939$ MeV and $m_{N^*} = 1535$ MeV. The chosen scale for the magnetic field is very large in order to show that the masses increase linearly for high field stregths. For small fields, the results are again very close to the analytical approximation, represented by the blue, dashed-dotted lines. Without magnetic catalysis the masses would both stay constant again, indicated for the nucleon by the red, dashed line.

particles, or in the case where the effect of magnetic catalysis is neglected, the masses stay constant again, indicated for the nucleon by the red, dashed line.

At the end of this chapter it is very instructive to compare the results of the two models. As explained before, the contribution of the chiral partner in the eLSM to the matter part of the free energy can be neglected, since we are working at energies well below the vacuum mass $m_{N^*} = 1535$ MeV. However, its contribution to the magnetic sea term can not be neglected. If one removes this contribution by hand, the obtained result is very close to the result in the Walecka model. This can be seen in Fig. 6.5. In Eq. (5.33) I have stated that states with mass squares larger than the regarded magnetic fields, i.e. $m \gg 2qB$, do not contribute. Nevertheless, the mass of the chiral partner is high enough to change the result significantly. This leads to the assumption that in a more complete treatment, additional charged hadronic states like pions or hyperons have to be taken into account.

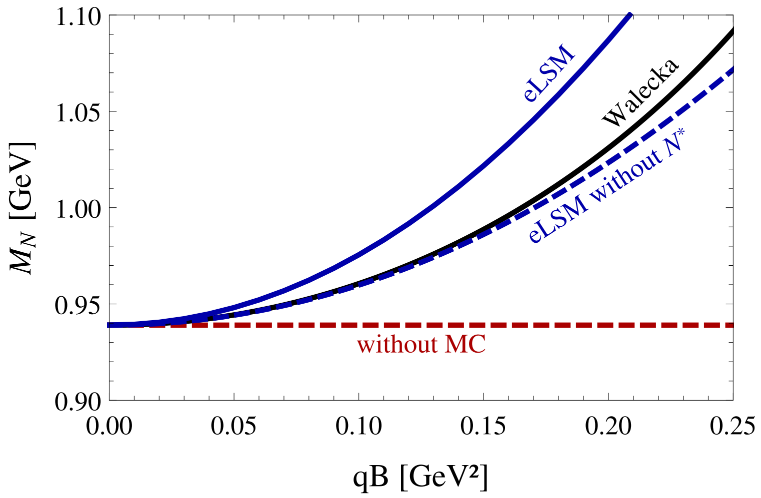

Figure 6.5: Comparison of the vacuum masses in the Walecka model and the eLSM. In principle, magnetic catalysis is even stronger in the eLSM. If one removes the influence of the chiral partner to the sea-contribution by hand, the results are much more similar, indicating that the main difference arises due to the presence of an additional hadronic state.

7 Baryon onset of nuclear matter

In this section I will calculate the onset of nuclear matter at $T = 0$ in both models, first starting at vanishing magnetic field, $B = 0$, and later on as a function of the magnetic field. The two corresponding equations 4.48 in the Walecka model respectively three in the eLSM 5.30 are solved numerically, where also the matter contributions have to be included. This allows us, for a given magnetic field, to calculate the effective mass as a function of the chemical potential. From this calculation only, it is not clear where the onset takes place, since it is lowered by the binding energy too. Without magnetic field, we expect the onset to take place at $\mu_0 = 922.7$ MeV per construction, since we have fitted both models to reproduce a binding energy of $E_{bind} = -16.3$ MeV at saturation. In principle, we already know how the vacuum mass responses as a function of the B-field, but also the binding energy changes with the field, leading to a non trivial behavior of the onset. How the onset can be computed is explained exemplarily in the following section in the Walecka model at $B = 0$. Beside the fact that in the eLSM and in presence of a magnetic field the equations are more complicated to solve, the principle of the calculation is unaffected, therefore I will only present the final results.

7.1 Vanishing magnetic field

As a first step we solve the self-consistency equations Eqs. (4.48) in the Walecka model for different values of the chemical potential at vanishing magnetic field. The result can be seen in Fig. 7.1. This plot is very instructive in order to understand the nature of the solution. The shaded area represents the vacuum, i.e. $\mu_* < M_N$. Since the vector condensate vanishes in the vacuum[3], i.e. $\bar{\omega}_0 = 0$, the effective chemical potential μ_* is equal to the thermodynamic chemical potential μ, so the vacuum can equivalently be characterized by $\mu < M_N$. In the vacuum, all solutions do not depend on μ, which results in the constant solution, plotted in solid black.

In the unshaded area, μ and μ_* differ due to the now existent condensate $\bar{\omega}_0$. In a certain regime, three solutions exist (in the figure, the three solutions are given by the solid, black line,

[3] At $B = 0$ this is true for both condensates, in presence of a magnetic field only the vector condensate vanishes in the vacuum.

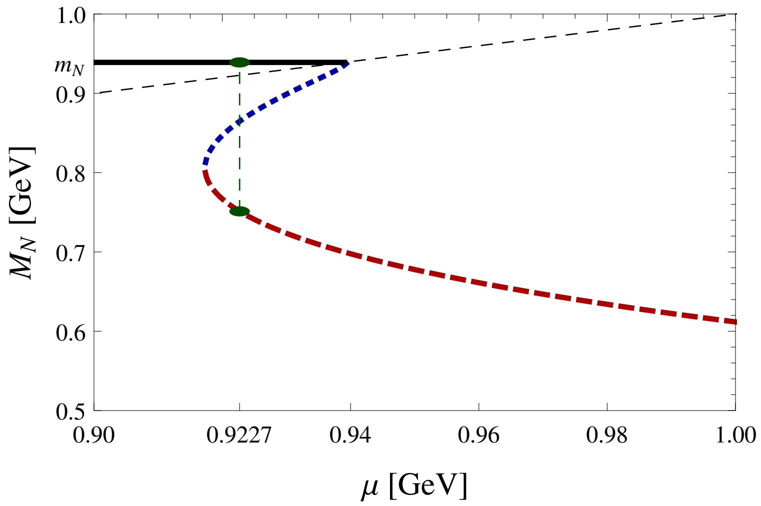

Figure 7.1: Effective mass at $B = 0$ in the Walecka model as a function of the chemical potential. The solid, black line represents the vacuum solution, which does not depend on μ. The shaded area marks the vacuum, i.e. $\mu_* < M_N$. Since the vector condensate vanishes in the vacuum this is equivalent to $\mu < M_N$. The dashed, vertical, green line marks the onset at $\mu_0 = 922.7$ MeV. At this point the effective mass changes discontinuously from $M_N = m_N$ to $M_N = 0.8\, m_N$. Both numerical values are obtained by construction, since they enter the parameter fit as an experimental input.

the dotted, blue line which reaches to the minimum of μ, and the dashed, red line). In order to decide which solution is realized in nature, one has to compute which one leads to the lowest free energy. Before the onset, the free energy of the vacuum is the lowest one. At the onset, the free energy of nuclear matter is exactly equal to the vacuum free energy and starts to be preferred from there on. This is a phase transition of the first order, since the first derivative of the potential is discontinuous. At the onset, the baryon density and the scalar density jump from zero to a finite value. Also the mass and the condensates are discontinuous at the onset, since all these quantities can be obtained by a first derivative of the potential. Therefore, one can calculate the onset by requiring the pressure of the vacuum to be identical to the pressure of nuclear matter (at $B = 0$ the vacuum pressure in the Walecka model is zero). In Fig. 7.2, the free energy for this case is plotted as a function of the chemical potential. Since the absolute value of the energy has no meaning for us due to the undetermined energy scale, we normalize it to the fourth order of the nucleon mass, rendering the plotted quantity dimensionless. In the vacuum the pressure is independent of the chemical potential (in this case even zero), therefore we obtain the constant, solid, black line corresponding to the constant vacuum solution $M_N = m_N$ in Fig. 7.1. Like in the plot of the effective mass, there is a region where three solution exist, each one corresponding to one solution in the mass diagram. The free energy now tells us which solution is energetically preferred at a given chemical potential and therefore realized in nature. As one can see, the blue, dotted line is never preferred. In plots of this kind, these region is often not shown in the mass plot since it has no physical significance. The meeting point of the two matter branches in the free energy corresponds to the point in the mass diagram with the lowest chemical potential, where the blue and the red solution meet. Following the dotted line up to the vacuum in the mass plot corresponds to following it in the free energy down to the vacuum solution, where it ends at $\mu = m_N$. Starting from the contact point of the matter branches again, we can follow the red, dashed line until it crosses the vacuum solution of the free energy. This is where the onset takes place, marked by the dashed vertical, green line in both figures. Physically, in the plot of the free energy we have

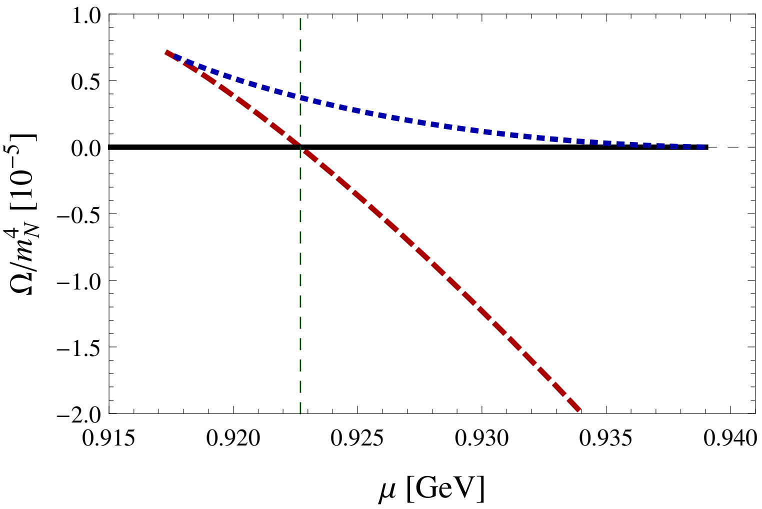

Figure 7.2: Free energy in the Walecka model at $B = 0$ as a function of the chemical potential μ. In the vacuum the pressure is zero, resulting in the constant black, solid line which reaches to the vacuum nucleon mass, $\mu = m_N = 0.939$ GeV. The dotted, blue line corresponds to the equivalently looking line in Fig. 7.1. Since this solution is energetically never preferred, it is not realized in nature. At the onset, marked by the vertical, dashed line at $\mu_0 = 922.7$ MeV, the energy of nuclear matter starts to be lower than the vacuum energy. Physically, we have to follow the black, solid line until the onset and then switch to the red, dashed line. Since this change is not continuously differentiable, the baryon onset is considered a first order phase transition.

to follow the vacuum solution until the crossing point with the lower matter solution (red, dashed line), and follow this solution from there on, which corresponds to a jump in the mass plot.

In the extended linear sigma model, the structure of the solution in the vicinity of the onset is completely the same, which proofs that the fit to the binding energy at saturation was successful in both models. In the extended linear sigma model, it would be possible to go to even higher chemical potentials and see a second phase transition, where the chiral symmetry is partially restored. At this point the mass of the chiral partner and the nucleon mass become nearly degenerated, due to the (nearly) vanishing chiral condensate. For vanishing magnetic field, the masses of the nucleon and its chiral partner are plotted in Fig. 7.3.

The scale off this plot is larger compared to the ones presented in the Walecka model in order to see the influence of the chiral partner in the calculations. Focusing on the solution of the nucleon mass first, which is presented by the solid, blue line starting at $M_N = m_N$ in the vacuum, i.e. the shaded area, one recognizes the same behavior as in the Walecka model. Per construction the onset of nuclear matter takes place at $\mu_0 = 922.7$ MeV, where the mass drops to $M_N = 0.8\, m_N$. It was stated before that neglecting the influence of the chiral partner to the matter contribution (not the sea-contribution) is an exact approximation close to the onset. This is proofed numerically by looking at the dashed, orange line. In vicinity of the onset, no difference between the two solutions can be found. The two functions start to differ at the point where the effective mass becomes lower than the effective chemical potential. In order to see this, the effective chemical potential is plotted with a dash-dotted, black line, and the mass of the chiral partner in solid red, starting at $M_N = m_{N^*} = 1535$ MeV. It is interesting to note that the mass of the chiral partner is not constant until it reaches the vacuum boundary. Its solution already starts to differ at the moment the nucleon sets in, which is clear by the structure of the self-consistency equations 5.30. Both partners are present in one equation, so the onset of the nucleon already starts to alter the vacuum solution of N^*. Therefore, in order to estimate the influence of N^* one has to check if $\mu_* > M_{N^*}$ since $\mu_* \neq \mu$ after the onset of N. The onset of the chiral partner alters the nucleon

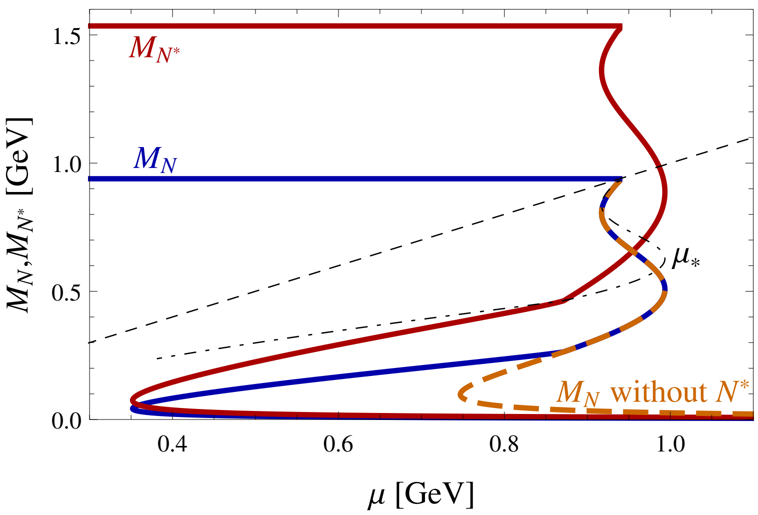

Figure 7.3: Effective mass of the nucleon and its chiral partner in the eLSM as a function of the chemical potential. Additionally, the effective nucleon mass is calculated without the contribution of the chiral partner to the matter part of the free energy, marked by the orange, dashed line. It can be seen that this approximation is exact in the vicinity of the onset. The two functions start to differ at the point where the mass of the chiral partner (red, solid line) becomes smaller than the effective chemical potential, plotted with a dash-dotted, black line.

mass drastically. However, the solution is not unique in this area since the chiral phase transition, where the chiral symmetry is partially restored, takes place at some value of $\mu > \mu_0$. Note that the two masses start to become nearly degenerate at this stage, as explained earlier in this thesis. This part of the diagram has no physical significance, since it is never energetically preferred. It would be very interesting to investigate the chiral phase transition in the eLSM in the presence of a magnetic field, which is beyond the scope of this work since I am focusing on the baryon onset only.

7.2 Nonzero magnetic field

In the presence of a magnetic field, two cases are possible: the onset can take place later than the onset at vanishing magnetic field, or even earlier. This happens if the binding energy, which is also altered by the magnetic field and makes creation of nuclear matter easier, dominates the effect of magnetic catalysis. In this case, a magnetic field can even facilitate the creation of nuclear matter. This is sometimes referred to as "inverse" magnetic catalysis (IMC) and first has been seen in the NJL model in Ref. [33]. This case never happens in the eLSM for our chosen set of parameters. Both cases are present in the Walecka model and are shown in Fig. 7.4. At the magnetic field chosen here, $qB = 0.07\,\mathrm{GeV}^2$, the effect of inverse magnetic catalysis is most pronounced. The binding energy at saturation can be defined by the amount of energy which facilitates the creation of nuclear matter compared to the creation of a single nucleon, i.e. the difference between the chemical potential at the onset and the effective vacuum mass of the nucleon.

$$E_{bind}(qB) = \mu_0(qB) - M_N(\mu = T = 0, qB)\,, \tag{7.1}$$

where $E_{bind}(qB = 0) \simeq -16.3\,\mathrm{MeV}$ was one of our fit parameters. This is the mathematical expression of the physical phenomenon which describes the onset as an interplay between the binding energy and magnetic catalysis, since a simple rearrangement gives $\mu_0(qB) = E_{bind}(qB) + M_N(\mu = T = 0, qB)$. With help of this definition, the binding energy can easily be read off from the

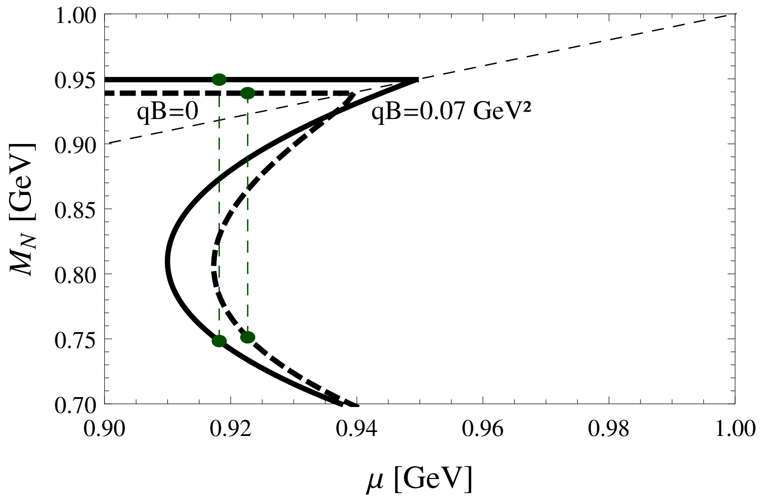

(a) At $qB = 0.07\,\text{GeV}^2$, the onset takes place earlier than without magnetic field. In this case, a magnetic field even facilitates the onset of nuclear matter since the increased binding effect dominates the effect of magnetic catalysis on the vacuum masses.

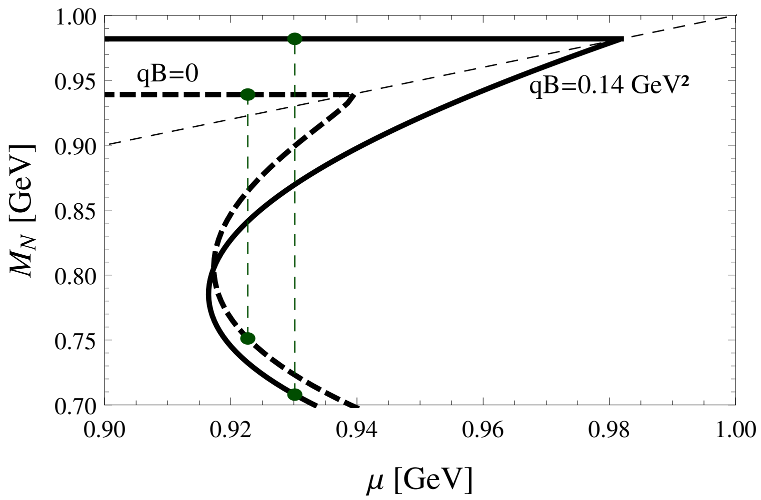

(b) At $qB = 0.14\,\text{GeV}^2$, the effect of magnetic catalysis has taken over completely, leading to a higher value of the critical chemical potential than without magnetic field.

Figure 7.4: Effective nucleon mass as a function of the chemical potential in the Walecka model for different fixed magnetic field strengths. For comparison, the $qB = 0$ result is plotted with a dashed line in both figures. All solutions are obtained in the lowest Landau level approximation.

mass plots as the length of the horizontal line between the actual onset and the vacuum boundary. The onset of nuclear matter can now be calculated numerically as a function of the magnetic field. The results are presented in Fig. 7.5.

The second figure shows oscillatory behavior due to the Landau levels, which are barley visible in the first plot since they happen at a very small range of the chemical potential. With raising magnetic field, less and less levels are occupied. In both models, the oscillations stop for a field larger than $qB \simeq 0.032\,\mathrm{GeV}^2$, meaning that above, only the lowest Landau level (LLL) is occupied. This also justifies the use of the LLL approximation for the calculation off the masses, which are performed at such high magnetic fields that the approximation is exact.

For sufficiently strong magnetic fields, magnetic catalysis dominates the onset in both models, making the creation of nuclear matter increasingly more difficult with increasing magnetic field. This happens due to the larger vacuum mass of the nucleon. For comparison, the wrong solutions, ignoring magnetic catalysis, are plotted for both models. The two dashed lines are barley distinguishable and show a qualitative difference to the correct renormalized case. At the maximal plotted magnetic field, the difference in the critical chemical potential is about $\sim 10\%$, for the saturation density at the onset the difference is about $\sim 25\%$ (Fig. 7.7)and the binding energy even differs by $\sim 90\%$ (Fig. 7.6). In the context of QCD, these results can be interpreted as follows. From lattice calculations it is known, that the chiral condensate increases monotonically with the magnetic field at zero temperature, leading to an increase in the quark masses. It is not clear a priori if this effect also leads to an increase of the nucleon mass, since the interaction between the quarks is also influenced by the magnetic fields. The Walecka model as well the eLSM treat nucleons as pointlike particles and neglect completely their inner structure, so these models show a simple increase of the vacuum masses too. Indeed, their are current calculations [57], concluding that the mass of the neutron decreases with the magnetic field. In these calculations, the inner structure is taken into account, whereas the influence of the chiral condensate is neglected. Therefore, one might expect that these two effects will counteract in a full treatment, where it is not a priori obvious which effect will dominate.

In our approach, the higher vacuum nucleon mass suggests a higher critical chemical potential, but also the interactions between the nucleons themselves are modified by the magnetic field, resulting in a dependence of the binding energy on the field. This effect is included in both models, since the nucleonic interactions are actually described by the meson exchange, which form a condensate and alter the mass. These two effects, binding energy and vacuum mass, counteract and lead to a non trivial behavior of the onset.

One significant difference of the considered models is the monotonic increase of the onset chemical potential in the extended linear sigma model, where as in the Walecka model a regime exists where inverse magnetic catalysis happens. This is consistent with the observations made in Fig. 6.5, where a stronger catalysis in the eLSM can be seen. There, the effect is too strong for the binding energy to overcome. This stronger catalysis in the eLSM was attributed to the existence of the chiral partner. If one removes the influence of the chiral partner to the sea contribution by hand, also the onset curves of the two models become very similar! This is also true if the hole sea contribution is neglected, as the dashed lines in Fig. 7.5 show. However, this seems to depend strongly on the choice of parameters, since slightly different parameters in the eLSM, which are able to reproduce vacuum properties better but fail at saturation, lead to a different behavior. In order to see the interplay between binding energy and magnetic catalysis at the onset it is instructive to calculate the binding energy itself (at the onset), which is done in Fig. 7.6. The solid lines show the result in both models. In the eLSM, the binding energy is even more affected by the correct renormalization. However, in both models the absolute value of the binding energy is even higher

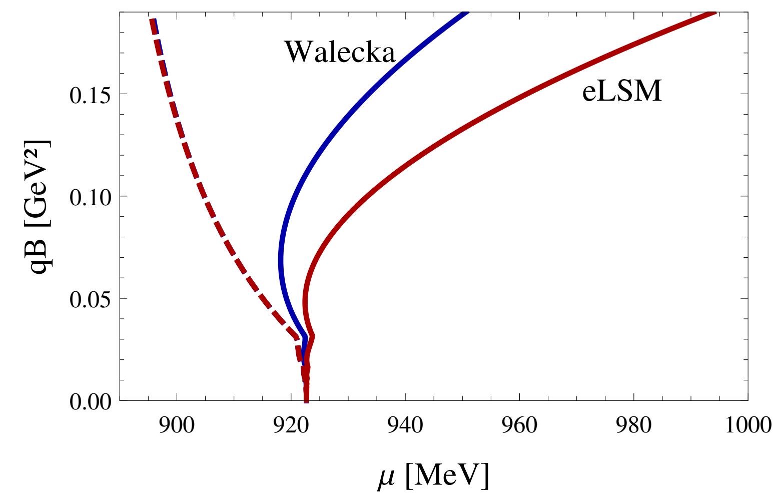

(a) The solid blue line shows the result in the Walecka model, the red one in the eLSM. For comparison, the barley indistinguishable dashed lines represent the solution without magnetic catalysis in both models, i.e. ignoring the $B-$dependent sea contribution, what has been done in the existing literature so far. This means, that the onset is totally driven by the binding energy.

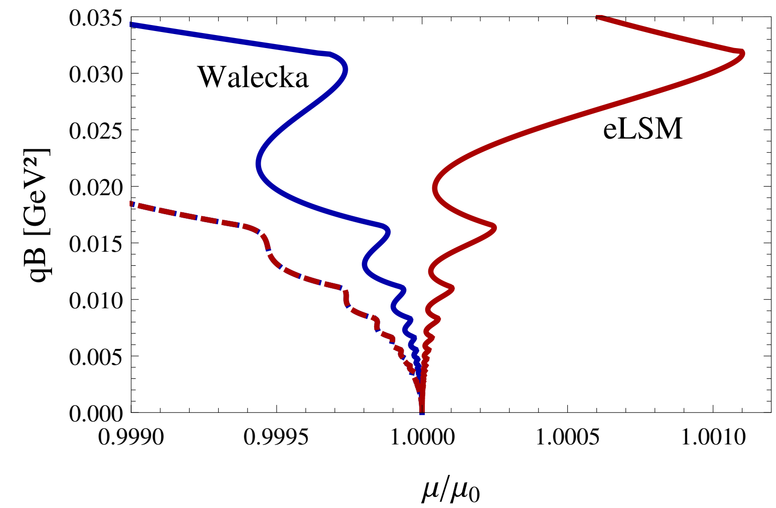

(b) Zoom in for small magnetic fields, showing oscillations due to the Landau level structure. The dashed lines represent again the solution without magnetic catalysis. All functions converge to the critical chemical potential at $qB = 0$, given by $\mu_0 = 922.7$ MeV.

Figure 7.5: Onset of nuclear matter as a function of the background magnetic field.

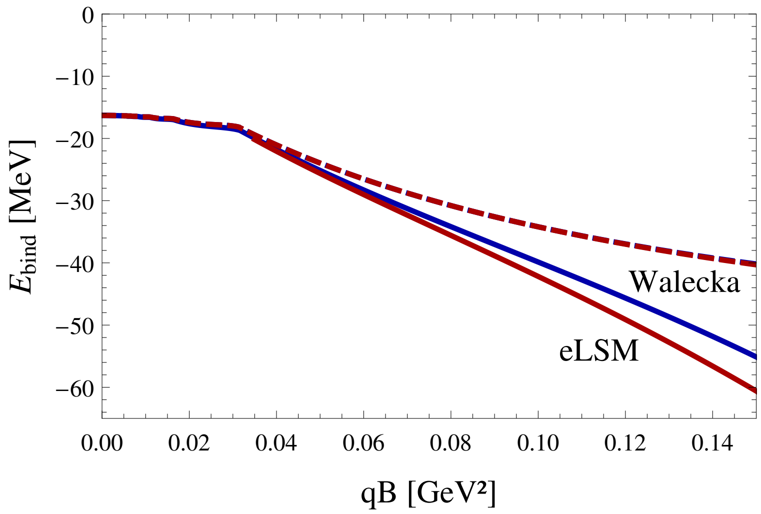

Figure 7.6: Binding energy along the onset of nuclear matter in both models. In the eLSM, the binding energy is slightly more affected by the correct renormalization than in the Walecka model. However, in both cases the absolute value of the binding energy is lowerd compared to the unrenormalized results, marked by the barley indistinguishable dashed lines. If one exchanges the axes, flips the plot by $\frac{\pi}{2}$ and subtracts the vacuum nucleon mass, the dashed lines are identical to the unrenormalized onset, since the binding energy completely drives its behavior.

than without correct renormalization, plotted with the barley indistinguishable dashed lines. If the magnetized sea contribution is neglected for the onset and the binding energy, the latter is solely responsible for the non trivial behavior of the onset. This can be seen if the wrong binding energy is rotated by 90°, i.e. the axes are exchanged, and corrected by the vacuum nucleon mass. The resulting curve is completely identical to the wrong onset curve. Mathematically this can be understood by recalling the definition of the binding energy, $E_{bind} = \mu_0 - M_N(\mu = T = 0, qB)$. Ignoring magnetic catalysis transforms the effective vacuum nucleon mass $M_N(\mu = T = 0, qB)$ to the constant mass m_N, $M_N \to m_N$, so rearranging the definition of the binding energy yields

$$\mu_0(qB) = E_{bind}(qB) + m_N \,. \tag{7.2}$$

Finally, Fig. 7.7 shows the baryon density at the onset. As expected, one can see De Haas–van Alphen oscillations, which stop at $qB \approx 0.032\,\mathrm{GeV}^2$, marking the onset of the lowest Landau level. In both models, incorporating magnetic catalysis leads to slightly higher densities compared to the wrong results, presented by the dashed lines.

NJL, Sakai Sugimoto??

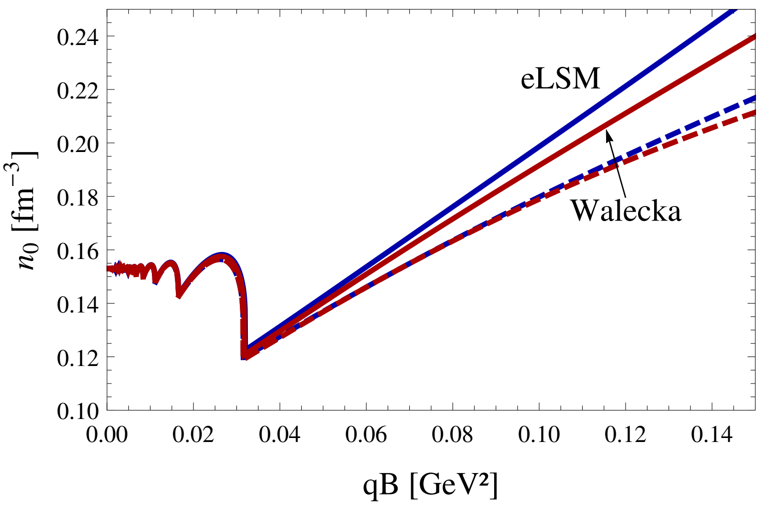

Figure 7.7: Baryon density along the onset of nuclear matter, showing De Haas–van Alphen oscillations. At $qB \approx 0.032\,\text{GeV}^2$, one can see the beginning of the lowest Landau level. The wrong results are presented as usual with the corresponding dashed line. Including the magnetized Dirac sea increases the density in both models.

8 Summary and Outlook

In this thesis and the resulting publication [51], we have discussed the influence of a background magnetic field on the onset of nuclear matter. After a short recap of chiral symmetry and magnetic catalysis in quantum chromo dynamics, we derived the correct renormalization of the free energy in a relativistic field theoretical approach in presence of a magnetic field. For this purpose, the solution of the corresponding Dirac equation was derived and discussed. As a next step I introduced two field theoretical models for relativistic, dense nuclear matter, the Walecka model and the extended linear sigma model (eLSM). Both models are fitted to the same properties of nuclear matter at saturation, the mean field approximation was applied and the equations for the self consistent determination of the appearing condensates were derived. The main goal has been to investigate the influence of the B-dependent contribution of the Dirac sea which has been omitted in previous studies on magnetized nuclear matter, but has been taken properly into account in similar studies of quark matter in background magnetic fields. This contribution can be physically interpreted as magnetic catalysis, which is defined as an enhancement of the chiral condensate by a background magnetic field. In the Walecka model, magnetic catalysis shows up indirectly by increasing the effective nucleon mass with the field, whereas in the eLSM it can be observed directly, leading to the increase of the absolute value of the chiral condensate. It has been shown that the influence to the transition from vacuum to dense nuclear matter, i.e. the baryon onset, is enormous. Whereas creating nuclear matter becomes less costly with increasing magnetic field due to the increased binding energy if the magnetized Dirac sea is ignored, taking magnetic catalysis properly into account leads to an increase of the vacuum mass of the nucleon. This effect dominates the effect of the increased binding energy for sufficiently large fields, rendering the creation of nuclear matter energetically more costly with increasing field strengths, even though the binding energy is also increased by magnetic catalysis. Although both models agree qualitatively they differ quantitatively, since magnetic catalysis is more pronounced in the eLSM. We have been able to show that this difference is mostly caused by the presence of an additional baryonic state in the eLSM, the chiral partner of the nucleon, $N(1535)$. Its presence in the Dirac sea leads to a stronger magnetic catalysis, although it is to heavy to be populated in nuclear matter. For the matter part, the mass has to be compared solely to the effective chemical potential in order to check if a state contributes, whereas for the magnetized vacuum, the magnetic field sets the scale! These observation suggest that in a more complete treatment, more charged hadronic states, like pions, rho mesons or even hyperons, should be taken into account.

Our investigations open up various interesting questions which could be addressed in the future. For example, the calculations should be extended in order to account for a more realistic description of nuclear matter. First of all, the magnetic field couples only to the charged states in our approach, since we neglect the anomalous magnetic moment (AMM) of the nucleons. Previous studies have accounted for the AMM by an effective approach, but magnetic catalysis has been ignored. This approach is not renormalizable and breaks down for high magnetic fields, where magnetic catalysis is most pronounced, making a more microscopic approach desirable.

For applications to compact stars, the condition of beta equilibrium and charge neutrality have to be fulfilled as well the models have to be extended to higher densities. As this seems to be straight forward by extending existing literature by our vacuum contribution it remains to calculate if magnetic catalysis has a sizable effect on the equation of state and therefore to mass radius relations, merger processes or other phenomenons which are affected by the equation of state.

As seen in Sec. 7.1, at larger values of the chemical potential, a second phase transition can be seen in the eLSM, where the chiral symmetry is approximately restored, an effect which can not be described in the Walecka model. It would be interesting to discuss the chiral phase transition in presence of a magnetic background field in our setup. In a more complete treatment, the incorporation of a chiral asymmetric phase in form of a chiral density wave could be instructive.

A Selfconsistency equations in more detail

In this Appendix I show that the $T = 0$ approximation can be applied before taking the derivatives of the pressure w.r.t. to the condensates. Since we convert the derivative into a derivative w.r.t. to the effective mass or chemical potential, this proof is true for the Walecka model as well the extended linear sigma model (eLSM).

In the Walecka model the equations to solve are given by

$$\frac{\partial\Omega_{N,mat}}{\partial\bar{\sigma}} = \frac{\partial M}{\partial\bar{\sigma}}\frac{\partial\Omega_{N,mat}}{\partial M} = -g_\sigma\frac{\partial\Omega_{N,mat}}{\partial M} \equiv 0\,, \tag{A.1}$$

$$\frac{\partial\Omega_{N,mat}}{\partial\bar{\omega}_0} = \frac{\partial\mu_*}{\partial\bar{\omega}_0}\frac{\partial\Omega_{N,mat}}{\partial\mu_*} = -g_\omega\frac{\partial\Omega_{N,mat}}{\partial\mu_*} \equiv 0\,. \tag{A.2}$$

In the eLSM we are dealing with three condensates, so we also obtain three equations. Additionally we have to sum over the two different masses M_N and M_{N^*}, which depend on the condensates $\bar{\sigma}$ and $\bar{\chi}$. The definition of the effective chemical potential is the same in both models.

$$\frac{\partial\Omega_{N,mat}}{\partial\bar{\sigma}} = \sum_{i=N,N^*}\frac{\partial M_i}{\partial\bar{\sigma}}\frac{\partial\Omega_{N,mat}}{\partial M_i} \equiv 0\,, \tag{A.3}$$

$$\frac{\partial\Omega_{N,mat}}{\partial\bar{\sigma}} = \sum_{i=N,N^*}\frac{\partial M_i}{\partial\bar{\chi}}\frac{\partial\Omega_{N,mat}}{\partial M_i} \equiv 0\,, \tag{A.4}$$

$$\frac{\partial\Omega_{N,mat}}{\partial\bar{\sigma}} = \frac{\partial\mu_*}{\partial\bar{\omega}_0}\frac{\partial\Omega_{N,mat}}{\mu_*} \equiv 0\,, \tag{A.5}$$

where the derivatives of the masses are given by

$$\frac{\partial M_i}{\partial\bar{\sigma}} = \frac{\left(\frac{g_1+g_2}{4}\right)^2\bar{\sigma}}{\sqrt{\left(\frac{g_1+g_2}{4}\right)^2\bar{\sigma}^2+(a\bar{\chi})^2}} \pm \frac{g_1-g_2}{4}\,, \tag{A.6}$$

$$\frac{\partial M_i}{\partial\bar{\chi}} = \frac{a^2\bar{\chi}}{\sqrt{\left(\frac{g_1+g_2}{4}\right)^2\bar{\sigma}^2+(a\bar{\chi})^2}}\,. \tag{A.7}$$

The plus sign in the first equation corresponds to M_N and the minus sign to the chiral partner M_{N^*}. In the case of the $\bar{\chi}$ condensate the contributions of the two states do not differ.

The contribution of the magnetic field can now be calculated independently of the model , except for the parameter M which differs.

$$\begin{aligned}\frac{\partial\Omega_{N,mat}}{\partial M} = & -\frac{qB}{2\pi^2}\theta\left(\mu_*-M\right)\sum_{\nu=0}^{\infty}\alpha_\nu\Bigg\{-\frac{M\mu_*}{k_{F,\nu}}-2M\ln\left(\frac{k_{F,\nu}+\mu_*}{\sqrt{M^2+2\nu qB}}\right)\\ & -\frac{\left(M^2+2\nu qB\right)\sqrt{M^2+2\nu qB}}{k_{F,\nu}+\mu_*}\frac{-\frac{m_i}{k_{F,\nu}}\sqrt{M^2+2\nu qB}-\frac{M(k_{F,\nu}+\mu_*)}{\sqrt{M^2+2\nu qB}}}{M^2+2\nu qB}\Bigg\}\end{aligned} \tag{A.8}$$

Now we are going to simplify the second line of the inner bracket, using the definition of $k_{F,\nu} =$

$\sqrt{\mu_*^2 - (M^2 + 2\nu qB)}$:

$$
\begin{aligned}
&= \left\{ \frac{\sqrt{M^2 + 2\nu qB}}{k_{F,\nu} + \mu_*} \left(\frac{M}{k_{F,\nu}} \frac{\left(M^2 + 2\nu qB\right)}{\sqrt{M^2 + 2\nu qB}} + \frac{M^2 \left(k_{F,\nu} + \mu_*\right)}{\sqrt{M^2 + 2\nu qB}} \right) \right\}, \\
&= \left\{ \frac{1}{k_{F,\nu} + \mu_*} \left(\frac{M}{k_{F,\nu}} \left(M^2 + 2\nu qB\right) + M \left(k_{F,\nu} + \mu_*\right) \right) \right\}, \\
&= \left\{ \frac{M}{k_{F,\nu} + \mu_*} \left(\frac{1}{k_{F,\nu}} \left(\mu_*^2 - k_{F,\nu}^2\right) + \left(k_{F,\nu} + \mu_*\right) \right) \right\}, \qquad \text{(A.9)} \\
&= \left\{ M \left(\frac{\left(\mu_* - k_{F,\nu}\right)}{k_{F,\nu}} + 1 \right) \right\}, \\
&= \frac{M\mu_*}{k_{F,\nu}}.
\end{aligned}
$$

This term cancels the first term of the bracket in the first line, so as a final result we obtain

$$
\begin{aligned}
\frac{\partial \Omega_{N,mat}}{\partial M} &= \frac{qB}{\pi^{2}} \theta\left(\mu_* - M\right) \sum_{\nu=0}^{\infty} \alpha_\nu M \ln \left(\frac{k_{F,\nu} + \mu_*}{\sqrt{M^2 + 2\nu qB}} \right), \qquad \text{(A.10)} \\
&= n_s(qB), \qquad \text{(A.11)}
\end{aligned}
$$

where we have introduced the scalar density n_s for charged fermions as follows:

$$
n_s(qB) = \frac{\partial \Omega_{N,mat}(qB)}{\partial M} = \frac{qB}{\pi^{2}} \theta\left(\mu_* - M\right) \sum_{\nu=0}^{\infty} \alpha_\nu M \ln \left(\frac{k_{F,\nu} + \mu_*}{\sqrt{M^2 + 2\nu qB}} \right). \qquad \text{(A.12)}
$$

The uncharged part is very similar to calculate,

$$
\begin{aligned}
\frac{\partial \Omega_{N,mat}}{\partial M} &= -\frac{\partial}{\partial M} \left\{ \frac{\Theta\left(\mu_* - M\right)}{8\pi^2} \left[\left(\frac{2}{3} k_F^3 - M^2 k_F \right) \mu_* + M^4 \ln \frac{k_F + \mu_*}{M} \right] \right\}, \\
&= -\frac{\Theta\left(\mu_* - M\right)}{8\pi^2} \left[-k_F M \mu_* - \frac{M^3}{k_F} \mu_* + 4M^3 \ln \frac{k_F + \mu_*}{M} - M^3 + \frac{M^5}{k_F \left(k_F + \mu_*\right)} \right], \\
&= -\frac{\Theta\left(\mu_* - M\right)}{8\pi^2} M^3 \left[-\frac{k_F \mu_*}{M} - \frac{\mu_*}{k_F} + 4 \ln \frac{k_F + \mu_*}{M} - 1 + \frac{\left(\mu_* - k_F\right)\left(\mu_* + k_F\right)}{k_F \left(k_F + \mu_*\right)} \right], \\
&= -\frac{\Theta\left(\mu_* - M\right)}{8\pi^2} M^3 \left[-\frac{k_F \mu_*}{M} - \frac{\mu_*}{k_F} + 4 \ln \frac{k_F + \mu_*}{M} - 1 + \frac{\left(\mu_* - k_F\right)}{k_F} \right], \\
&= -\frac{\Theta\left(\mu_* - M\right)}{8\pi^2} M^3 \left[-\frac{k_F \mu_*}{M} - \frac{\mu_*}{k_F} + 4 \ln \frac{k_F + \mu_*}{M} - 1 + \frac{\left(\mu_* - k_F\right)}{k_F} \right], \\
&= \frac{\Theta\left(\mu_* - M\right) M}{2\pi^2} \left[k_F \mu_* - M^3 \ln \frac{k_F + \mu_*}{M} \right], \\
&= n_s\left(qB = 0\right). \qquad \text{(A.13)}
\end{aligned}
$$

In the last line we have defined in complete analogy to the magnetic case the scalar density

$$
n_s\left(qB = 0\right) = \frac{\partial \Omega_{N,mat}}{\partial M} \left(qB = 0\right) = \frac{\Theta\left(\mu_* - M\right) M}{2\pi^2} \left[k_F \mu_* - M^3 \ln \frac{k_F + \mu_*}{M} \right]. \qquad \text{(A.14)}
$$

The derivative w.r.t. the effective chemical potential is also split into a charged and an uncharged contribution. Including the magnetic field, one obtains

$$
\begin{aligned}
\frac{\partial\Omega_{N,mat}}{\partial\mu_*} &= -\frac{\partial}{\partial\mu_*}\left\{\frac{qB}{4\pi^2}\Theta\left(\mu_*-M\right)\sum_{\nu=0}^{\nu_{max}}\alpha_\nu\left[\mu_* k_{F,\nu}-\left(M^2+2\nu qB\right)\ln\frac{k_{F,\nu}+\mu_*}{\sqrt{M^2+2\nu qB}}\right]\right\}\,, \\
&= -\frac{qB}{4\pi^2}\Theta\left(\mu_*-M\right)\sum_{\nu=0}^{\nu_{max}}\alpha_\nu\left[k_{F,\nu}+\frac{\mu_*^2}{k_{F,\nu}}-\frac{\left(M^2+2\nu qB\right)}{k_{F,\nu}}\right]\,, \\
&= -\frac{qB}{4\pi^2}\Theta\left(\mu_*-M\right)\sum_{\nu=0}^{\nu_{max}}\alpha_\nu\left[k_{F,\nu}+\frac{\mu_*^2}{k_{F,\nu}}-\frac{\mu_*^2-k_{F,\nu}^2}{k_{F,\nu}}\right]\,, \\
&= -\frac{qB}{2\pi^2}\Theta\left(\mu_*-M\right)\sum_{\nu=0}^{\nu_{max}}\alpha_\nu k_{F,\nu}\,, \\
&= -n_B(qB)\,,
\end{aligned}
\tag{A.15}
$$

where we found the negative of the baryon density for charged fermions,

$$
n_B = \frac{qB}{2\pi^2}\Theta\left(\mu_*-M\right)\sum_{\nu=0}^{\nu_{max}}\alpha_\nu k_{F,\nu}\,. \tag{A.16}
$$

For uncharged fermions the derivation is again not very different,

$$
\begin{aligned}
\frac{\partial\Omega_{N,mat}}{\partial\mu_*} &= -\frac{\partial}{\partial\mu_*}\left\{\frac{\Theta\left(\mu_*-M\right)}{8\pi^2}\left[\left(\frac{2}{3}k_F^3-M^2k_F\right)\mu_*+M^4\ln\frac{k_F+\mu_*}{M}\right]\right\}\,, \qquad \text{(A.17)} \\
&= -\frac{\Theta\left(\mu_*-M\right)}{8\pi^2}\left[\left(2k_F\mu_*-M^2\frac{\mu_*}{k_F}\right)\mu_*+\left(\frac{2}{3}k_F^3-M^2k_F\right)+\frac{M^4}{k_F}\right]\,, \\
&= -\frac{\Theta\left(\mu_*-M\right)}{8\pi^2}\left[\frac{8}{3}k_F^3+k_FM^2-M^2\frac{\mu_*^2}{k_F}+M^2\frac{\mu_*^2-k_F^2}{k_F}\right]\,, \\
&= -\frac{\Theta\left(\mu_*-M\right)}{8\pi^2}\left[\frac{8}{3}k_F^3\right]\,, \\
&= -\frac{\Theta\left(\mu_*-M\right)}{3\pi^2}k_F^3\,, \\
&= n_B(qB=0)\,.
\end{aligned}
$$

In the last line the expression for the uncharged baryon number density appears,

$$
n_B(qB=0) = -\frac{\partial\Omega_{N,mat}}{\partial\mu_*} = \Theta\left(\mu_*-M\right)\frac{k_F^3}{3\pi^2}\,. \tag{A.18}
$$

If one compares these result to the derivation in the main text one can indeed see that it does not matter at which point the $T=0$ approximation is applied.

B Renormalization of the B-independent vacuum in the Walecka model

In this appendix I want to show that the B-independent vacuum contribution in the Walecka model is negligible at the onset. Therefore, we have to regularize the integral

$$\Omega_{vac} = -4 \int \frac{d^3\boldsymbol{k}}{(2\pi)^3} \epsilon_k \,, \tag{B.1}$$

with $\epsilon_k = \sqrt{k^2 + M_N^2}$, which is indefinite. Carrying out the angular integral after changing to spherical coordinates yields

$$\Omega_{vac} = -\frac{4 \cdot 4\pi}{8\pi^3} \int_o^\infty dk\, k^2 \sqrt{k^2 + M_N^2} \,. \tag{B.2}$$

There are three possibilities to regularize this divergent integral:

1. We can simply take the result from our calculations including the magnetic field and multiply the result for $B \to 0$ by a factor of 2 because of the isospin degeneracy.
2. We can use the proper time regularization again where we use the Schwinger representation only for the dispersion relation and multiply the resulting proper time integral with the factor k^2 arising from the Jacobi determinant.
3. We can use a simple momentum cutoff for the integral.

I will proceed with number the third option, which leads, as expected, to the same result as method two that is shown in the appendix of Ref. [51]. The B-independent vacuum contribution with the momentum cutoff Λ is given by

$$\Omega_{vac} = -\frac{2}{\pi^2} \int_o^\Lambda dk k^2 \sqrt{k^2 + M_N^2} \,. \tag{B.3}$$

This integral can be solved analytically and can be expanded into a power series where we neglect all terms indirect proportional to Λ or even lower since they vanish in the limit $\Lambda \to \infty$.

$$\Omega_{vac} = -\frac{\Lambda^4}{2\pi^2} - \frac{M_N^2 \Lambda^2}{2\pi^2} - \frac{M_N^4}{16\pi^2} - \frac{M_N^4 \ln\left(\frac{M_N}{2\Lambda}\right)}{4\pi^2} \,. \tag{B.4}$$

In order to separate the effective mass and the cutoff in the logarithm we introduce a renormalization scale ℓ and add it to the energy via the identity $0 = \ln 1 = \ln \frac{\ell}{\ell}$.

$$\Omega_{vac} = -\frac{\Lambda^4}{2\pi^2} - \frac{M_N^2 \Lambda^2}{2\pi^2} - \frac{M_N^4}{16\pi^2} - \frac{M_N^4}{4\pi^2} \left(\ln\left(\frac{M_N}{\ell}\right) - \ln\left(\frac{2\Lambda}{\ell}\right) \right) \,. \tag{B.5}$$

No we include counterterms to our Lagrangian up to the fourth order of the scalar meson condensate, where we additionally add a linear term:

$$b = b_r + \delta b, \qquad c = c_r + \delta c, \qquad m_\sigma^2 = m_{\sigma,r}^2 + \delta m_\sigma^2 \,. \tag{B.6}$$

The new part of the Lagrangian is termed $\delta\mathcal{L}$ and looks like

$$\delta\mathcal{L} = -\delta a m_N^3 \left(g_\sigma \sigma\right) - \frac{\delta m_\sigma^2}{2}\sigma - \frac{\delta b}{3} m_N \left(g_\sigma \sigma\right)^3 - \frac{\delta c}{4}\left(g_\sigma \sigma\right)^4 \,, \tag{B.7}$$

where we have added appropriate factors of the nucleon mass in order to keep the couplings dimensionless. The corresponding change in the tree-level potential, sorted in orders of the effective mass M_N, reads

$$\begin{aligned}\delta U &= \left(\delta a + \frac{\delta m_\sigma^2}{2 g_\sigma^2 m_N^2} + \frac{\delta b}{3} + \frac{\delta c}{4}\right) m_N^4 - \left(\delta a + \frac{\delta m_\sigma^2}{g_\sigma^2 m_N^2} + \delta b + \delta c\right) m_N^3 M_N \\ &+ \left(\frac{\delta m_\sigma^2}{2 g_\sigma^2 m_N^2} + \delta b + \frac{3\delta c}{2}\right) m_N^2 M_N^2 - \left(\frac{\delta b}{3} + \delta c\right) m_N M_N^3 + \frac{\delta c}{4} M_N^4 \,. \end{aligned} \tag{B.8}$$

Since the dynamical mass M_N depends implicitly on μ and T, also some of the cutoff dependent terms are altered with changing temperature and chemical potential. Therefore, we require the counterterms to cancel the cutoff terms in each order of the cutoff and obtain a nested system of coupled equations for the counterterms:

$$\left(\delta a + \frac{\delta m_\sigma^2}{g_\sigma^2 m_N^2} + \delta b + \delta c\right) m_N^3 = 0 \,, \tag{B.9}$$

$$\left(\frac{\delta m_\sigma^2}{2 g_\sigma^2 m_N^2} + \delta b + \frac{3\delta c}{2}\right) m_N^2 = -\frac{\Lambda^2}{2\pi^2} \,, \tag{B.10}$$

$$-\left(\frac{\delta b}{3} + \delta c\right) m_N = 0 \,, \tag{B.11}$$

$$\frac{\delta c}{4} = -\frac{1}{16\pi^2} + \frac{1}{4\pi^2}\ln\left(\frac{2\Lambda}{\ell}\right) . \tag{B.12}$$

The last equation determines $\delta c = -\frac{1}{4\pi^2} - +\frac{1}{\pi^2}\ln\left(\frac{\Lambda}{\ell}\right)$ directly. By inserting the solution upstairs like in a pyramid we obtain:

$$\delta c = -\frac{1}{4\pi^2} + \frac{1}{\pi^2}\ln\left(\frac{2\Lambda}{\ell}\right) = \frac{1}{\pi^2}\ln\left(\frac{\Lambda}{\ell'}\right) , \tag{B.13}$$

$$\delta b = -3\delta c = \frac{3}{4\pi^2} - \frac{3}{\pi^2}\ln\left(\frac{2\Lambda}{\ell}\right) = -\frac{3}{\pi^2}\ln\left(\frac{\Lambda}{\ell'}\right) , \tag{B.14}$$

$$\frac{\delta m_\sigma^2}{g_\sigma^2 m_N^2} = -\frac{\Lambda^2}{m_N^2\pi^2} + 3\delta c = -\frac{\Lambda^2}{m_N^2\pi^2} + \frac{3}{\pi^2}\ln\left(\frac{\Lambda}{\ell'}\right) , \tag{B.15}$$

$$\delta a = 2\delta c - \frac{\delta m_\sigma^2}{g_\sigma^2 m_N^2} = \frac{\Lambda^2}{m_N^2\pi^2} + \frac{1}{4\pi^2} - \frac{1}{\pi^2}\ln\left(\frac{2\Lambda}{\ell}\right) = \frac{\Lambda^2}{m_N^2\pi^2} - \frac{1}{\pi^2}\ln\left(\frac{\Lambda}{\ell'}\right) . \tag{B.16}$$

Here we have absorbed the constant term $\frac{1}{4}$ into a new renormalization scale $\ell' = \frac{1}{2}\exp\left(\frac{1}{4}\right)\ell$. Now, per construction, all terms beside the one proportional to M_N^0 vanish in δU. To all calculated counterterms we can add a finite, cutoff independent contribution which we will call $\delta\tilde{a}$, and so on. Finally, the free energy reads

$$\Omega = -\frac{\Lambda^4}{2\pi^2} - \frac{m_N^4}{4\pi^2}\ln\frac{\Lambda}{\ell'} + \frac{\Lambda^2 m_N^2}{2\pi^2} + U + \Delta\Omega_N + \Omega_{N,mat} \,. \tag{B.17}$$

The tree-level potential U and the matter contribution now only depend on the renormalized quantities and $\Delta\Omega_N$ is given by

$$\Delta\Omega_N = \delta\tilde{a} m_N^3 (g_\sigma\bar{\sigma}) + \frac{\delta\tilde{m}_\sigma^2}{2}\bar{\sigma}^2 + \frac{\delta\tilde{b}}{3} m_N (g_\sigma\bar{\sigma})^3 + \frac{\delta\tilde{c}}{4}(g_\sigma\bar{\sigma})^4 - \frac{M_N^4}{8\pi^2}\ln\left(\frac{M_N^2}{\ell^2}\right) . \tag{B.18}$$

We may require the finite (tilded) counterterms to cancel the higher than fourth order terms of $\bar{\sigma}$,$\mathcal{O}(\bar{\sigma}^4)$, in $\Delta\Omega_N$, in such a way that it only changes the free energy in fifth order of the condensate or higher. For this purpose we expand the logarithmic term around $\bar{\sigma} = 0$ up to the fourth order and require each order of $\bar{\sigma}$ to vanish separately.

$$
\begin{aligned}
-\frac{M_N^4}{8\pi^2}\ln\frac{M_N^2}{\ell^2} &= -\frac{1}{8\pi^2}\left(m_N - g_\sigma\bar{\sigma}\right)^4 \ln\left(\frac{\left(m_N - g_\sigma\bar{\sigma}\right)^2}{\ell^2}\right) \qquad \text{(B.19)}\\
&= -\frac{1}{8\pi^2}\ln\frac{m_N^2}{\ell^2} + \frac{1}{4\pi^2}g_\sigma m_N\left(1 + 2\ln\frac{m_N^2}{\ell^2}\right)\bar{\sigma} - \frac{g_\sigma m_N^2}{8\pi^2}\left(7 + 6\ln\frac{m_N^2}{\ell^2}\right)\bar{\sigma}^2\\
&\quad + \frac{g_\sigma^3 m_N}{12\pi^2}\left(13 + 6\ln\frac{m_N^2}{\ell^2}\right)\bar{\sigma}^3 - \frac{g_\sigma^4}{48\pi^2}\left(25 + 6\ln\frac{m_N^2}{\ell^2}\right)\bar{\sigma}^4 + \mathcal{O}\left(\bar{\sigma}^5\right).
\end{aligned}
$$

Comparison order by order yields

$$
\begin{aligned}
\delta\tilde{a} &= -\frac{1}{4\pi^2}\left(1 + 2\ln\frac{m_N^2}{\ell^2}\right), &\text{(B.20)}\\
\frac{\delta\tilde{m}_\sigma^2}{g_\sigma^2 m_N^2} &= \frac{1}{4\pi^2}\left(7 + 6\ln\frac{m_N^2}{\ell^2}\right), &\text{(B.21)}\\
\delta\tilde{b} &= -\frac{1}{4\pi^2}\left(13 + 6\ln\frac{m_N^2}{\ell^2}\right), &\text{(B.22)}\\
\delta\tilde{c} &= \frac{1}{12\pi^2}\left(25 + 6\ln\frac{m_N^2}{\ell^2}\right). &\text{(B.23)}
\end{aligned}
$$

If we require that $\bar{\sigma} = 0$, i.e. $M_N = m_N$, stays the solution of the vacuum equations we have to choose the renormalization scale $\ell = m_N$. The change in the free energy due to the counter terms then reads

$$
\Delta\Omega_N = -\frac{1}{4\pi^2}\left[m_N^3(g_\sigma\bar{\sigma}) - \frac{7}{2}m_N^2(g_\sigma\bar{\sigma})^2 + \frac{13}{3}m_N(g_\sigma\bar{\sigma})^3 - \frac{25}{12}(g_\sigma\bar{\sigma})^4 + M_N^4\ln\frac{M_N}{m_N}\right]. \qquad \text{(B.24)}
$$

This additional term has to be considered in the self-consistency equations, its derivative is given by

$$
\begin{aligned}
\frac{\partial\left(\Delta\Omega_N\right)}{\partial\bar{\sigma}} &= -\frac{1}{4\pi^2}\left[m_N^3 g_\sigma - 7m_N^2 g_\sigma^2\bar{\sigma} + 13 m_N g_\sigma^3\bar{\sigma}^2 - \frac{25}{3}g_\sigma^4\bar{\sigma}^3 - g_\sigma 4M_N^3\ln\frac{M_N}{m_N} - g_\sigma M_N^3\right],\\
&= \frac{g_\sigma}{\pi^2}\left[m_N^2\left(g_\sigma\bar{\sigma}\right) - \frac{5}{2}m_N\left(g_\sigma\bar{\sigma}\right)^2 + \frac{11}{6}\left(g_\sigma\bar{\sigma}\right)^3 + M_N^3\ln\frac{M_N}{m_N}\right], \qquad \text{(B.25)}
\end{aligned}
$$

where we have inserted the definition for the effective mass into the pure cubic term to obtain the second line. For the parameter fit we require our model to reproduce the compression modulus K. In the calculation of K we can see $\Delta\Omega_N$ as additional part to the tree-level potential and perform the same fit procedure as in the no sea approximation. The parameters we obtain are

g_ω	g_σ	b	c
8.1617	8.5062	1.0784×10^{-2}	-6.22205×10^{-3}

.

The negative value of the parameter c leads to an unbounded tree-level potential for $\bar{\sigma}$. This problem can be cured by including the exchange of ρ mesons in the nucleon nucleon interaction, see Refs. [34, 38, 39, 65]. In these references also a vacuum contribution $\Delta\Omega_\sigma$ due to σ loop contributions is included. This contribution can be found in the references mentioned above and reads

$$
\Delta\Omega_\sigma = \frac{m_\sigma^4}{(8\pi)^2}\left[(1+\phi_3)^2\ln(1+\phi_3) - \phi_3 - \frac{3}{2}\phi_3^2 - \frac{1}{3}\phi_1^2(\phi_1 + 3\phi_2) + \frac{1}{12}\phi_1^4\right], \qquad \text{(B.26)}
$$

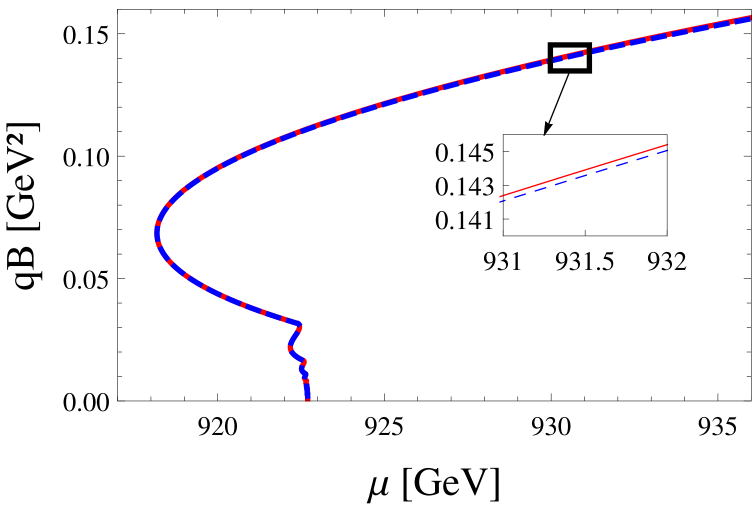

Figure B.1: Effect of the B-independent sea contribution $\Delta\Omega_N$ to the onset of nuclear matter in the Walecka model. The difference between the dashed line, which includes the correction, and the solid line, where only the B-dependent sea contribution is taken into account, is barley visible. Therefore, this correction is neglected in the main part of this thesis.

with the abbreviations

$$\phi_1 \equiv 2bm_N\frac{g_\sigma^2}{m_\sigma^2}(g_\sigma\bar{\sigma})\,, \qquad \phi_2 \equiv 3c\frac{g_\sigma^2}{m_\sigma^2}(g_\sigma\bar{\sigma})^2\,, \qquad \phi_3 \equiv \phi_1 + \phi_2\,. \tag{B.27}$$

Additionally including this contribution, the parameter set has to be changed again where $\Delta\Omega_\sigma$ can bee seen as a change of the tree-level potential in the calculations. The set of parameters we obtain are

g_ω	g_σ	b	c
8.1617	8.1487	5.2855×10^{-3}	-2.3611×10^{-2}

.

In the mean field approximation, all meson loops are neglected in the medium, therefore I neglect this contribution in the vacuum too and will proceed solely with $\Delta\Omega_N$.

It is now straightforward to extend this renormalization to the case with nonvanishing magnetic field. We can simply treat the B-independent and B-dependent vacuum contributions separately, i.e. we can put together the result from the main part and the result from this appendix,

$$\Omega = U + \Delta\Omega_N + \frac{B^2}{2} + \Omega_{N,\text{sea}} + \Omega_{N,\text{mat}}\,, \tag{B.28}$$

with $\frac{B^2}{2} + \Omega_{N,\text{sea}}$ given in Eq.(3.56). In the B-independent sea contribution discussed here, a specific choice of ℓ is needed in order to keep $\bar{\sigma} = 0$ a solution of the vacuum equations. In contrast, in the B-dependent sea contribution, ℓ only appears in a constant term, and the specific choice of ℓ does not matter for our purposes. Therefore, any choice (such as $\ell = m_N$) is compatible with the renormalization discussed in the main text of this thesis.

The influence of this additional terms in the free energy on the vacuum masses and the onset is shown in Fig. B.2 and Fig. B.2. For the vacuum masses the change is visible but rather small whereas at the onset the difference between the two curves is barley visible and shown in the inset of the figure. For the onset, only $\Delta\Omega_N$ was taken into account due to the reasons mentioned before. Since all these contributions change the results only quantitatively, but have no influence on the nature of the results presented in this thesis, it seems justified to neglect the loop contributions for the biggest part of our calculations.

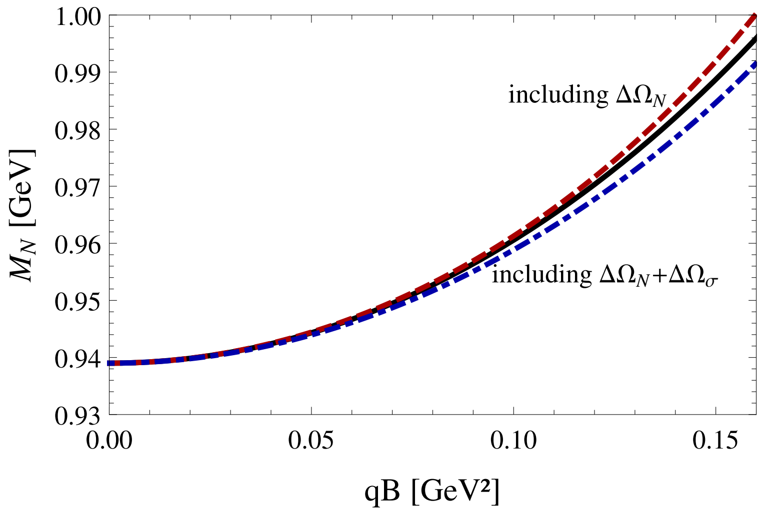

Figure B.2: Effects of the nucleon and meson loop corrections to the vacuum mass of the nucleon in the Walecka model as a function of the magnetic field. The black, solid line is the same shown in the main text, the dashed line includes the nucleon loop corrections and the dash-dotted line takes both, meson and nucleon loop corrections into account.

C Vacuum solution in the eLSM

In this appendix I want to show how to rewrite the general solution for the chiral condensate in the vacuum by using the relations for the parameters derived in Sec. 5.1. Our requirement $\bar{\sigma} = Zf_\pi$, where $f_\pi = 92.4$ MeV represents the pion decay constant and $Z = 1.67$ is the pion wave function renormalization constant, yields a numerical value of $\bar{\sigma} = 154.3$ MeV. The equation to solve is the vacuum self-consistency equation for the chiral condensate,

$$\epsilon + m^2\bar{\sigma} - \lambda\bar{\sigma}^3 + \frac{2g^2\bar{\sigma}^3}{m_\chi^2} = 0\,, \tag{C.1}$$

where I have already used $\bar{\chi} = \frac{g\bar{\sigma}^2}{m_\chi^2}$. The relations we use for the constants are derived in Sec. 5.1,

$$\lambda = \frac{1}{2\,(Zf_\pi)^2}\left(m_\sigma^2 - \frac{m_\pi^2}{Z^2}\right),\; m^2 = \frac{1}{2}\left(m_\sigma^2 - \frac{3m_\pi^2}{Z^2}\right) - \frac{2g^2\,(Zf_\pi)^2}{m_\chi^2},\; \epsilon = \frac{f_\pi m_\pi^2}{Z}\,. \tag{C.2}$$

Inserting this in Eq. (C.1) yields

$$\frac{f_\pi m_\pi^2}{Z} + \frac{1}{2}\left(m_\sigma^2 - \frac{3m_\pi^2}{Z^2}\right)\bar{\sigma} - \frac{1}{2\,(Zf_\pi)^2}\left(m_\sigma^2 - \frac{m_\pi^2}{Z^2}\right)\bar{\sigma}^3 \quad = \quad 0\,, \tag{C.3}$$

where we have backtranslated $Zf_\pi = \bar{\sigma}$ in order to cancel the terms proportional to $\frac{g\bar{\sigma}^3}{m_\chi^2}$. This equation is obviously fulfilled for $\bar{\sigma} = Zf_\pi$, which can be checked by insertion. The general solution to Eq. (C.1), found by solving it directly using the analytic solution for cubic polynomials is given by

$$\bar{\sigma} = \frac{2m}{\underbrace{\sqrt{3}\sqrt{\lambda - \frac{2g^2}{m_\chi^2}}}_{:=c}}\cos\left[\frac{1}{3}\arccos\left(\frac{3\sqrt{3}\epsilon}{2m^3}\sqrt{\lambda - \frac{2g^2}{m_\chi^2}}\right)\right] \approx 154.3\,\mathrm{MeV}\,, \tag{C.4}$$

where we inserted the constants obtained by the parameter fit performed in Sec. 5.1. Since the numerical values coincident, it should be possible to show the conjecture between the two solutions analytically. This means that I want to proof that, if we insert the relations between the parameters and the constants given in (C.2), we end up with $\bar{\sigma} = Zf_\pi$ again.

$$\bar{\sigma} = \frac{2m}{\sqrt{3}c} \cos\left[\frac{1}{3}\arccos\left(\frac{3\sqrt{3}\epsilon}{2m^3}c\right)\right], \tag{C.5}$$

$$\frac{\sqrt{3}c\bar{\sigma}}{2m} = \cos\left[\frac{1}{3}\arccos\left(\frac{3\sqrt{3}\epsilon}{2m^3}c\right)\right], \tag{C.6}$$

$$\arccos\left(\frac{\sqrt{3}c\bar{\sigma}}{2m}\right) = \frac{1}{3}\arccos\left(\frac{3\sqrt{3}\epsilon}{2m^3}c\right). \tag{C.7}$$

Now we use the fact the the $\arccos(z)$ of a complex number z can be expressed as the principal branch of the complex natural logarithm,

$$\arccos z = -i \ln\left(x + i\sqrt{1-x^2}\right). \tag{C.8}$$

We apply this to the last line of the recent equation and cancel the factor $-i$ on both sides. Then we use the general rules for the natural logarithm to absorb the factor $\frac{1}{3}$ into the argument: $\frac{1}{3}\ln x = \ln x^{\frac{1}{3}}$. This allows us to apply the exponential function on both sides which cancels the logarithm and yields

$$\left(\frac{\sqrt{3}c\bar{\sigma}}{2m}\right) + i\sqrt{1 - \frac{3c^2\bar{\sigma}^2}{4m^2}} = \left\{\frac{3\sqrt{3}\epsilon}{2m^3}c + i\sqrt{1 - \frac{27\epsilon^2}{4m^3}c^2}\right\}^{1/3}, \tag{C.9}$$

$$\left\{\left(\frac{\sqrt{3}c\bar{\sigma}}{2m}\right) + i\sqrt{1 - \frac{3c^2\bar{\sigma}^2}{4m^2}}\right\}^3 = \left\{\frac{3\sqrt{3}\epsilon}{2m^3}c + i\sqrt{1 - \frac{27\epsilon^2}{4m^3}c^2}\right\}. \tag{C.10}$$

Now we compare the real and the imaginary part of the equation above separately. The cube of a complex number of the form $(a + ib)$ with $a, b \in \mathbb{R}$ is given by

$$(a + ib)^3 = \left(a^3 - 3ab^2\right) + i\left(3a^2b - b^3\right). \tag{C.11}$$

The real part of the equation is hence computed to be

$$\begin{aligned}
\left(\frac{\sqrt{3}c\bar{\sigma}}{2m}\right)^3 - 3\left(\frac{\sqrt{3}c\bar{\sigma}}{2m}\right)\left(1 - \frac{3c^2\bar{\sigma}^2}{4m^2}\right) &= \frac{3\sqrt{3}\epsilon}{2m^3}c, \\
\frac{c^2\bar{\sigma}^3}{4} - \bar{\sigma}\left(m^2 - \frac{3}{4}c^2\bar{\sigma}^2\right) &= \epsilon, \\
\epsilon + m^2\bar{\sigma} + \left\{-\frac{3}{4}c^2 - \frac{1}{4}c^2\right\}\bar{\sigma}^3 &= 0, \\
\epsilon + m^2\bar{\sigma} - \lambda\bar{\sigma}^3 + \frac{2g^2}{m_\chi^2}\bar{\sigma}^3 &= 0.
\end{aligned} \tag{C.12}$$

In the last line we reinserted the definition of $c^2 := \lambda - \frac{2g^2}{m_\chi^2}$. Since we have backtransformed the general solution to the original equation, which is solved, as seen before, by $\bar{\sigma} = Zf_\pi$, we have proven the equivalence of the two solutions. As a check we calculate the imaginary part too:

$$\sqrt{1-\frac{27\epsilon^2}{4m^3}c^2} \;=\; 3\left(\frac{\sqrt{3}c\bar{\sigma}}{2m}\right)^2\sqrt{1-\frac{3c^2\bar{\sigma}^2}{4m^2}}-\left(1-\frac{3c^2\bar{\sigma}^2}{4m^2}\right)^{3/2}, \tag{C.13}$$

$$\begin{aligned}1-\frac{27\epsilon^2}{4m^3}c^2 \;=\;& \left(\frac{27}{4}\frac{c^2\bar{\sigma}^2}{m^2}\right)^2\left(1-\frac{3c^2\bar{\sigma}^2}{4m^2}\right)+\\ &\left(1-\frac{3c^2\bar{\sigma}^2}{4m^2}\right)^3-6\left(\frac{\sqrt{3}c\bar{\sigma}}{2m}\right)^2\left(1-\frac{3c^2\bar{\sigma}^2}{4m^2}\right)^2.\end{aligned} \tag{C.14}$$

In this case the easiest way to proceed is to insert the ansatz $\bar{\sigma} = Zf_\pi$ and the parameters from Eq. ((C.2)) and to show that this identity is true which can be done by hand or with the help of Mathematica. Inserting the parameters and abbreviating $a := m_\sigma^2 - \frac{m_\pi^2}{Z^2}$, $b := m_\sigma^2 - \frac{3m_\pi^2}{Z^2}$ one ends up with

$$\frac{81}{16}\left(\frac{a}{b}\right)^2\left(1-\frac{3}{4}\frac{a}{b}\right)+\left(1-\frac{3}{4}\frac{a}{b}\right)^3-\frac{9}{2}\frac{a}{b}\left(1-\frac{3}{4}\frac{a}{b}\right)^2 \;=\; 1-\frac{27m_\pi^4}{Z^4}\frac{a}{b^3}, \tag{C.15}$$

$$\frac{27a\left[Z^4\left(a-b\right)^2-4m_\pi^4\right]}{4b^3Z^4} \;=\; 0, \tag{C.16}$$

$$27a\left[Z^4\frac{4m_\pi^4}{Z^4}-4m_\pi^4\right] \;=\; 0, \tag{C.17}$$

$$4m_\pi^4 \;=\; 4m_\pi^4\,.\,q.e.d. \tag{C.18}$$

This finally proves the equivalence of the solutions if the parameters are related as in ((C.2)).

m_σ [MeV]	m_ω [MeV]	m_N [MeV]	g_ω	g_σ	b	c
550	782	939	8.672	8.685	7.950×10^{-3}	6.952×10^{-4}

Table D.1: Different parameter set for the Walecka model. All properties at saturation are taken from Tab. 4.1, except for the effective mass at the onset, which is changed to $M_N = 0.78\, m_N$.

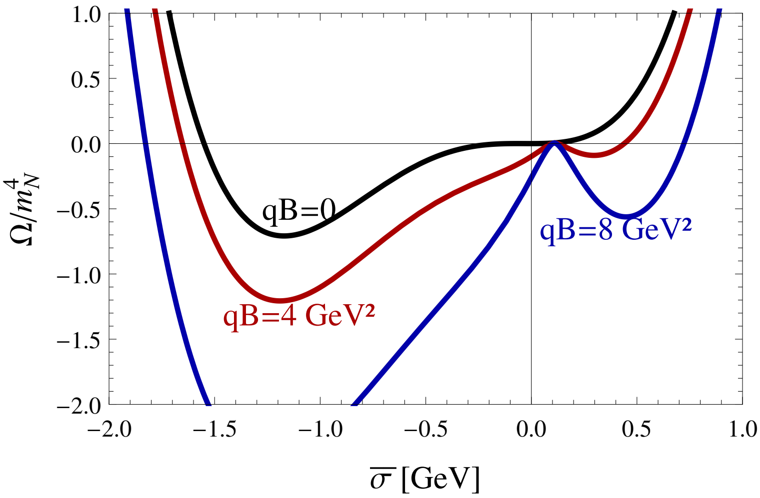

Figure D.1: Free energy in the Walecka model for different background fields with the alternative parameter set. For small or zero magnetic field there is a local minimum close to $\bar{\sigma} = 0$, which is the only existent solution in the parameter set of the main text. In this set there is always a nearly constant global minimum at large negative values of the condensate. At large magnetic fields, a second local minimum around $\bar{\sigma} = 0.5$ GeV develops, whereas a local maximum at small negative values only exists at small magnetic fields.

D Walecka model with different parameter set

In this appendix I want to show that some properties of the vacuum solutions and the baryon onset are indeed dependent on the choice of parameters. However, the conclusions from the main text are not changed.

For this appendix we fit all parameters to the same saturation properties except for the effective mass at the onset, which is chosen to be $M_N = 0.78\, m_N$, leading to the parameters which are often found in standard literature [38, 53] and are presented in Tab. D.1. For $B = 0$ there are, beside the physical solution $\bar{\sigma} = 0$, other solutions for the scalar condensate in the vacuum. Inserting these parameters into the solution of the quadratic equation, given in Eq. (6.2), one obtains for the condensate respectively the mass

$$\begin{aligned} \bar{\sigma} &= -0.0654\,\text{GeV} &\rightarrow\quad & M_{N,2} = 1.5067\,\text{GeV}\,, \\ \bar{\sigma} &= -1.1711\,\text{GeV} &\rightarrow\quad & M_{N,1} = 11.1106\,\text{GeV}\,. \end{aligned} \tag{D.1}$$

These three solutions and their dependence on the magnetic field can be read off from the free energy, which is shown in Fig. D.1.

In comparison to the main text, the free energy now shows several extremal values. In the vacuum, $\bar{\sigma} = 0$ stays a solution to the gap equations, which ceases to exist around $qB = 0.3\,\text{GeV}^2$. For all field strengths, there exists a rather constant global minimum at large negative values of the condensate, which means that this solution is actually preferred from a energetic point of view. For larger magnetic fields, a local maximum, which is of no physical interest, vanishes and another local minimum at positive values of $\bar{\sigma}$ starts to exist. These other minima are both energetically

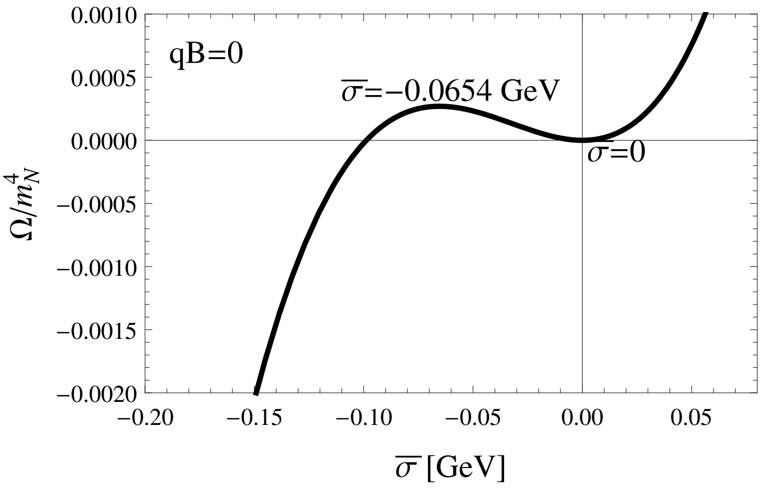

Figure D.2: Zoom in of the vacuum free energy at $qB = 0$. Beside the physical solution $\bar{\sigma} = 0$, a local maximum at $\bar{\sigma} = -0.0654$ GeV can be seen, which converges with increasing magnetic field to the local minimum developing from $\bar{\sigma} = 0$ and ceases to exist at the same time.

preferred, but lead to very unphysical, i.e. unnatural high or negative, values of the effective mass, rendering the physical solution a metastable state. However, since these extrema strongly depend on the choice of parameters, and only the physical solution always exists, it is safe to neglect these other states. In Fig. D.2 I present a zoom in to the physical solution at $qB = 0$, where a local maximum can be seen too. With increasing field, this maximum converges to the physical vacuum solution and both ceases to exist at the same time .

The exact behavior of these extrema, which are the expectation value of the condensate $\bar{\sigma}$ in the vacuum, are shown in Fig. D.3.

D.1 B=0 Solutions

The change in the structure of the free energy also reflects in the behavior of the effective mass as a function of the chemical potential at vanishing background magnetic field, see Fig. D.4. Since there are three vacuum solutions, they complete structure of the matter part is "S-shaped". At the vacuum solutions, the "S" would enter the shaded vacuum area and is cut out. If the magnetic field is that high, that the lowest two solutions do not exist any more, the "S" is completely right of the vacuum boundary. It is instructive to study the form of the free energy for this case, which is done in Fig. D.5. In principle there are three constant, μ-independent solutions, whereas two of them can only be distinguished in the inset, which is a zoom in. The part of the free energy, which allows us to determine the onset at $\mu_0 = 922.7$ MeV and is presented in the main text, is barley visible even in the inset and is marked by the second dashed box (in the inset). Since the physical parts of the free energy and the mass as a function of the chemical potential to not differ qualitatively from the ones presented in the main text, they are omitted in this appendix.

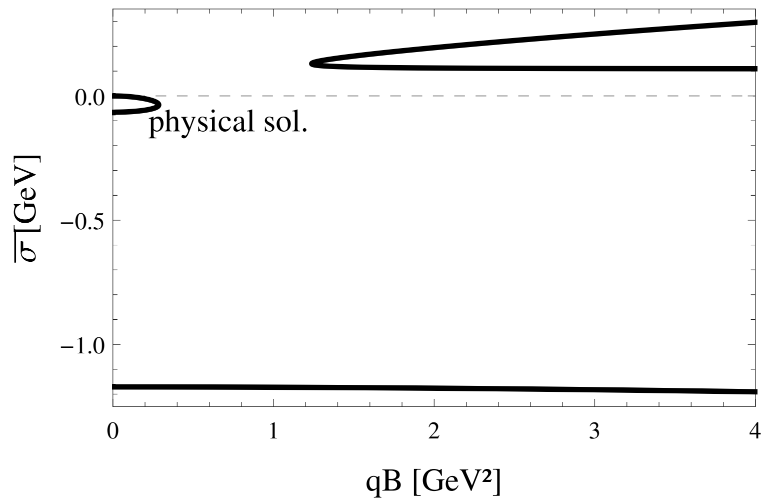

(a) All solutions to the gap equation for the scalar condensate as a function of the magnetic field. The rather constant solution at large negative values of the condensate, i.e. for a huge effective mass, is actually preferred and has to be neglected. The positive solutions, starting around $qB = 1.3\,\mathrm{GeV}^2$, lead to unphysical negative masses and have to be neglected too.

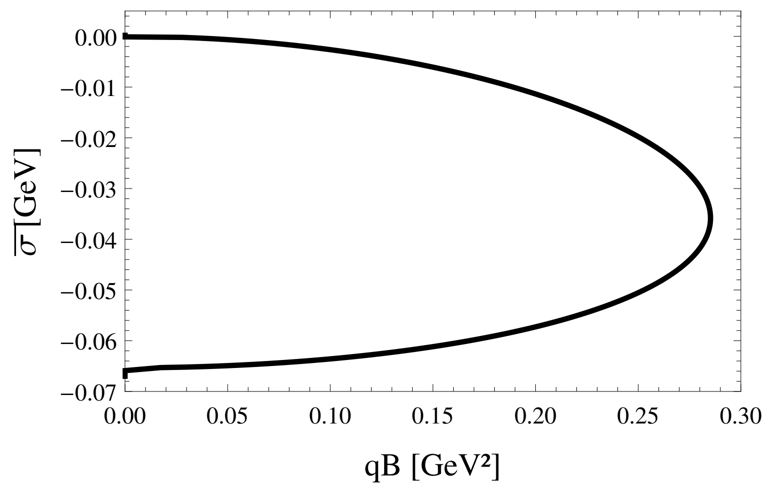

(b) Zoom in to the physical solution, which starts at $\bar{\sigma} = 0$ and converges to the solution coming from the local maximum in the free energy and ceases to exist slightly before $qB = 0.3\,\mathrm{GeV}^2$.

Figure D.3: Scalar condensate in the Walecka model as a function of the magnetic field.

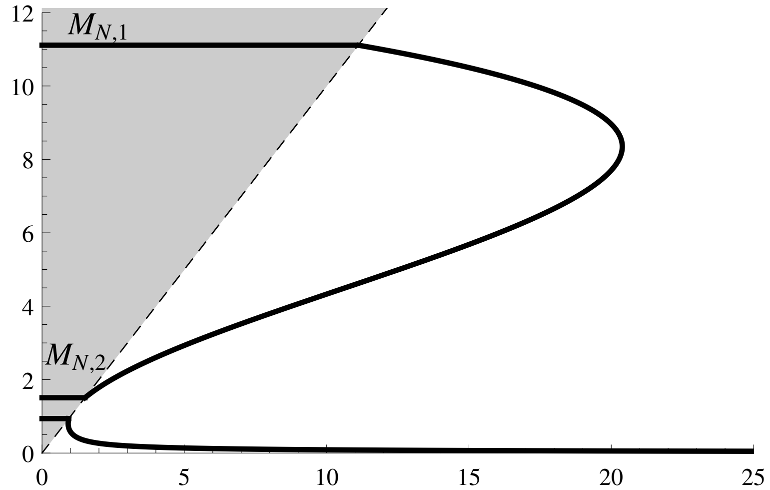

Figure D.4: Effective mass in dependence of the chemical potential at $qB = 0$, where the shaded area corresponds to the vacuum. The three vacuum solutions are given by Eq. (D.1). The lowest solution, starting at $M_N = m_N$ is the physical solution which does not differ qualitatively from the solutions in the main text.

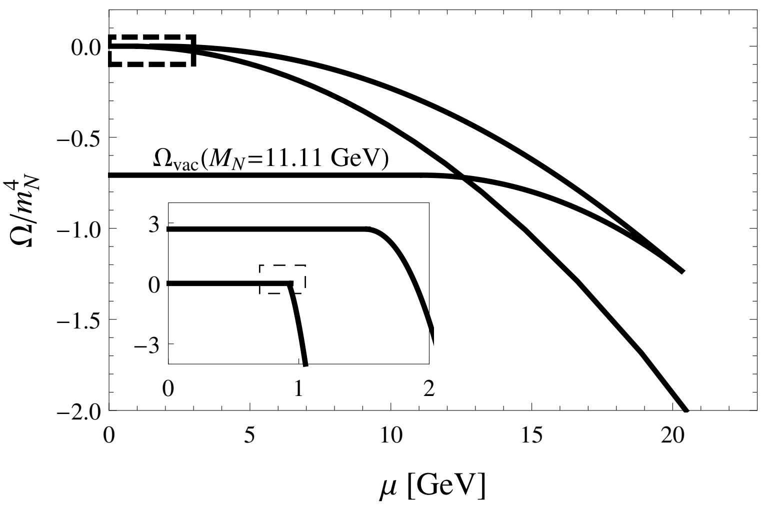

Figure D.5: Free energy at $qB = 0$ as a function of the chemical potential. The inset shows a zoom in, where the two constant lines correspond to the vacuum solutions $M_{N,2} = 1.5067\,\mathrm{GeV}$ and m_N. The dashed box marks the area which we have to look at in order to determine the actual onset, which is presented in the main text, and is barley visible here. One can see that the physical solution is actually not energetically preferred, therefore the other solutions have to be neglected.

Acknowledgements

At first I want to thank my advisor Andreas Schmitt for the opportunity to write my thesis under his supervision. His endless support allover they entire time was really great. For a master student it is something special to be coauthor of a publication, I really appreciate this.

I also want to thank Florian Preis, who performed a lot of calculations for the paper, brought a lot of input into this project and helped me with several minor questions. Additionally I am grateful to Denis Parganilja who spent endless hours to explain the subtle details of the extended linear sigma model to me, additionally I also learned a lot for my thesis in his lectures on QCD. I do not want to forget my office colleagues David Müller, Christian Ecker and Frederic Brünner for a lot of useful and not so useful discussions, help with quantum field theory, Mathematica, which really can drive someone crazy, and a lot of funny moments. A lot of thanks goes to my girlfriend Michaela for her constant support and for taking a look at my horrible English writing. I certainly want to thank my family and especially my parents for the ongoing moral and financial support during my studies. Not everyone has the possibility to focus completely on his studies, I am grateful that I could. Finally I want to say thank you to all the people who maid my time at the University enjoyable and fun.

References

[1] R. C. Duncan and C. Thompson, "Formation of very strongly magnetized neutron stars - implications for gamma-ray bursts," *Astrophys.J.* **392** (1992) L9.

[2] D. Lai and S. Shapiro, "Cold equation of state in a strong magnetic field - Effects of inverse beta-decay," *Astrophys.J.* **383** (1991) 745–751.

[3] E. J. Ferrer, V. de la Incera, J. P. Keith, I. Portillo, and P. L. Springsteen, "Equation of state of a dense and magnetized fermion system," *Phys. Rev. C* **82** (Dec, 2010) 065802.

[4] J. S. Read, L. Baiotti, J. D. E. Creighton, J. L. Friedman, B. Giacomazzo, *et al.*, "Matter effects on binary neutron star waveforms," *Phys.Rev.* **D88** (2013) 044042, `arXiv:1306.4065 [gr-qc]`.

[5] D. M. Siegel, R. Ciolfi, A. I. Harte, and L. Rezzolla, "Magnetorotational instability in relativistic hypermassive neutron stars," *Phys.Rev.* **D87** no. 12, (2013) 121302, `arXiv:1302.4368 [gr-qc]`.

[6] K. Klimenko, "Three-dimensional Gross-Neveu model in an external magnetic field," *Theor.Math.Phys.* **89** (1992) 1161–1168.

[7] K. Klimenko, "Three-dimensional Gross-Neveu model at nonzero temperature and in an external magnetic field," *Theor.Math.Phys.* **90** (1992) 1–6.

[8] V. Gusynin, V. Miransky, and I. Shovkovy, "Catalysis of dynamical flavor symmetry breaking by a magnetic field in (2+1)-dimensions," *Phys.Rev.Lett.* **73** (1994) 3499–3502, `arXiv:9405262 [hep-ph]`.

[9] V. Gusynin, V. Miransky, and I. Shovkovy, "Dynamical flavor symmetry breaking by a magnetic field in (2+1)-dimensions," *Phys.Rev.* **D52** (1995) 4718–4735, `arXiv:9407168 [hep-th]`.

[10] V. Gusynin, V. Miransky, and I. Shovkovy, "Dimensional reduction and dynamical chiral symmetry breaking by a magnetic field in (3+1)-dimensions," *Phys.Lett.* **B349** (1995) 477–483, `arXiv:9412257 [hep-ph]`.

[11] I. Shushpanov and A. V. Smilga, "Quark condensate in a magnetic field," *Phys.Lett.* **B402** (1997) 351–358, `arXiv:9703201 [hep-ph]`.

[12] N. O. Agasian, "Chiral thermodynamics in a magnetic field," *Phys.Atom.Nucl.* **64** (2001) 554–560, `arXiv:0112341 [hep-ph]`.

[13] V. Miransky and I. Shovkovy, "Magnetic catalysis and anisotropic confinement in QCD," *Phys.Rev.* **D66** (2002) 045006, `arXiv:0205348 [hep-ph]`.

[14] I. A. Shovkovy, "Magnetic Catalysis: A Review," *Lect.Notes Phys.* **871** (2013) 13–49, `arXiv:1207.5081 [hep-ph]`.

[15] D. Kharzeev, K. Landsteiner, A. Schmitt, and H.-U. Yee, "Strongly Interacting Matter in Magnetic Fields," *Lect.Notes Phys.* **871** (2013) 1–624.

[16] M. D'Elia, S. Mukherjee, and F. Sanfilippo, "QCD Phase Transition in a Strong Magnetic Background," *Phys.Rev.* **D82** (2010) 051501, `arXiv:1005.5365 [hep-lat]`.

[17] M. D'Elia and F. Negro, "Chiral Properties of Strong Interactions in a Magnetic Background," *Phys.Rev.* **D83** (2011) 114028, arXiv:1103.2080 [hep-lat].

[18] G. Bali, F. Bruckmann, G. Endrődi, Z. Fodor, S. Katz, *et al.*, "The QCD phase diagram for external magnetic fields," *JHEP* **1202** (2012) 044, arXiv:1111.4956 [hep-lat].

[19] G. Bali, F. Bruckmann, G. Endrődi, Z. Fodor, S. Katz, *et al.*, "QCD quark condensate in external magnetic fields," *Phys.Rev.* **D86** (2012) 071502, arXiv:1206.4205 [hep-lat].

[20] J. Walecka, "A Theory of highly condensed matter," *Annals Phys.* **83** (1974) 491–529.

[21] B. D. Serot and J. D. Walecka, "Recent Progress in Quantum Hadrodynamics," *International Journal of Modern Physics E* **6** (1997) 515–631, nucl-th/9701058.

[22] C. E. DeTar and T. Kunihiro, "Linear σ Model With Parity Doubling," *Phys.Rev.* **D39** (1989) 2805.

[23] D. Jido, Y. Nemoto, M. Oka, and A. Hosaka, "Chiral symmetry for positive and negative parity nucleons," *Nucl.Phys.* **A671** (2000) 471–480, arXiv:9805306 [hep-ph].

[24] D. Jido, M. Oka, and A. Hosaka, "Chiral symmetry of baryons," *Prog.Theor.Phys.* **106** (2001) 873–908, arXiv:0110005 [hep-ph].

[25] D. Zschiesche, L. Tolos, J. Schaffner-Bielich, and R. D. Pisarski, "Cold, dense nuclear matter in a SU(2) parity doublet model," *Phys.Rev.* **C75** (2007) 055202, arXiv:0608044 [nucl-th].

[26] S. Gallas, F. Giacosa, and G. Pagliara, "Nuclear matter within a dilatation-invariant parity doublet model: The role of the tetraquark at nonzero density," *Nuclear Physics A* **872** no. 1, (2011) 13 – 24.

[27] S. Gallas, F. Giacosa, and D. H. Rischke, "Vacuum phenomenology of the chiral partner of the nucleon in a linear sigma model with vector mesons," *Phys.Rev.* **D82** (2010) 014004, arXiv:0907.5084 [hep-ph].

[28] A. Heinz, S. Strüber, F. Giacosa, and D. Rischke, "Role of the tetraquark in the chiral phase transition," *Physical Review D* **79** no. 3, (Feb., 2009) 037502, arXiv:0805.1134 [hep-ph].

[29] A. Heinz, F. Giacosa, and D. H. Rischke, "Chiral density wave in nuclear matter," arXiv:1312.3244 [nucl-th].

[30] A. Broderick, M. Prakash, and J. Lattimer, "The Equation of State of Neutron Star Matter in Strong Magnetic Fields," *The astrophysical journal* **537** (July, 2000) 351–367, astro-ph/0001537.

[31] M. Sinha, B. Mukhopadhyay, and A. Sedrakian, "Hypernuclear matter in strong magnetic field," *Nucl.Phys.* **A898** (2013) 43–58, arXiv:1005.4995 [astro-ph.HE].

[32] A. Rabhi, P. Panda, and C. Providência, "Warm and dense stellar matter under strong magnetic fields," *Physical Review C* **84** no. 3, (Sept., 2011) 035803, arXiv:1105.0254 [nucl-th].

[33] F. Preis, A. Rebhan, and A. Schmitt, "Holographic baryonic matter in a background magnetic field," *Journal of Physics G Nuclear Physics* **39** no. 5, (May, 2012) 054006, arXiv:1109.6904 [hep-th].

[34] J. Dong, W. Zuo, and J. Gu, "Magnetization of neutron star matter," *Phys.Rev.* **D87** (2013) 103010, `arXiv:1305.4533 [astro-ph.SR]`.

[35] R. Casali, L. Castro, and D. Menezes, "Hadronic and hybrid stars subject to density dependent magnetic fields," *Phys.Rev.* **C89** (2014) 015805, `arXiv:1307.2651 [astro-ph.SR]`.

[36] A. Broderick, M. Prakash, and J. Lattimer, "Effects of strong magnetic fields in strange baryonic matter," *Phys.Lett.* **B531** (2002) 167–174, `arXiv:0111516 [astro-ph]`.

[37] R. C. R. de Lima, S. S. Avancini, and C. Providência, "Effect of strong magnetic fields on the nuclear "pasta" phase structure," *Physical Review C* **88** no. 3, (Sep, 2013) .

[38] N. Glendenning, *Compact Stars Nuclear Physics, Particle Physics and General Relativity.* Springer, 1996.

[39] N. K. Glendenning, "Vacuum polarization effects on nuclear matter and neutron stars," *Nuclear Physics A* **493** (Mar., 1989) 521–548.

[40] N. K. Glendenning, "Vacuum polarization effects in the non-linear σ, ω-model," *Physics Letters B* **208** (July, 1988) 335–338.

[41] F. Preis, A. Rebhan, and A. Schmitt, "Inverse Magnetic Catalysis in Field Theory and Gauge-Gravity Duality," in *Lecture Notes in Physics, Berlin Springer Verlag*, D. Kharzeev, K. Landsteiner, A. Schmitt, and H.-U. Yee, eds., vol. 871 of *Lecture Notes in Physics, Berlin Springer Verlag*, p. 51. 2013. `arXiv:1208.0536 [hep-ph]`.

[42] D. Ebert, K. Klimenko, M. Vdovichenko, and A. Vshivtsev, "Magnetic oscillations in dense cold quark matter with four fermion interactions," *Phys.Rev.* **D61** (2000) 025005, `arXiv:9905253 [hep-ph]`.

[43] T. Inagaki, D. Kimura, and T. Murata, "Four fermion interaction model in a constant magnetic field at finite temperature and chemical potential," *Prog.Theor.Phys.* **111** (2004) 371–386, `arXiv:0312005 [hep-ph]`.

[44] D. Menezes, M. Benghi Pinto, S. Avancini, A. Perez Martinez, and C. Providência, "Quark matter under strong magnetic fields in the Nambu-Jona-Lasinio Model," *Phys.Rev.* **C79** (2009) 035807, `arXiv:0811.3361 [nucl-th]`.

[45] R. Gatto and M. Ruggieri, "Quark Matter in a Strong Magnetic Background," *Lect.Notes Phys.* **871** (2013) 87–119, `arXiv:1207.3190 [hep-ph]`.

[46] G. N. Ferrari, A. F. Garcia, and M. B. Pinto, "Chiral Transition Within Effective Quark Models Under Magnetic Fields," *Phys.Rev.* **D86** (2012) 096005, `arXiv:1207.3714 [hep-ph]`.

[47] J. O. Andersen and A. Tranberg, "The Chiral transition in a magnetic background: Finite density effects and the functional renormalization group," *JHEP* **1208** (2012) 002, `arXiv:1204.3360 [hep-ph]`.

[48] J. O. Andersen and R. Khan, "Chiral transition in a magnetic field and at finite baryon density," *Phys.Rev.* **D85** (2012) 065026, `arXiv:1105.1290 [hep-ph]`.

[49] V. V. Skokov, A. Y. Illarionov, and V. D. Toneev, "estimate of the magnetic field strength in heavy-ion collisions," *International Journal of Modern Physics A* **24** no. 31, (2009) 5925–5932, `http://www.worldscientific.com/doi/pdf/10.1142/S0217751X09047570`.

[50] E. S. Fraga and L. F. Palhares, "Deconfinement in the presence of a strong magnetic background: an exercise within the MIT bag model," *Phys.Rev.* **D86** (2012) 016008, `arXiv:1201.5881 [hep-ph]`.

[51] A. Haber, F. Preis, and A. Schmitt, "Magnetic catalysis in nuclear matter," `arXiv:1409.0425 [nucl-th]`.

[52] A. Schmitt, "Thermal field theory-lecture notes." 2013.

[53] A. Schmitt, "Dense matter in compact stars: A pedagogical introduction," *Lect.Notes Phys.* **811** (2010) 1–111, `arXiv:1001.3294 [astro-ph.SR]`.

[54] Y. Nambu and G. Jona-Lasinio, "Dynamical model of elementary particles based on an analogy with superconductivity. i," *Phys. Rev.* **122** (Apr, 1961) 345–358.

[55] Y. Nambu and G. Jona-Lasinio, "Dynamical model of elementary particles based on an analogy with superconductivity. ii," *Phys. Rev.* **124** (Oct, 1961) 246–254.

[56] V. Gusynin, V. Miransky, and I. Shovkovy, "Dynamical chiral symmetry breaking by a magnetic field in QED," *Phys.Rev.* **D52** (1995) 4747–4751, `arXiv:9501304 [hep-ph]`.

[57] M. Andreichikov, B. Kerbikov, V. Orlovsky, and Y. A. Simonov, "Neutron in Strong Magnetic Fields," *Phys.Rev.* **D89** (2014) 074033, `arXiv:1312.2212 [hep-ph]`.

[58] J. Kapusta and C. Gale, *Finite-Temperature Field Theory: Principles and Applications*. Cambridge Monographs on Mathematical Physics. Cambridge University Press, 2006.

[59] M. N. Kuznetsov Alexander, *Electroweak Processes in External Active Media*, vol. 252 of *Springer Tracts in Modern Physics*. Springer, 2013. ISBN: 978-3-642-36225-5.

[60] G. Endrődi, "Qcd equation of state at nonzero magnetic fields in the hadron resonance gas model," *Journal of High Energy Physics* **2013** no. 4, (2013) 1–19, `arXiv:1301.1307 [hep-ph]`.

[61] J. Schwinger, "On gauge invariance and vacuum polarization," *Phys. Rev.* **82** (Jun, 1951) 664–679.

[62] G. V. Dunne, "Heisenberg-Euler effective Lagrangians: Basics and extensions," in *From fields to strings, Vol. 1*, M. Shifman, A. Vainshtein, and J. Wheater, eds., pp. 445–522. World Scientific, 2004. `arXiv:0406216 [hep-th]`.

[63] M. H. Johnson and E. Teller, "Classical field theory of nuclear forces," *Phys. Rev.* **98** (May, 1955) 783–787.

[64] H.-P. Duerr, "Relativistic effects in nuclear forces," *Phys. Rev.* **103** (Jul, 1956) 469–480.

[65] B. D. Serot and J. D. Walecka, "The Relativistic Nuclear Many Body Problem," *Adv.Nucl.Phys.* **16** (1986) 1–327.

[66] J. Boguta and A. Bodmer, "Relativistic calculation of nuclear matter and the nuclear surface," *Nuclear Physics A* **292** no. 3, (1977) 413 – 428.

[67] J. D. Walecka, *Theoretical Nuclear and Subatomic Physics*. World Scientific, 2nd ed., 2004.

[68] J. Walecka, "Nuclear hydrodynamics in a relativistic mean field model." 2009.

[69] K. e. a. P. D. G. Olive, "Review of particle physics," *Chin. Phys. C* **38** no. 38, (2014) .

[70] W. Myers, "Droplet model of atomic nuclei," *New York, Plenum* (1977) .

[71] W. Myers and W. Swiatecki *Nuclear Physics* **81** (1966) 1.

[72] R. Barret *Reg.Prog.Phys* **37** (1974) 1.

[73] Y. N. Kim, *Mesic atoms and nuclear structure*. North-Holland Pub. Co, Amsterdam, 1971.

[74] P. Möller, W. Myers, W. Swiatecki, and J. Treiner *Atomic Data and nuclear Data Tables* **39** (1988) 225.

[75] D. Youngblood, Y. Lui, H. Clark, B. John, Y. Tokimoto, *et al.*, "Isoscalar E0 - E3 strength in Sn-116, Sm-144, Sm-154, and Pb-208," *Phys.Rev.* **C69** (2004) 034315.

[76] J. Blaizot, J. Berger, J. Decharge, and M. Girod, "Microscopic and macroscopic determinations of nuclear compressibility," *Nucl.Phys.* **A591** (1995) 435–457.

[77] C. Johnson, D. Horen, and C. Mahaux, "Unified description of the neutron- Pb-208 mean field between -20 and + 165 MeV from the dispersion relation constraint," *Phys.Rev.* **C36** (1987) 2252–2273.

[78] G. Li, R. Machleidt, and R. Brockmann, "Properties of dense nuclear and neutron matter with relativistic nucleon-nucleon interactions," *Phys.Rev.* **C45** (1992) 2782–2794.

[79] M. Jaminon and C. Mahaux, "Effective Masses in Relativistic Approaches to the Nucleon Nucleus Mean Field," *Phys.Rev.* **C40** (1989) 354–367.

[80] R. Furnstahl, J. J. Rusnak, and B. D. Serot, "The Nuclear spin orbit force in chiral effective field theories," *Nucl.Phys.* **A632** (1998) 607–623, `arXiv:9709064 [nucl-th]`.

[81] A. Heinz, F. Giacosa, and D. H. Rischke, "Chiral density wave in nuclear matter," `arXiv:1312.3244 [nucl-th]`.

[82] B. Lee, *Chiral Dynamics*. Documents on modern physics. Gordon and Breach Science Publishers, 1972.

[83] S. Gasiorowicz and D. Geffen, "Effective lagrangians and field algebras with chiral symmetry," *Rev. Mod. Phys.* **41** (July, 1969) 531.

[84] T. D. Cohen, R. J. Furnstahl, D. K. Griegel, and X. Jin, "QCD sum rules and applications to nuclear physics," *Progress in Particle and Nuclear Physics* **35** (1995) 221–298, `hep-ph/9503315`.

[85] D. Parganlija, "Quarkonium Phenomenology in Vacuum," `arXiv:1208.0204 [hep-ph]`.

[86] D. Parganlija, F. Giacosa, and D. H. Rischke, "Vacuum Properties of Mesons in a Linear Sigma Model with Vector Mesons and Global Chiral Invariance," *Phys.Rev.* **D82** (2010) 054024, `arXiv:1003.4934 [hep-ph]`.

[87] T. D. Cohen, D. A. McGady, and E. S. Werbos, "The Chiral condensate in a constant electromagnetic field," *Phys.Rev.* **C76** (2007) 055201, `arXiv:0706.3208 [hep-ph]`.

[88] N. Callebaut and D. Dudal, "On the transition temperature(s) of magnetized two-flavour holographic QCD," *Phys.Rev.* **D87** (2013) 106002, arXiv:1303.5674 [hep-th].